

https://dspace.org/

# Delineating the current and potential distributions of prosopis glandulosa in the square kilometre array South Africa, Karoo site

**Buthelezi, Nomcebo Siphesihle**

**2019**

https://hdl.handle.net/10539/29576

Buthelezi, Nomcebo Siphesihle (2019) Delineating current and potential distributions of prosopis glandulosa in the SKA SA Karoo Site, University of the Witwatersrand, Johannesburg, <http://hdl.handle.net/10539/29576>

Downloaded from a DSpace repository. https://dspace.org/

# Delineating the Current and Potential Distributions of *Prosopis glandulosa* in the Square Kilometre Array South Africa, Karoo Site

**Nomcebo Siphesihle Buthelezi (672456)**




**Supervisors:** **Prof Jasper Knight**

**Prof Fethi Ahmed**

**MSc Geographical Information Systems and Remote Sensing**

SKA AFRICA
SQUARE KILOMETRE ARRAY

NRF National Research Foundation

# Declaration

I declare that this research report is my own, unaided work. It is being submitted for the Degree Master of Science in the University of Witwatersrand, Johannesburg. It has not been submitted before for any degree or examination in any other University.

Candidate: Nomcebo Buthelezi

Date:

# Abstract

*Prosopis* species (also known as Mesquite), in particular *P. glandulosa* (Honey Mesquite) have a negative impact on indigenous biodiversity and the livelihood of communities in the semi-arid and arid parts of South Africa. The spread of these species is a threat to the environments in which they have been introduced as they spread at high rates, increase the mortality of indigenous trees and disrupt important ecosystem processes such as hydrological and nutrient cycles. Due to the negative impacts of *Prosopis* on important ecosystem services and South Africa's native biodiversity, it is essential for the distribution of these species to be identified, controlled and monitored in order to mitigate their spread and restore damaged ecosystems. The objectives of this study were to use Remote Sensing and Geographic Information Systems (GIS) tools to: (i) delineate the distribution of *Prosopis* using high resolution satellite imagery, (ii) determine the changes in spatial distribution of these species in the period 2003-2017, and (iii) use moderate spatial resolution satellite imagery and ancillary environmental data to predict areas susceptible to future invasion.. The study area used in this investigation is the Square Kilometre Array (SKA SA) site, situated in Northern Cape Province, South Africa. Satellite images were classified using Multi-layer Perceptron (MLP) Neural Network classification algorithm to improve the land use land cover classification accuracy. A WordView-3 image with 1.24 m spatial resolution was used to delineate the distribution of *Prosopis* in the study area for the year 2016. Landsat images from the years 2003, 2008, 2013 and 2017 were used to conduct a change detection analysis. The prediction model developed in the study was able to predict *Prosopis* cover for the years 2017 and 2022 cover using ancillary environmental data and land use land cover maps. The study was also able to quantify the area covered by *Prosopis* species for the years 2017 and 2022.

# Contents

Abstract ..... ii
List of Figures ..... v
List of Tables ..... vi
1. Introduction ..... 1
1.1 Problem Statement ..... 3
1.2 Research Questions ..... 6
1.3 Aims ..... 6
1.4 Objectives ..... 6
1.5 Justification ..... 6
2. Literature Review ..... 7
2.1 Introduction ..... 7
2.2 Description of *Prosopis* ..... 7
2.3 Introduction and spread of *Prosopis* into South Africa ..... 8
2.4 Impacts of Alien Invasive Species ..... 9
2.4.1 Ecological Impacts ..... 9
2.4.2 Socio economic Impacts ..... 11
2.5 South African Legislation Relating to Alien Invasive Species ..... 12
2.6 Remote Sensing Techniques for Invasive Control ..... 13
2.6.1 *Prosopis* mapping in Africa ..... 13
2.6.2 Predictive Modelling ..... 18
3. Materials and Methods ..... 20
3.1 Study Area ..... 20
3.2 Data Acquisition ..... 22
3.2.1 Satellite Data ..... 22
3.2.2 Digital Elevation Model ..... 24
3.3 Field Survey ..... 25
3.4 Pre-processing ..... 31
3.5 Data Analysis ..... 31
3.5.1 Image Classification of WorldView-3and Landsat Satellite Image ..... 32
3.5.2 Land Use Land Cover Change detection ..... 34
3.5.3 *Prosopis* Land Cover Change Prediction ..... 36
4. Results ..... 40
4.1 2016 Worldview-3 Land Cover Classification ..... 40

4.1.1 Results ..... 40
4.2 Change Detection Analysis ..... 43
4.2.1 Results ..... 43
4.3 Change Prediction ..... 59
4.3.1 Results ..... 59
5. Discussion ..... 67
5.1 WorldView-3 Land Cover Classification ..... 67
5.2 Change Detection Analysis ..... 68
5.3 Change Prediction ..... 69
6. Conclusions ..... 71
7. Recommendations ..... 73
8. References ..... 74

# List of Figures

Figure 1. False colour composite Landsat image highlighting the vegetation (shown in green) at the SKA site (including) *Prosopis* ..... 5
Figure 2. Land cover classification results: (A) Pleiades, (B) Senitinel-2 in the urban area of Marigat. Pleiades had a higher accuracy in mapping for Prosopis and Vachellia as the sensor has an improved capacity to detect the location of smaller features (Ng *et al*., 2017) ..... 17
Figure 3. Map illustrating the SKA SA site in the Northern Cape Province, South Africa. ..... 21
Figure 4. Example of density categories identified during field survey (scale 66 m) ..... 26
Figure 5. Map illustrating the density of Prosopis surveyed during fieldwork ..... 28
Figure 6. Images of Prosopis glandulosa in the study area. These species are located along watercourses and drainage line (a, b and d) and close to manmade dams and boreholes (d). ..... 29
Figure 7. Map illustrating the height of the ground reference Prosopis species collected ..... 30
Figure 8. Flowchart illustrating the processes followed when classifying the high resolution WorldView 3 image ..... 33
Figure 9. Flowchart illustrating the processes followed when conducting the land use land cover change detection ..... 35
Figure 10. Flowchart illustrating the processes followed when conducting the 2017 and 2022 land cover prediction ..... 36
Figure 11. RMS plot for the 2016 neural network classification ..... 41
Figure 12. 2016 land cover classification using WorldView 3 satellite imagery. ..... 42
Figure 13. 2003 Land cover classification using Landsat satellite image ..... 45
Figure 14. 2008 Land cover classification using Landsat satellite image ..... 47
Figure 15. Gains and Losses graph for the year 2003-2008 ..... 48
Figure 16. Net change graph for the year 2003-2008 ..... 49
Figure 17. 2013 Land cover classification using Landsat 8 satellite imagery**Error! Bookmark not defined.**
Figure 18. Gains and Losses graph for the year 2008-2013 ..... 52
Figure 19. Net change graph for the year 2008-2013 ..... 52
Figure 20. Contributions to Net Change in Built-up land ..... 52
Figure 21. 2017 Land cover classification using Landsat 8 satellite imagery ..... 54
Figure 22. Gains and losses for the year 2013-2017 ..... 56
Figure 23. Net change for the year 2013-2017 ..... 56
Figure 24. *Prosopis*land over changes from 2003-2017 ..... 56
Figure 25. RMS plots. a) 2003 classification RMS plot, b)2008 classification RMS plot, c)2013 classification RMS plot, d) 2017 classification RMS plot ..... 58
Figure 26. 2003-2013 gains and losses graph for land cover prediction ..... 59
Figure 27. 2003-2013 Change analysis change map for prediction model ..... 60
Figure 28. Driver variables used in the change prediction model ..... 61
Figure 29. 2017 Land cover prediction map ..... 63
Figure 30. Pixel comparison of 2017 real LULC map and 2017 predicted LULC map ..... 64
Figure 31. 2022 Land cover prediction map ..... 66

# List of Tables

Table 1. Worldview 3 sensor specifications ..... 22
Table 2. Landsat 5 ETM and Landsat 8 sensor specifications ..... 24
Table 3. LULC classes collected including training and testing dataset ..... 27
Table 4. LULC classes showing the test and training data ..... 35
Table 5. Confusion matrix for 2016 Worldview land cover classification ..... 40
Table 6. Confusion matrix for 2003 Landsat 5 land cover classification ..... 43
Table 7. 2003 Accuracy assessment statistics ..... 43
Table 8. 2008 Confusion matrix ..... 48
Table 9. 2008 Accuracy assessment statistics ..... 48
Table 10. Confusion matrix for 2013 Landsat land cover classification ..... 51
Table 11. 2013 Accuracy assessment statistics ..... 51
Table 12. Confusion matrix 2017 land cover classification ..... 55
Table 13. 2017 Accuracy assessment statistics ..... 55
Table 14. Statistical model validation ..... 62
Table 15. Confusion matrix for 2017 prediction map ..... 65

# 1. Introduction

*Prosopis* species also known as mesquite, are evergreen, alien invasive plant species commonly found in the arid north-western parts of South Africa (Zimmermann and Pasiecznik, 2005). These species were introduced into the country in the 1880s from North and South America for a number of functions such as providing shade for livestock, fuel wood, pods for fodder and wood for construction and furniture production (Zachariades *et al.*, 2011). With the establishment and production of this plant being encouraged by the government in the 1950s, farmers deliberately planted these trees in large parts of the country (Van Wilgen *et al*., 2001). In the Western Cape, Northern Cape, Free State and North West provinces, *Prosopis* species have been spreading at high rates, having negative environmental, economic and social impacts (Abdi, 2001; Zachariades *et al*., 2011). *Prosopis* in South Africa covers approximately 1.8 million ha, with an estimated expansion in area ranging from 3.5-18.0% per annum (Zachariades *et al.*, 2011).

There are numerous species and their hybrids that are major invaders in the arid interior regions of South Africa (Shackleton *et al.,* 2015). The most common species are *Prosopis glandulosa* (Honey Mesquite)*, P. veltutina* and *P. chilensis.* In addition, *P. alba, P. juliflora, P. laevigata, P. pubescens* and *P. pallid* are also present in the country but are not as common (Shackleton *et al.,* 2015). The spread of *Prosopis* has severe negative impact on the arid and semi-arid environments in which they have been introduced as they spread at high rates, increase the mortality of native trees, and disrupt important ecosystem processes such as altering hydrology and nutrient cycles (Van Wilgen *et al*., 2001; Shackleton *et al.,* 2015). The detrimental threat *Prosopis* has on indigenous biodiversity and ecosystem services highlights the importance of identifying, controlling and mitigating their spread in order to restore damaged ecosystems and protect potential invasion areas (Roura-Pascual *et al*., 2009; Ndhlovu *et al*., 2016).

The successful control of *Prosopis* depends on early detection of these species and rapid monitoring and management (West *et al*., 2016). Information on the distribution and abundance of *Prosopis* is required when controlling and reducing the extent of spread of these species (Van Klinken *et al*., 2007). This information, captured at the correct scale and accuracy, is also essential for predicting future spread and devising appropriate management plans and control policies (Van Klinken *et al*., 2007). Remote sensing and geographical information systems (GIS) can be utilized to map and model the distribution of *Prosopis* (Wakie *et al.*, 2014). In predicting the areas that are more likely to be infested by invasive alien plant species, it is important to identify the environmental conditions under

which these species grow and spread. The relationships between these environmental conditions are then used to predict areas with similar conditions to those where the species are found (Wakie *et al*., 2014). Remote sensing technology has provided multispectral and multitemporal data that are cost effective and cover large, complex and inaccessible terrains and ecosystems (Joshi *et al*., 2004; Cho *et al*., 2015). The integration of GIS, remote sensing and modelling algorithms has been utilised successfully in numerous alien invasion studies in Africa (Van den Berg *et al.*, 2013; Wakie *et al.*, 2014; Abdou *et al*., 2016; West *et al.*, 2016). GIS and remote sensing tools favour the delineation of *Prosopis* in large areas, therefore allowing for effective monitoring.

With the *Prosopis* invasion expanding within the Northern Cape Province, the Square Kilometer Array South Africa (SKA SA) requires a way of detecting and controlling these species. Remote sensing and GIS technologies provide an effective way of detecting, quantifying and predicting vulnerable areas that require monitoring for any future invasion. This technology will assist with mapping and monitoring invasive species, allowing for effective control of these species.

## 1.1 Problem Statement

Alien invasive species negatively impact indigenous biodiversity and the livelihood of locals in the Northern Cape (Van den Berg *et al*., 2013). *Prosopis glandulosa* is a significant problem in some parts of the SKA SA site, especially along drainage lines. There are hundreds of hectares in the study area which are currently affected and a dedicated and coordinated approach will be required to bring the invasion under control. This control is essential in order to reduce the negative impacts *Prosopis* has on limited water resources, limited agricultural potential and native biodiversity of the semi-arid region (Van den Berg *et al*., 2013). Acquiring information on the distribution and location of *Prosopis* is important in order to stop further spread in these arid regions.

There are numerous studies that have attempted to estimate the spatial extent of alien invasive species in the Northern Cape (Henderson, 1998, Van den Berg *et al*., 2013, Mureriwa *et al*., 2016). These were aimed at delineating the affected areas and attempting to address the alien invasive problems faced in the province (Van den Berg *et al*., 2013). Comprehensive records illustrating the invasion in the country are available. This includes records by Henderson (1998) which is the South African Plant Invader Atlas (SAPIA). The SAPIA project was launched in 1994 and was aimed at collecting information on the abundance, distribution, geographic extent and habitat types of different alien invasive plant species in southern Africa (Henderson, 1999). The database consists of information that was collected between 1994 and 1998 (Henderson, 1998). The problem with most records is that they may be outdated and due to the nature of *Prosopis*, being a fast growing species, it is suspected that their spread rate may not be the earlier predicted 3.5-18.0% in area per annum, but now can be estimated to be as high as 30-40% in area per annum (Zachariades *et al*., 2011; Wise *et al*., 2012). The rate of spread is based on the area of the invaded land. Van den Berg (2013) estimated that the area covered by *Prosopis* in the Northern Cape Province increased from 127 821 ha in 1974 to 1 473 953 ha in 2007, with a mean annual increase of 7.4% in area. There may also be local variations in the rate of spread of these species.

Numerous past studies that attempted to estimate invasive plant species extent were conducted using traditional field survey techniques and local expert knowledge (Van den Berg *et al*., 2013; Wakie *et al.,* 2014). This is a problem as not all invaded areas could be accessed and large areas could not be delineated using these traditional techniques (Van den Berg *et al*., 2013; Wakie *et al.,* 2014). This meant new strategies for monitoring natural resources had to be developed. Remote sensing has proven to be an essential tool in detecting and monitoring land cover changes due to its ability to cover large areas in the fraction of time required by field surveys and being cost effective (Cho *et al*.,

2015). The availability of remote sensing data made it possible for more *Prosopis* studies to be carried out (Van den Berg *et al*., 2013; West *et al*., 2016). This has improved our understanding and estimation of species distribution, but most sensors used were of a lower resolution. This affects the accuracy and details one may obtain from the low resolution satellite imagery. Research using high resolution images is required as this will give a more detailed overview of the spread of *Prosopis* in the country (Joshi *et al*., 2004).

Figure 1 is a false colour composite image of the SKA site using Bands 4, 5 and 6 to allow for vegetation to be detected. Based on past environmental assessments and studies undertaken on the SKA site, the site consists of a number of plant species namely, *Rhigozum trichotomum*, *Acacia karroo*, *Stipagrostis* and *Prosopis.* Of these species, assessments have shown that *Prosopis* is by far the most abundant plant on site (Milton, 2017).

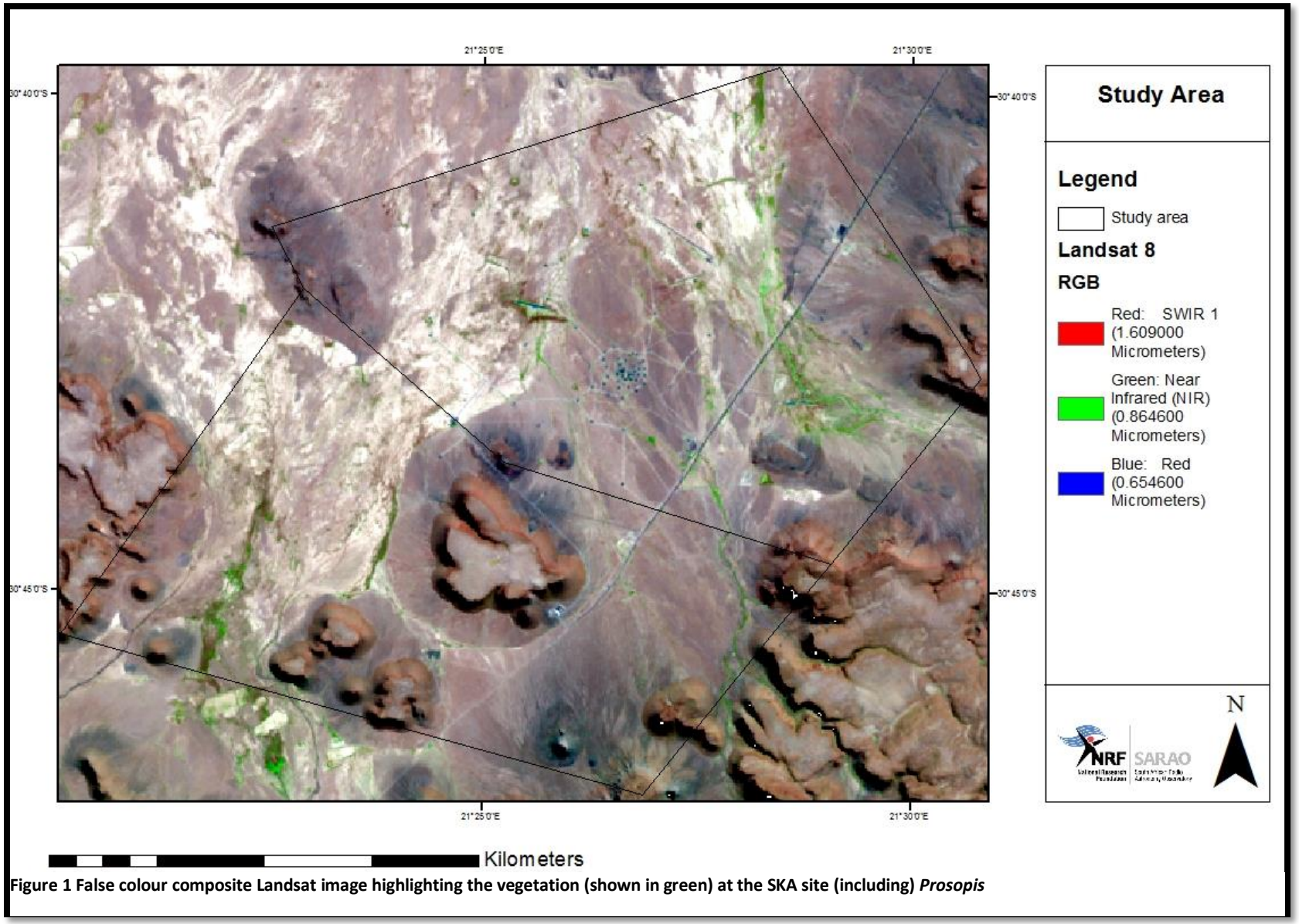



**Figure 1 False colour composite Landsat image highlighting the vegetation (shown in green) at the SKA site (including) *Prosopis***

## 1.2 Research Questions

1. Which areas were covered by *Prosopis glandulosa* in the SKA SA Karoo site in 2016?
2. How has the land cover changed in the past 14 years within the study area?
3. Which areas are susceptible to the establishment and growth of *Prosopis* in the future?

## 1.3 Aims

1. The aim of the study was to delineate *Prosopis gladulosa* and other land use / land cover (LULC) classes and predict areas susceptible to future invasion.

## 1.4 Objectives

1. Delineate the distribution of *Prosopis glandulosa* and other LULC classes using high resolution WorldView-3 satellite imagery and Multi-layer Perceptron (MLP) Neural Network algorithm.
2. Determine the change in spatial distribution of *Prosopis* species from the years 2003, 2008, 2013 and 2017.
3. Determine the areas that are likely to be infested by *Prosopis* in 2017 and 2022 using remotely sensed data, ancillary environmental data and the IDRISI Land Change Modeller.

## 1.5 Justification

The results of this study will provide the SKA South Africa, Infrastructure and Site Operations department with detailed information on the distribution, quantity and potential invading areas of *Prosopis* on site. This will assist with the establishment of land management strategies and programmes that will deal with effectively controlling and removing *Prosopis*, which is required by the South African National Environmental Management Act: Biodiversity Act No 10 of 2004 (NEMBA). This control is essential in order to reduce the negative impacts *Prosopis* has on limited water resources, limited agricultural potential and native biodiversity of the semi-arid region (Van den Berg *et al*., 2013). The National Environmental Management: Biodiversity Act, 2004 also requires landowners to clear invasive plant species in their property.

# 2. Literature Review

## 2.1 Introduction

Quantifying areas occupied by *Prosopis* is important in order to determine the ecological and socio-economic impacts of the invasive plant species as well as the feasibility of the management strategies designed to reduce its expansion (Mirik and Ansley, 2012). This literature review will cover a number of themes. *Prosopis* species will first be defined, by describing their appearance, their characteristics and the location in which these plant species are commonly found. This will lead to a brief description of their native areas and the ways in which they were introduced into South Africa. The environmental, economic and social impacts *Prosopis* has on the communities of South Africa will be evaluated, looking at how these species affect the environment and people within infested areas. Laws and regulations to combat and control the spread of *Prosopis* will also be highlighted. Studies related to modelling the spread of *Prosopis* using remote sensing and GIS have increased over the years. These will be dealt with in the literature review looking at their methodologies and their success in delineating the distribution of invasive plant species.

## 2.2 Description of *Prosopis*

*Prosopis* shrubs or trees may be defined as evergreen, woody perennials belonging to the Leguminosae family (Zachariades *et al*., 2011). In South Africa, these species are usually referred to as Meskietboom or Mesquites. There are 44 recognized species of the genus *Prosopis* which are native to the Americas, Asia and Africa (Choge *et al*., 2007). Of the 44 *Prosopis* species, 40 are native to the Americas with only one species, *Prosopis africana*, being native to African countries such as Senegal, Sudan, Uganda and Ethiopia (Geesingis *et al*., 2004). These species are usually found in arid and semi-arid environments. This is as a result of these species being drought and heat resistant (Sawal *et al*., 2004). The *Prosopis* taxa shrubs or trees may grow to approximately 3-15m high; with either one main stem that is usually 6-9 m in height or in multiple stems (Van Klinken and Campbell, 2001). *Prosopis* consists of bark that is usually a dark red colour and is rough. The species' branches mostly consist of hard thorns (Sawal *et al*., 2004). The foliage is feathery, usually dark green, but can sometimes be bluish green. The species flowers are greenish cream to yellow and consists of seed pods that are about 5-20 cm long (Van Klinken and Campbell, 2001).

The growth of *Prosopis* is influenced by a number of factors. This includes their ability to establish and grow in a variety of temperatures, soil types, moistures and light conditions (Weltzin *et al*., 1998). *Prosopis* species have the ability to grow at fast rates and are drought resistant, nitrogen fixing species

that are able to adapt to poor and saline soils in arid and semi-arid environments and are tolerant of disturbances (Choge *et al*., 2007). *Prosopis* species are not entirely dependent on rainfall. Their deep root system allows for these species to use groundwater supplies Geesingis *et al*., 2004). The roots of these species can adapt in a variety of soil conditions. *Prosopis* roots have been classified as being the most extensive root system of any plant species in the world (Hoshino *et al*., 2012). This is a result of *Prosopis* roots grow upwards to exploit surface water and also growing long roots that may even reach a depth of 80 m (Hoshino *et al*., 2012). The complete and detailed taxonomy of the *Prosopis* genus was compiled by Burkart (1976).

## 2.3 Introduction and spread of *Prosopis* into South Africa

*Prosopis* species were originally introduced into South Africa between 1800 and 1960 (Zachariades *et al*., 2011). These species were introduced from America, promoted to give socioeconomic and ecological benefits to farmers and locals in arid environments where other tree species failed to survive (Zachariades *et al*., 2011). By the 1960s, the promotion of the deliberate planting of these trees ceased. This decision was made as a result of the spread and densification of these plant species (Wise *et al.,* 2012). *Prosopis* spread out from the designated plantation areas, and today these invasive species cover several million hectares in the Northern Cape, Western Cape, Free State and North West provinces (Choge *et al*., 2007; Zachariades *et al*., 2011).

The dispersal of *Prosopis* seeds has been both deliberate and accidental in South Africa. Humans have transported *Prosopis* globally for their benefits such as providing firewood, timber, shade and aesthetic value (Mwangi and Swallow, 2005; Zachariades *et al*., 2011). In recent years, the spread and infestation of these species have been influenced by a number of agents. These include floodwaters, animals and runoff (Van Klinken and Campbell, 2001). Water plays an important role in the spread of *Prosopis* seeds because they float. Seed dispersal is enhanced by water flow during high rainfall event or floodwaters. This is observed by the concentration of *Prosopis* along ephemeral water courses and low lying areas (Zachariades *et al*., 2011). Animals, both wild and domesticated are also main drivers of the dispersal of seeds by feeding on them (Pasiecznik *et al*., 2001). This is due to the high sugar content of *Prosopis* pods. A variety of herbivores sought after this food source resulting in the dispersal of seeds in dung (Pasiecznik *et al*., 2001). *Prosopis* has therefore been seen establishing around livestock water points and kraals where livestock and game shelter. Grazing also has an influence in the growth of these species. Livestock grazing results in a reduction in competition with grasses which may also increase *Prosopis* spreading rate (Weltzin *et al*., 1998).

## 2.4 Impacts of Alien Invasive Species

The spread of alien invasive species is a major threat to biodiversity, economic development and human wellbeing in South Africa (Burgiel and Muir, 2010; Abdi, 2011; Tessema, 2012; Wilson *et al*., 2013). The negative impacts on biodiversity include the displacement of native species, alteration of soil chemistry, hydrological cycles, nutrient cycles and alteration of disturbance regimes (fire, erosion and flooding) (Charles and Dukes, 2008). Alien invasive species also affect humans by altering ecosystem services including services such as water availability and food security (Charles and Dukes, 2008). Many studies in South Africa have focused on how alien invasive species impact the country's water resources (Le Maitre *et al*., 2000, 2015). This is as a result of the country's overall dry climate (Van den Berg, 2013; Le Maitre *et al*., 2015). Such services are important for human wellbeing and survival therefore alien invasive plant species need to be closely monitored to reduce such negative impacts (Tessema, 2012).

### 2.4.1 Ecological Impacts

Alien invasive species have an impact on natural systems and biodiversity due to their ability to produce large numbers of offspring, to grow fast and tolerate extreme environmental conditions. These species are also able to displace indigenous biodiversity and have long distance dispersal capabilities which affect the natural environment negatively. Alien invasive species affect the ecosystems by altering their structure and functions which are responsible for producing and maintaining ecosystem services (Wakie *et al*., 2014).

Invasive alien plant species have been observed to alter evapotranspiration rates and timing, runoff and groundwater recharge (Charles and Dukes, 2008). This may result in stream flow and groundwater recharge reduction, affecting water supply, quality and regulation (Chamier *et al*., 2012). These species have the ability to use more water than indigenous species, therefore decreasing water available for human use and native species (Charles and Dukes, 2008). The increased water use by invasive species is as a result of a number of factors. According to Le Maitre *et al*. (2015) these factors are the plant traits such as having little dependence on rainfall, its size, root depth, leaf area and transpiration rates (Le Maitre *et al*., 2000, 2015). Deep roots in a number of alien invasive plant species such as *Prosopis* can give rise to increased water use as these roots allow such species to access groundwater and soil moisture in deep soils. *Prosopis* species are described as being evergreen and this characteristic also has a great impact as native species are seasonally dormant during winter (Charles and Dukes, 2008; Maitre *et al*., 2015). This increased water use is a problem in South Africa as the country is dry and is

prone to droughts. If invasive species are left uncontrolled, this may result in water shortages in the future for human consumption and biodiversity.

In 1996, the Council for Scientific and Industrial Research (CSIR) was appointed by the Water Research Council to assess the impacts of alien invasive plants on surface water resources (Le Maitre *et al*., 2000). An appropriate and reliable model was utilized to estimate the water use of alien invasive plant species. The information used in the model, captured at an appropriate scale, consisted of data from a catchment experiment which compared the stream flow under natural vegetation and under commercial plantations. The model used the idea of forest water used being linked to leaf area which is linked to biomass, growth and productivity. Bosch *et al*. (1980) explored the idea of water used being related to biomass and this was later taken further by Le Maitre *et al*. (1996) in which a model was created that converted biomass estimates into estimates of stream flow reduction. The study concluded that South Africa and Lesotho have approximately 10 million ha of invaded area. The invaded areas can also be evaluated by observing the 'condensed' invasion which illustrates the extent to which areas are fully invaded (altered to cover 100%). The 'condensed' invaded area which if fully invaded is approximately 1.7 million ha. The estimated incremental water use in South Africa and Lesotho by alien species is approximately 3300$m^3$per year (33mm/yr) or 6.67% of the mean annual runoff when calculated using the total invaded area of 10.1 million ha. In a 'condensed' area, the estimated incremental water use is 1 900 $m^3$ per ha (19 mm/yr) or910$m^3$/ha/yr. The extent to which the alien species covers the country varies from province to province, with the Northern Cape and Western Cape being considered some of the extensively invaded provinces in South Africa. The species which invaded the largest total area include *Melia azedarach, Acacia mearnsii, Prosopis* species and *Lantana camaral*; where *Prosopis* species were mainly found in the Northern Cape Province. The Northern Cape Province was also observed to be the province with the highest impact percentage where the invaders, mainly *Prosopis*, uses approximately 910 $m^3$ /ha/yr which is about 17% of mean annual runoff. The study concluded by comparing the water used in plantations and in areas invaded by alien species. The plantation water use was approximately 93 mm/yr, with invaded areas using more water of approximately 190 mm/yr. One of the reasons for this is as a result of alien species establishing close to water resources (Le Maitre *et al*., 2000).

Soil properties change in response to the introduction of new species. Enhrenfeld (2003) studied the effects that alien plants have on soil nutrient cycling processes. Changes in species dominance patterns affect nutrient cycling. These changes are as a result of the changes in the physical properties of the soil caused by the new species. This study stated that alien invasive plants tend to have more

extractable inorganic nitrogen and exotic invasive plants have increased rate of nitrogen mineralization (Enhrenfeld, 2003).

The spread of alien invasive species threatens native biodiversity. Invasive species such as *Prosopis are* able to take advantage over native species in the regions that they invade (Richardson and Van Wilgen, 2004). These species are able to alter community structure and transform ecosystems by using resources excessively, by adding resources that may not be needed, by affecting soil properties, and by accumulating and redistributing litter and salts (Richardson and Van Wilge, 2004). This results in population decline of native species. Alien invasive species may also lead to habitat destruction, fragmentation and loss. This can lead to a collapse of the indigenous ecosystem (Reaser *et al*., 2007).

### 2.4.2 Socio economic Impacts

*Prosopis* and other invasive plant species have an economic impact because they may be in conflict with other human land uses (Geesingis *et al*., 2004). These species have an influence on the goods and services that may be provided by ecosystems needed by humans. Alien invasive tree and shrub species affect important resources needed by humans such as water availability, food security and reduce grazing lands (Admasu, 2008). Food productivity and availability for the consumption of humans and livestock is negatively affected by invasive alien species (Richardson and Van Wilgen, 2004). This takes place when grazing land is invaded. This reduces grazing potential and reduces indigenous species (Richardson and Van Wilgen, 2004).

Haji and Mohammed (2013) conducted a study aimed at evaluating the impacts of *Prosopis juliflora* on rural communities in Dire Dawa Administration, Ethiopia. The study assessed the income generated from livestock and crop production in households that are invaded by *Prosopis* and the households that are not invaded. A comparative assessment was done using a propensity matching technique which was developed by Rosenbaum and Rubin (Rosenbaum and Rubin, 1983; Haji and Mohammed, 2013). Out of the 155 households that were randomly sampled, 98% of the respondents had experience with *Prosopis* in the last 5-7 years. The findings showed that in invaded agropastoral households, approximately 59% of the respondents perceived *Prosopis* as a detrimental and undesired plant. The remaining 35% stated the plant was both beneficial and destructive with only 5% of respondents finding it beneficial. The main effects that the respondents observed were the decrease in the availability of grazing land and fodder (60%), reduced ground water levels (9%), the loss of biodiversity (7%) and threat to health such as poisonous thorn and allergic reactions (9%).The respondents mentioned that grass species in their communities have declined, resulting in their cattle suffering and decreased fodder. This resulted in an increased pressure in available pastures, leading

to conflict with other neighbouring pastoral and agropastoral communities (Haji and Mohammed, 2013).

Invasion by alien invasive species also affects the tourism sector (Pejchar and Mooney, 2009). South Africa has a unique plant and animal diversity. If alien invasive species continue to displace native species, this will threaten this unique biodiversity and therefore result in financial losses for the country due to the negative impacts these species have on the natural ecosystem (Richardson and Van Wilgen, 2004). Invasive species such as *Prosopis* are also health risks for humans and livestock. These species have thorns which may physically harm humans and animals (Richardson and Van Wilgen, 2004).

## 2.5 South African Legislation Relating to Alien Invasive Species

Section 64 of The National Environmental Management: Biodiversity Act (NEMBA), 2004, aims to prevent the unauthorized introduction and spread of alien invasive species, to manage and control these species, and to reduce harm that may cause to the environment and biodiversity. The Act also aims to formulate strategies to eradicate alien invasive species. Section 67 of this Act compels the SKA SA as an organ of state to prepare an invasive species monitoring, control and eradication plan for land under their control, as part of their environmental plans in accordance with section 11 of the National Environmental Management Act. Out of the four categories of Invasive Alien Plans listed in the NEMBA Alien and Invasive Species Regulations (2004), *Prosopis* species have been declared as Category 2 invaders under the Act and its regulations. This means that *Prosopis* and other species such as *Eucalytus grandis, Ricinus communis, Psidium guajava, Acacoa mearnsii* and *Leucaena leucocephala* have a commercial or utility value. These are species that may be used for economic purposes that are of benefits to humans such as providing timber, animal fodder etc. These species are permitted in demarcated areas under controlled conditions and in controlled areas. They are however not permitted within 30m of the 1:50 year flood line of a watercourse unless authorized by the Department of Water and Sanitation. This law has not been implemented in many parts of the country as most areas that are invaded are privately owned and landowners are not taking responsibility. The Conservation of Agricultural Resources Act, 1983, (Act No.43 of 1983) is another act that aims to reduce the spread of invasive alien species. This act states that landowners are responsible for the clearing of invasive species on their property, but owners do not comply, resulting in more challenges to reduce the spread.

The South African government has initiated programmes that will assist with the fight against invasive alien species. The largest programme is the Working for Water Programme. The *Working for Water Programme* is a government programme that is aimed at controlling and reducing invasive alien species. This programme was established in 1995 and is currently administrated by the Department of Environmental Affairs.

## 2.6 Remote Sensing Techniques for Invasive Control

Remote sensing and GIS has been identified by a number of researchers as being a useful tool for mapping and monitoring invasive alien species and factors that facilitate their dispersal (Joshi *et al*., 2004;Amboka and Ngigi, 2015). Due to this technology's ability to collect information in large, complex and inaccessible areas, a number of environmentalists, policy makers and resource managers have been able to analyze the colonization and spread of invasive alien species (Van Klinken and Robinson, 2007). Remote sensing techniques provide a wide range of sensors which consists of a variety of resolutions which allow for a number of vegetation analyses to take place. Landscape mapping is necessary for understanding the colonization processes, quantifying impacts and establishing on ground management policies (Van Klinken and Robinson, 2007). The variety of sensors available, with different characteristics and abilities, has provided the potential for remote sensing data to detect a number of forms of invasive species all over the world (Amboka and Ngigi, 2015). Remote sensing is a non-destructive way of assessing vegetation distribution and allows for the quantification of such resources in inaccessible and complex terrains (Mirk and Ansley, 2012).

### 2.6.1 *Prosopis* mapping in Africa

The use of remotely sensed data for detecting *Prosopis* species has been used widely by a number of researchers in Africa (Van den Berg *et al*., 2013; Wakie *et al*., 2014; Abdou *et al*., 2016; Mureriwa *et al*.,2016; Meroni *et al*., 2017; Ng *et al*., 2017). This includes the use of aerial photographs, multispectral scanners, and ground based spectrometer instruments (Amboka and Ngigi, 2015). The use of multispectral sensors was done by Van den Berg *et al*. (2013), Wakie *et al*. (2014), Abdou *et al*. (2016), Meroni *et al*. (2017) and Ng *et al*. (2017), where Landsat and Moderate Resolution Imaging Spectroradiometer (MODIS) multispectral sensors were utilized to delineate *Prosopis* in South Africa, Ethiopia, Niger, Somalia and Kenya respectively. Mureriwa *et al*. (2016) recently used *in situ* spectroscopy data to delineate *Prosopis* and discriminate these species from other vegetation within the semi-arid region of the Northern Cape, South Africa. These spatial information technologies have been successful for a number of years in mapping the distribution of natural resources (Van Klinken and Robinson, 2007).

Multispectral sensors that have been used in past alien invasive plant species studies include Landsat, Satellite Pour l'Observation de la Terre (SPOT) and MODIS products (Joshi *et al*., 2004; Van den Berg *et al.*, 2013; Wakie *et al.*, 2014). These sensors provided satellite imagery that had a spatial resolution of 30 m, 20 m and 250 m respectively and have not been considered useful for mapping at species level, unless the stand of these species is large (Joshi *et al.*, 2004). Van den Berg *et al*. (2013) utilized MODIS and Landsat to delineate areas in the Northern Cape Province susceptible to *Prosopis* invasion in the future, quantify the current extent and densities of invasion, and to describe the spatial dynamics of these species in the province. Field observations were also conducted to record information such as tree height, density, terrain and other dominant species and soil properties (soil colour, clay content and limestone availability) (Van den Berg *et al.*, 2013). Other datasets that were utilized include the NASA Shuttle Radar Topography Mission (SRTM) Digital Elevation Model (DEM) and environmental ancillary data (Van den Berg *et al.*, 2013). Wakie *et al*. (2014) conducted a similar study whereby the current and potential distribution of *Prosopis* was mapped for the Afar region of Ethiopia. Wakie *et al*. (2014) not only used DEMs and MODIS satellite images, but also included climate predictors to delineate areas susceptible to *Prosopis* invasion. The two studies used the same sensor but had different data analysis methods with Wakie *et al*. (2014) using the maximum entropy modelling software and Van den Berg *et al*. (2013) using ArcGIS 9.3.2 Model Builder. The studies were able to delineate current *Prosopis* distribution. They were also able to predict potential areas for future invasion both using MODIS images in different African countries. Even though the studies successfully delineated *Prosopis*, there were a number of shortfalls and limitations which may have affected the quality of their final products. MODIS and Landsat have a moderate to low spatial resolution. Spatial resolution may be described as a measure of the smallest feature that can be observed on an image (Kerle *et al.,* 2004). The lower the spatial resolution, the limited number of small features one can observe. Images with a low resolution provide limited information therefore affecting the kind of detail one may obtain (Van den Berg *et al.*, 2013). They may also allow for inaccurate classification as pixels may consist of multiple land cover or vegetation types.

Hoshino *et al*. (2012) utilized Landsat imagery to map *Prosopis* in Sudan. Landsat has been utilized since it was launched in 1972 and has allowed researchers to assess land cover change effectively. Hoshino *et al*. (2012) and Van den Berg *et al*. (2013) used this sensor to map the then current distribution of *Prosopis.* Both of these studies used the Near Infrared/Red band ratio to discriminate *Prosopis* from other vegetation (Hoshino *et al*., 2012; Van den Berg *et al*., 2013). This band ratio was used on images selected from the growing season with the assumption that *Prosopis* is the greenest

plant than other vegetation and that *Prosopis* will be the only plant species that will be detected. This resulted in other tree species being detected, making the discrimination of *Prosopis* to other vegetation not being achieved completely. The confusion of *Prosopis* with other trees was analysed by Meroni *et al*. (2017) when their study aimed to evaluate the spectral signature of *Prosopis* with other natural vegetation present in their area of interest. This study revealed the importance of using spectral information as this has an impact on the outcome of one's study. It was observed that healthy *Acacia* spp and some of the driest *Prosopis* had similar spectral signatures (Meroni *et al*., 2017). This may result in these tree species being confused, therefore affecting the accuracy of the classification even during dry seasons where *Prosopis* is observed to be healthier and greener than other indigenous trees (Meroni *et al*., 2017).

Recent developments in remote sensing technology have the potential to enable improved accuracy in mapping invasive plant species and their characteristics (Joshi *et al.*, 2004). These developments include sensors such as WorldView-3, IKONOS, RapidEye and Sentinel-2 that have a higher spatial and spectral resolution (Malahlela *et al.*, 2014). Such sensors address the spatial resolution problem as they have higher spatial resolution and accuracy which makes it suitable for the study as it allows for a variety of features to be easily identified (Malahlela *et al*., 2014). Ng *et al*. (2017) assessed the potential of Sentinel-2B and Pléiades 1A to detect *Prosopis* and *Vachellia* spp around Lake Baringo in Kenya and to estimate the areas covered. These sensors have a spatial resolution of 10 m and 2 m respectively. The study concluded that the accuracy of the delineation of *Prosopis* and *Vachellia* was higher in the image with the higher spatial resolution, which was the Pléiades sensor, with a 2 m resolution. The high resolution Pleiades image was able to detect small habitat patches that the Sentinel-2B 10 m resolution sensor missed (Boyle *et al*., 2014; Ng *et al*., 2017). Shrubs and single trees were sometimes not detected by Sentinel-2 as they were too small (Ng *et al*., 2017). High resolution satellite images assist in detecting narrow, linear features such as riparian corridors (Boyle *et al*., 2014). When one attempts to detect *Prosopis* species, such satellite imagery will be beneficial due to the nature of the species and its establishment in riparian habitats. These sensors also have spectral characteristics that improve vegetation cover mapping. WorldView-3, RapidEye and Sentinel-2 satellite consists of new bands such as the red edge band which provide additional sources of information on vegetation analysis and discrimination (Mahlahlela *et al*., 2014).

The spectral resolution of the Sentinel-2 and Pléiades sensors played a noticeable role in the classification results of *Prosopis* and *Vachellia* spp. Pléiades 1A has four multispectral bands with a resolution of 2 m (red, green, blue and near infrared) and one panchromatic band with a resolution of

0.5 m. Sentinel-2B has a total of 13 spectral bands with four 1 m multispectral (MS) bands (red, blue, green and near infrared bands), 20 m red edge 1-3, near infrared-2, short wave infrared 1 and 2 bands and 3 atmospheric correction bands (retrieval of aerosol, water vapour, cirrus) (Ngi *et al*., 2017). The Out-of-Bag accuracy was used as a measure for assessing and validating the results. The higher spectral resolution of Sentinel-2B was able to partly compensate for the lower spatial resolution. This is evident in Sentinel-2 receiving an equal or better Out-of-Bag result in some vegetation classes classified as the additional spectral bands contributed to the improved delineation and differentiation of vegetation type and cover (Ngi *et al*., 2017). Figure 2 is the land cover classifications around Lake Baringo in Kenya; with image A being the land cover classification conducted using the Pléiades sensor and image B being the land cover classification created using Sentinel-2 imagery.

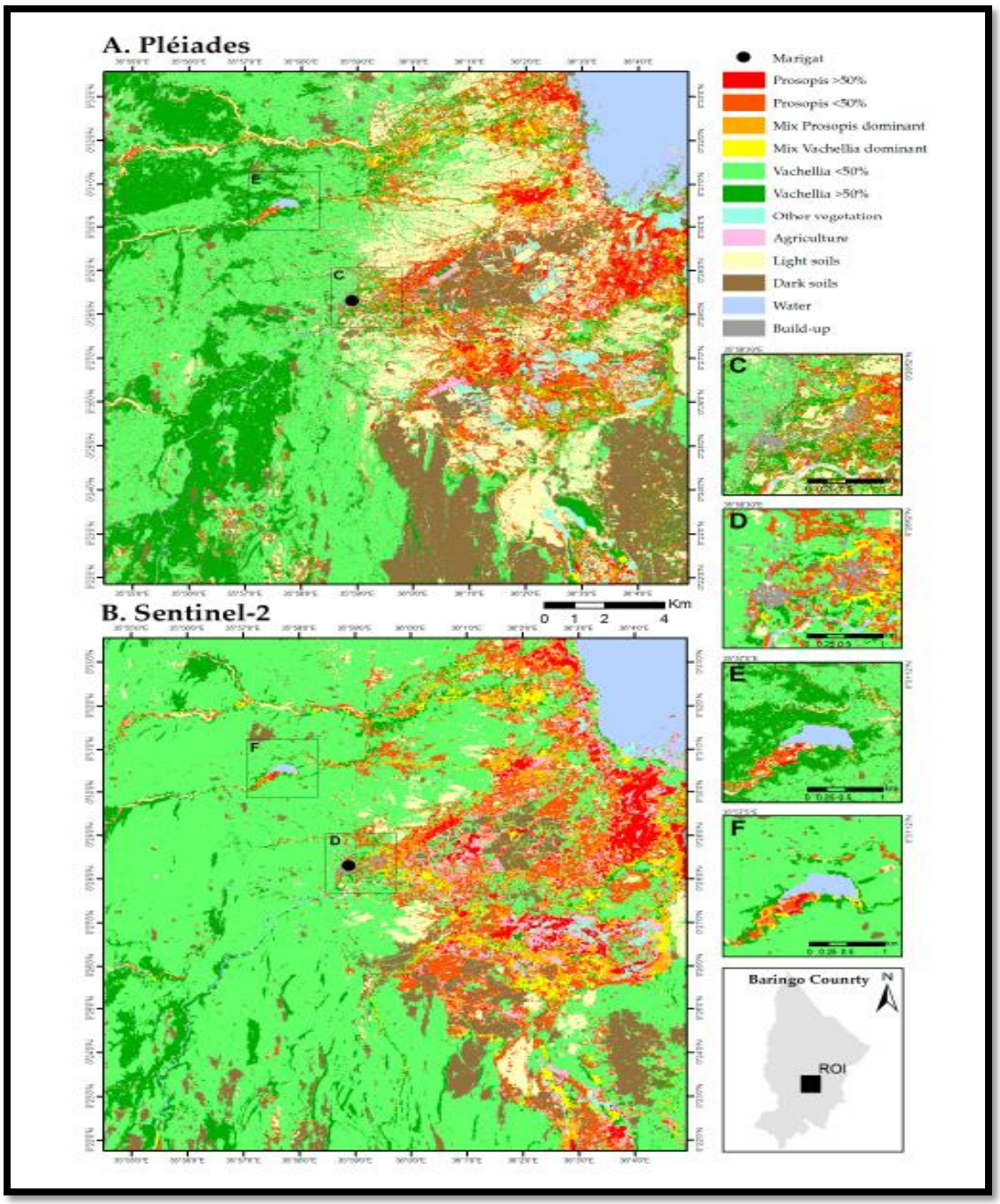



**Figure 2. Land cover classification results: (A) Pleiades, (B) Senitinel-2 in the urban area of Marigat. Pleiades had a higher accuracy in mapping for Prosopis and Vachellia as the sensor has an improved capacity to detect the location of smaller features (Ng *et al*., 2017)**

The spatial and spectral characteristics of high resolution satellite images make it a potentially useful tool for vegetation characterization but their availability and cost are one of the issues one may faces when attempting to uses them (Boyle *et* al., 2014; Ngi *et al*., 2017). High resolution sensors such as WorldView have limited dates as they were established in the 2000s whereas moderate resolution sensors such as Landsat have long term time series data which allow for long term monitoring (Boyle *et al*., 2014).

### 2.6.2 Predictive Modelling

A number of studies have used GIS and modelling algorithms to predict potential areas likely to be invaded by invasive alien species (Wakie *et al*., 2014; Abdou *et al*., 2016; West *et al*., 2016). Predictive modelling of *Prosopis* is essential in order to establish effective monitoring and controlling strategies of these species. The most commonly used species distribution model (SDM) is the maximum entropy model, which is commonly known as Maxent (West *et al*., 2016). The Maxent model is a machine learning and statistical method which relates known locations of a species (presence-only data) with the environmental conditions of these locations to predict the potential geographical locations of a species (Fourade *et al*., 2014). Maximum entropy models have been used more frequently in predicting species distribution due to its ability to work with limited data which can be presence only data (Elith *et al*., 2011). Presence point data also known as occurrence points and training data may be described as the species georeferenced locations which describe the species distribution (Kuloba *et al*., 2015). Another important advantage is that the Maxent models allows for the use of environmental data, which is useful when presence data are limited. Through the use of presence data and environmental data, the Maxent model can attempt to identify the environmental conditions that are associated with the occurrence of *Prosopis*. Wakie *et al*. (2014) and Abdou *et al*. (2016) utilized the Maxent model to predict potential *Prosopis* invasion areas in Ethiopia and Niger respectively. Both Wakie *et al*. (2014) and Abdou *et* al. (2016) used climate variables to predict the potential distribution of *Prosopis*, with Wakie *et al*. (2014) including slope and elevation datasets. Both studies were able to successfully produce good predictions as the model area under curve (AUC) were 0.94 and 0.953 respectively, which indicate the models had very good predictions and therefore producing distribution maps with high accuracies (Wakie *et al*., 2014; Abdou *et al*., 2016; West *et al*., 2016). One of the limitations of using Maxent is that it needs a high computational power. It is difficult to deal with it computationally. Another limitation of using Maxent it is mostly considered as a black box-style modelling environment with new and underdeveloped statistics (Pollock, 2015).

This research utilized the IDRISI Land Change Modeller (LCM), which is an integrated software environment used for analyzing and predicting land cover and land use change (LULCC) (Mishra *et al*., 2014; Megahed *et al*., 2015). The LCM has been successfully utilized to predict land cover and land use changes in studies conducted by Mishra *et al*. (2014), Roy *et al*. (2014) and Megahed *et al.* (2015) to predict change in India, France and Egypt respectively. There are four main procedures in the LCM; which are the change detection analysis, transition potential modelling, change prediction, and model validation. The change detection analysis analyzes land cover changes between two different times (Mishra *et al*., 2014; Megahed *et al*., 2015; Eastman, 2016). These changes are illustrated in the form of graphs and maps. The transition potential modelling procedure is responsible for determining the

locations of potential change through the creation of transition potential maps (Mishra *et al*., 2014; Megahed *et al*., 2015; Eastman, 2016). The LCM then utilizes change rates calculated from the change detection analysis, as well as the created transition potential maps and Markov Chain analysis to predict future land cover land use classes (Mishra *et al*., 2014; Megahed *et al*., 2015; Eastman, 2016). The LCM uses the Markov Chain model matrix to quantify the change and the spatial distribution of change is given by the Multi-Layered Perceptron (Mishra *et al*., 2014; Megahed *et al*., 2015; Eastman, 2016). To assess the quality of the model predictions, the validation procedure needs to be conducted. There are two approaches used to validate a model; namely the statistical approach and the visual approach. The statistical approach includes the calculation of Kappa accuracy indices. The visual approach includes the cross tabulation between the created prediction map and the map in reality to illustrate the accuracy of the model results (Roy *et al*., 2014; Eastman, 2016).

# 3. Materials and Methods

## 3.1 Study Area

The SKA site is located in the Northern Cape Province, South Africa. The study area consists of two farms, namely Losberg Farm and Meysdam Farm, which together have an area of approximately 135 $km^2$.The two farms are situated across two local municipalities which are Kareeberg Local Municipality and Karoo-Hoogland Local Municipality. The study area is situated approximately 85 km southeast of Carnarvon, 147 km northwest of Brandvlei and 100 km south west of Williston (Figure 3).

The Northern Cape climate may be described as arid and semi-arid. The province is considered to be the driest province in South Africa with an average annual rainfall of approximately 200 mm. The Northern Cape is hot and dry, with its evaporation levels being higher than the annual rainfall. The summers are hot with temperatures often reaching $40^oC$ in most parts of the province. Winter day temperatures are mild with a temperature of approximately $22^oC$, with night temperatures dropping to below $0^oC$. The annual rainfall in Brandvlei (100 km away from SKA) is 127 mm and in Carnarvon (80 km away from SKA) is 209 mm. The peak rainfall season throughout the area is late summer to autumn (February to April).

The Orange River with its tributaries is the main surface water resource in the Northern Cape. Groundwater is an important water resource to a large rural population for domestic and agricultural use. This source of water is essential for communities that are far from rivers.

Most of the vegetation in the study area is classified as Bushmanland Nama Karoo of the Karoo Biome. The vegetation types are Bushmanland Basin Shrubland and Upper Karoo Hardevel (Hoffman, 1996; Mucina and Rutherford, 2004).

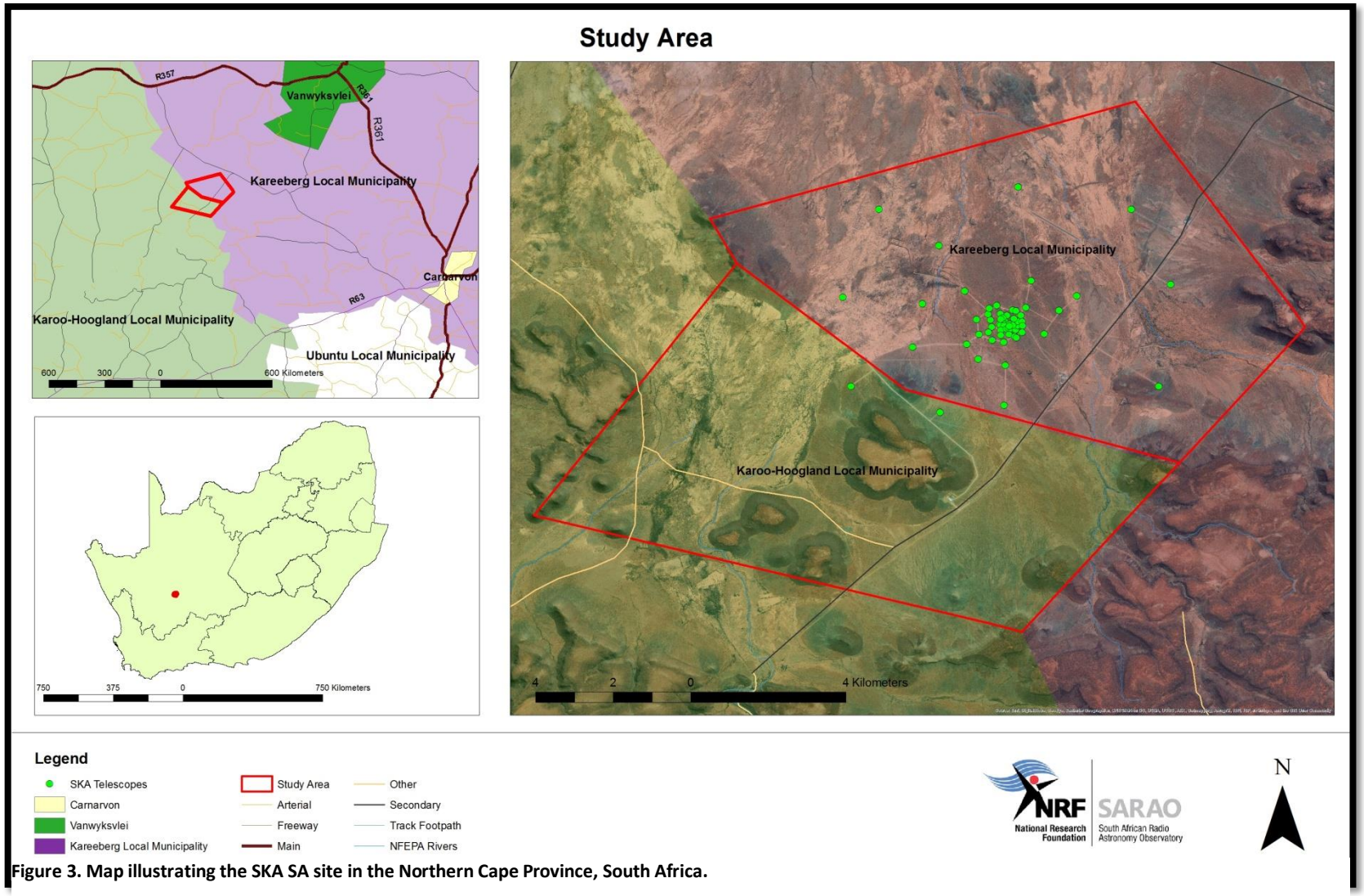



**Figure 3. Map illustrating the SKA SA site in the Northern Cape Province, South Africa.**

## 3.2 Data Acquisition

### 3.2.1 Satellite Data

Cloud free Worldview-3 and Landsat satellite images were used in this study. To delineate *Prosopis* species accurately, a number of sensor specifications were evaluated. These include the sensors spatial, spectral and radiometric resolutions. These determine the quality and quantity of information one may obtain from the different satellite images.

**WorldView-3**

A 2016 WorldView-3 satellite image was used to delineate the current distribution of *Prosopis* in the study area. This satellite was selected as a result of its high spectral and spatial resolution. High resolution images allow for more accurate delineation and quantification of the feature analysed. In Table 1, the WorldView-3 specifications are presented. This sensor has a spatial resolution of 1.24 m. WorldView images allow for the mapping of small, linear features such as riparian corridors (Boyle *et al*., 2014). These areas are difficult to detect with lower resolution satellite images. *Prosopis* species are found in areas along water sources making the choice of using WorldView-3 more suitable. WorldView-3 has 8 spectral bands which include 4 standard bands (red, green, blue, NIR-1) and 4 additional new bands (yellow, NIR-2, coastal blue and red-edge) (Table 1). The new bands allow for enhanced vegetation analysis and delineation (Malahlela *et al*., 2015).

**Table 1. Worldview 3 sensor specifications**

| **Launch Date** | 13 August 2014 | |
|---|---|---|
| **Spectral Resolution** | **Bands** | **Spatial Resolution** |
| | Panchromatic (450-800 nm) | 0.31 m |
| | Coastal (400-450 nm), | 1.24 m |
| | Red (626 - 696 nm), | |
| | Blue (450 - 510 nm), | |
| | Red Edge (630 - 769 nm), | |
| | Green (510 - 580 nm), | |
| | Near-IR1(770 - 895 nm), | |
| | Yellow (585 - 625 nm), | |
| | Near-IR2 (860 - 1040 nm) | |
| **Temporal Resolution** | <1 day | |

(https://www.digitalglobe.com/)

**Data selection**

Spectral characteristics and image resolution are not the only variables that must be considered when one is about to acquire remotely sensed data and analyse *Prosopis* distributions (Joshi et al., 2004). It is ideal that one gets imagery that is captured during the peak time of plant activity (Van den Berg et al., 2013). This means one must have an understanding of phenological processes of *Prosopis*. Meroni et al. (2017) assessed the spectral signature of *Prosopis* species and indigenous trees. The study revealed that *Prosopis* has a different spectral signature which is more distinct during drier seasons. In the Northern Cape, Van den Berg et al. (2013) concluded that the best imagery to obtain must be captured in February to May, therefore confirming that the date in which satellite images were captured is important in order for one to discriminate *Prosopis* accurately without confusing it with other vegetation in the study area. The Worldview-3 imagery available within the preferred period (February – May) was captured on the 1st and 7th of April 2016. These two scenes were mosaicked.

**Landsat 5 and Landsat 8 OLI/TIRS**

Landsat satellite images from the years 2003, 2008, 2013 and 2017 were used for the LULC change detection and to predict future land cover changes. The satellite images used for the years 2003 and 2008 were acquired from the Landsat 5 sensor. The Landsat 5 mission was launched with a Thematic Mapper (TM) on the 1 March 1984. Landsat 5 TM has seven spectral bands, with a spatial resolution of 30 m (six reflective bands) and 120 m (thermal band) (Chander *et al*., 2007).

The satellite images used for the years 2013 and 2017 were acquired from the Landsat 8 sensor. The Landsat 8 satellite was launched on the 11 February 2013 with two sensors, the Operational Land Imager (OLI) and the Thermal Infrared sensor (TIRS). Landsat 8 sensor specifications are presented on Table 2. Landsat 8 consists of 11 spectral bands. The OLI consists of eight bands with a spatial resolution of 30 m, one panchromatic band with a resolution of 15 m (Skakun *et al*., 2016).

This sensor was selected as it is one of the few moderate resolution sensors that have images that date back to the early 2000s. This sensor is ideal for land use land cover change analysis as it has been collecting images of the earth's surface since 1972 and has great historical archives (Ma and Xu, 2010). Table 2 states the Landsat sensors' specifications.

**Table 2. Landsat 5 ETM and Landsat 8 sensor specifications**

| Sensor | Landsat 5TM | Landsat 8 OLI/TIR |
|---|---|---|
| **Launch Information** | 1 March 1984 | 11 February 2013 |
| **Sensor Bands(µm)** | Band 1 (30 m) 0.45-0.52 µm<br>Band 2 (30 m) 0.52-0.60 µm<br>Band 3 (30 m) 0.63-0.69 µm<br>Band 4 (30 m) 0.76-0.90 µm<br>Band 5 (30 m) 1.55-1.75 µm<br>Band 6 (120*30 m) 10.40-12.50 µm<br>Band 7 (30 m) 2.08-2.35 µm | Band 1 (30 m)0.435 - 0.451 µm<br>Band 2 (30m)0.452 - 0.512 µm<br>Band 3 (30m)0.533 - 0.590 µm<br>Band 4 (30m)0.636- 0.673 µm<br>Band5 (30m) 0.851 - 0.879 µm<br>Band6 (30 m) 1.566 - 1.651 µm<br>Band 7 (30 m) 2.107 - 2.294 µm<br>Band 8 (15 m) 0.503 - 0.676 µm<br>Band 9 (30 m) 1.363 - 1.384 µm<br>Band 10 (100m) 10.60-11.19 µm<br>Band 11 (100m) 11.50-12.51 µm |
| **Temporal Resolution** | 16 days | 16 days |
| **Sensor Resolution** | 30 m<br>Pan 15 m | 30m<br>Pan 15m |
| **Image Acquisition date & Image ID** | 24/09/2008<br>LT05_L1TP_174081_20080924_20161029_01<br><br>14/11/2003<br>LT05_L1TP_174081_20031114_20161203_01 | 22/09/2013<br>LC08_L1TP_174081_20130922_20170502_01<br><br>17/09/2017<br>LC08_L1TP_174081_20170917_20170929_01 |
| **Path & Row** | Path 174; Row 81 | Path 174; Row 81 |

(https://landsat.usgs.gov/)

### 3.2.2 Digital Elevation Model

A Shuttle Radar Topography Mission (SRTM) digital elevation model (DEM) was used to analyse the terrain and flow paths of the study area. A DEM carries vital elevation information in raster format that can be used in various hydrologic and geomorphologic studies (Hancock *et al*., 2006). The SRTM was launched on the 11 February 2000. This mission was as a result of a collaborative effort by the National Aeronautics and Space Administration (NASA), the National Imagery and Mapping Agency (NIMA), the German space agency and Italian space agency (Hancock *et al*., 2006). The SRTM DEM has a spatial resolution of approximately 30 m (1 arc-second).

*Prosopis* species are mainly located in low lying areas and areas close to a water source. The DEM was used to delineate and extract drainage lines using the ArcGIS Hydro tool. The ArcGIS Hydro tool uses a DEM to automatically model the flow of water across a surface (Yang *et al*., 2010). The 30 m SRTM DEM was used to delineate drainage lines to the study area.

The DEM was also used to analyse the terrain of the study area by creating a slope and elevation map. Analysing the terrain was essential as *Prosopis* species have been observed to be located in specific

terrains, mostly low lying areas. The created drainage lines, slope and elevation maps were used to model the 2017 and 2022 land cover land use.

## 3.3 Field Survey

Field surveys in the study area were conducted from 26 September-4 October 2017 and 1-3 November 2017. These surveys were conducted to collect ground reference data used for image classification (training) and the accuracy assessment. The sampling strategy that was used to collect this information was the Stratified Random Sampling technique, which has been considered as one of the most convenient and effective techniques (Liu *et al*., 2010). A WorldView-3 false colour composite image was used to locate *Prosopis* and other land cover types. More ground reference points were taken from low lying areas and along drainage lines as *Prosopis* has been observed to be situated in areas with these environmental conditions. The benefits of utilizing stratified random sampling are not only limited to cost efficiency, but it also allows for groups to be assessed differently as the desired precision is not the same for all groups (Köhl *et al.*, 2006; Liu *et al*., 2010).

A total of 573 field data points were collected using the Garmin Montana 680 handheld GPS and high aerial photographs. *Prosopis* and other land cover types were recorded including tree species, location (longitude, latitude and altitude), tree height, number of stems, a description of the surrounding landscape, and canopy density. Four canopy density classes were identified during the field survey. These density classes were closed, medium, moderate and sparse density. The GPS points collected during the field survey were also overlaid on a high resolution satellite imagery to evaluate the density classes recorded during the field work for verification. Figure 4 illustrates the density categories identified.

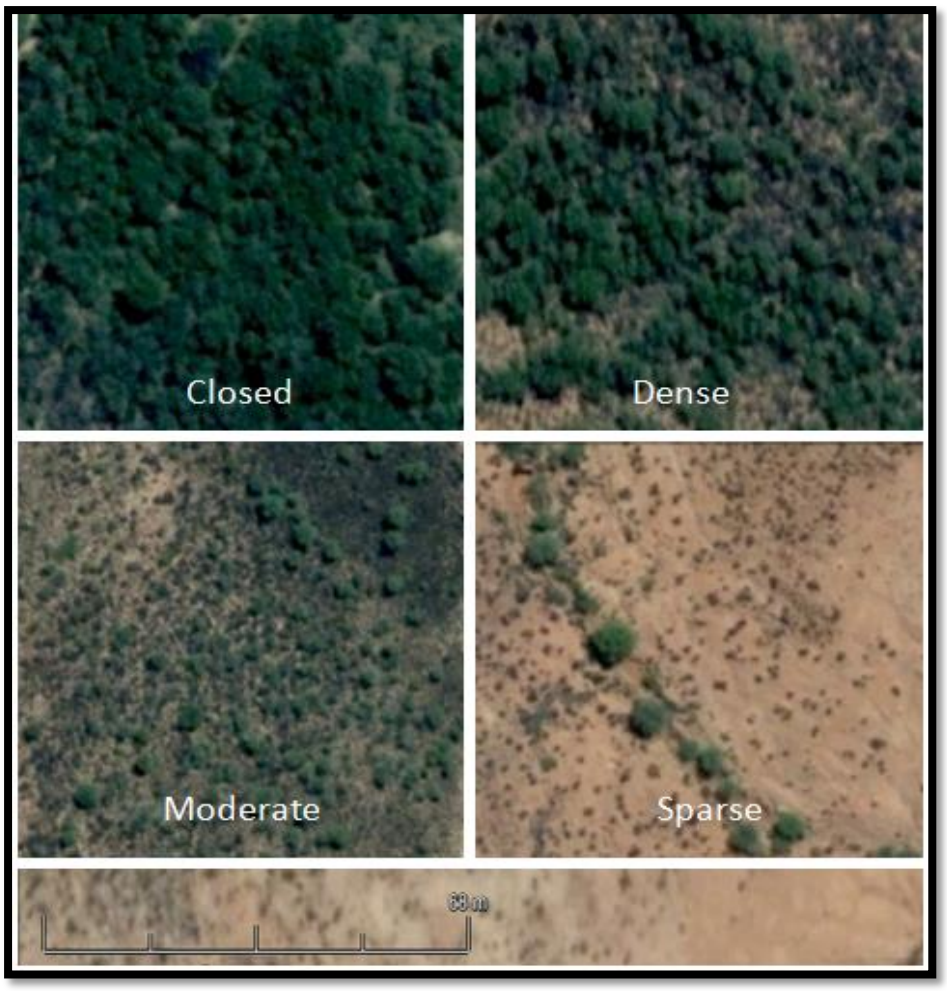



**Figure 4. Example of density categories identified during field survey (scale 66 m)**

Out of the 573 collected ground reference points, 148 were of *Prosopis*. Information collected on these species included their height, number of stems, surrounding terrain, distance from water source and density. Figure 5 is a map illustrating density categories of the ground referenced *Prosopis* sites. The study area consists of mostly dense *Prosopis* populations. Out of the 148 *Prosopis* sites, 26 were of closed density, 55 were dense, 34 were moderate and 33 were sparse. Information on the abundance of *Prosopis* is essential for the control and prevention of these species. When one attempts to implement eradication and conservation strategies, one must have knowledge of the location of these species and their extent (Holdmes *et al*., 2008). This informs the appropriate control and eradication strategies such as establishing priority areas and methods of clearing.High priority areas may include areas with a light*Prosopis* infestation. The clearing of alien invasive plant species in lightly infested areas is essentialto stop the further spread to surrounding areasand limit intensification of these plant species(Holdmes *et al*., 2008). Table 3 illustrates the LULC classes collected with the number of training and test dataset for each class.

**Table 3. LULC classes collected including training and testing dataset**

| Class | Training | Test | Total |
|---|---|---|---|
| Bare rock | 46 | 20 | 66 |
| Bare soil | 59 | 26 | 85 |
| Built-up land | 47 | 21 | 68 |
| Quiver tree | 42 | 18 | 60 |
| *Prosopis* | 103 | 45 | 148 |
| Waterbodies | 44 | 20 | 64 |
| Shrubland | 57 | 25 | 82 |

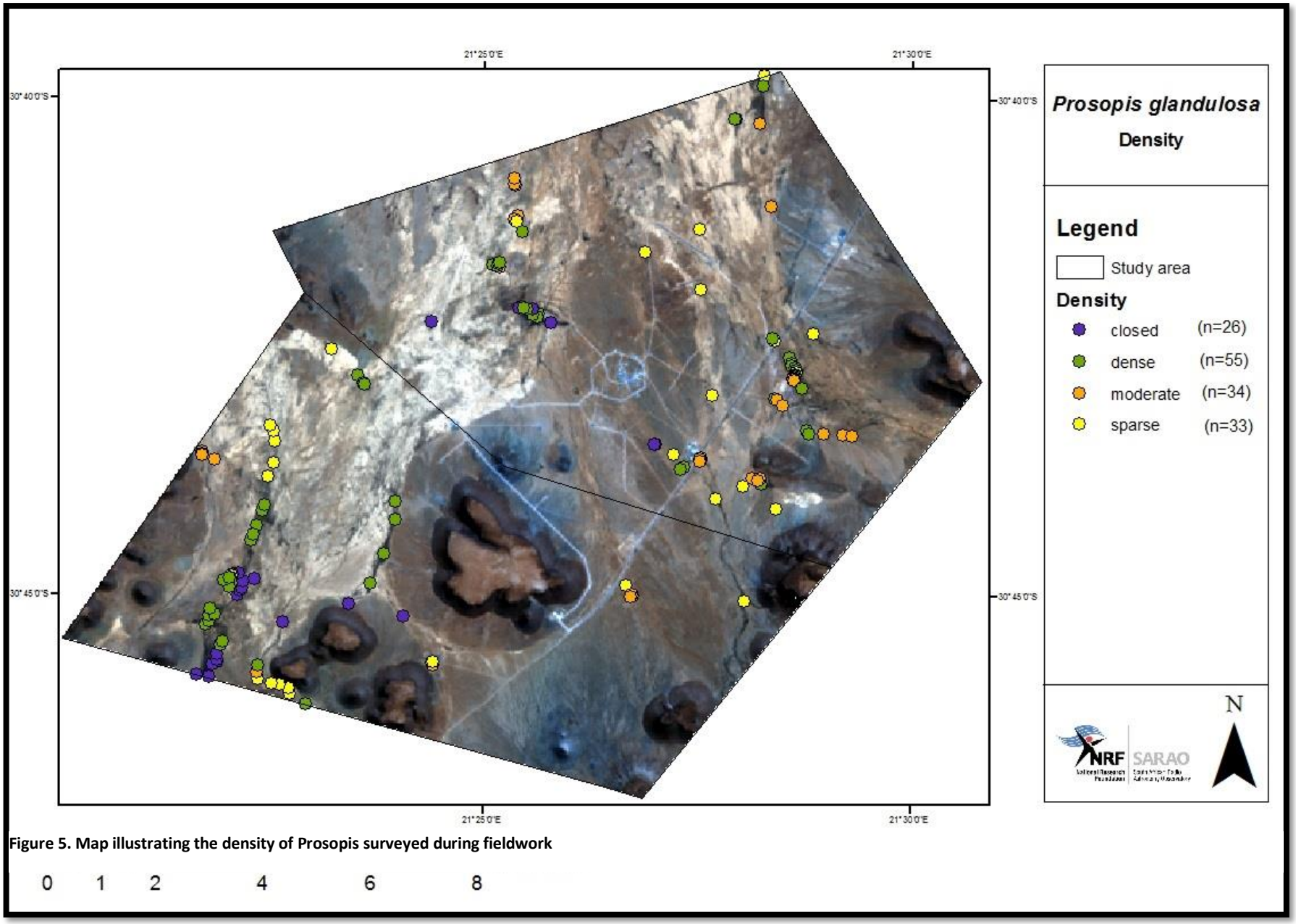



**Figure 5. Map illustrating the density of Prosopis surveyed during fieldwork**

The height of these tree species was also measured. Figure 6 illustrate the varying height of the *Prosopis* species found on site. The scale used was approximately 1 m. Figure 7 is a map illustrating the height of the ground referenced *Prosopis* points. Most of the surveyed species were of a height between 2-4 m.

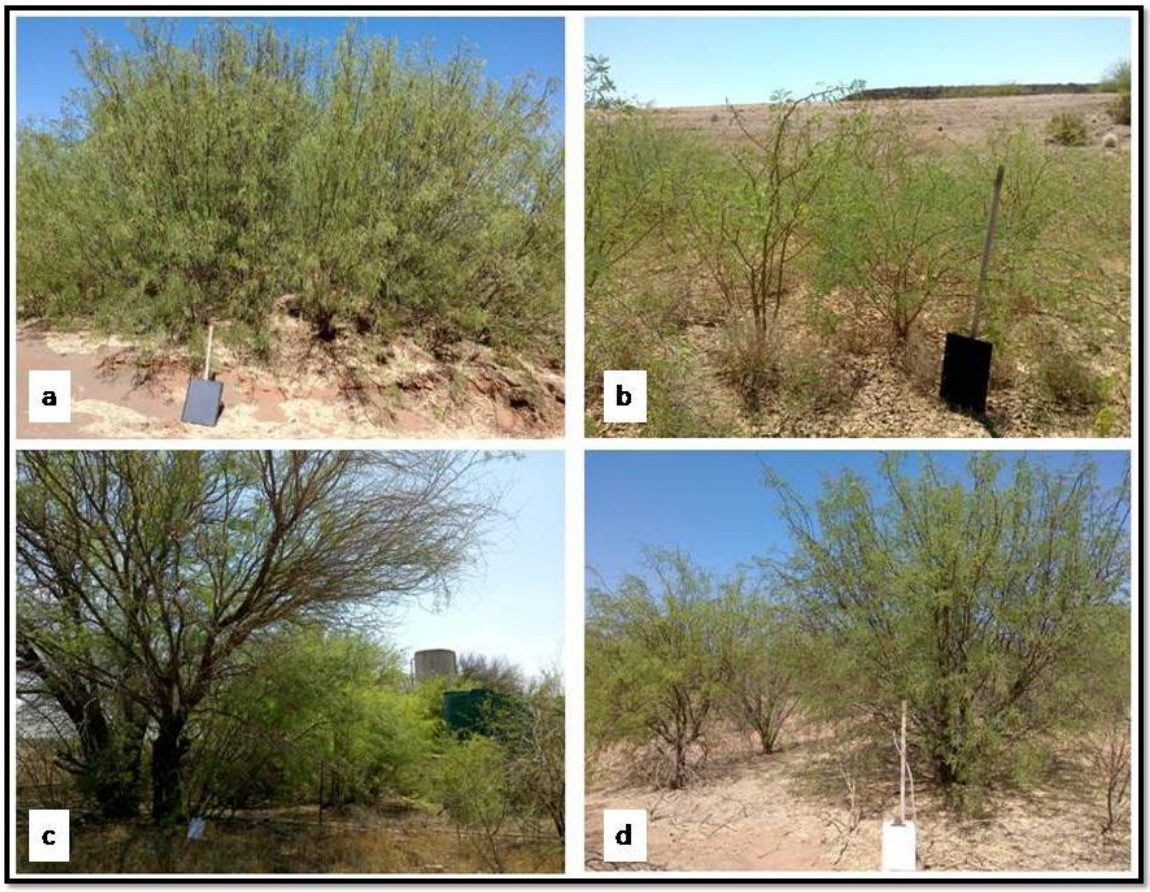



**Figure 6. Images of *Prosopis glandulosa* in the study area. These species are located along watercourses and drainage line (a, b and d) and close to manmade dams and boreholes (d).**

The ground reference data was randomly split and regions of interest (ROIs) were created. In total, 70% of the ground reference points (for each class) were used for training (image classification) and 30% was used to test the accuracy of the classification through conducting an accuracy assessment on ENVI 5.2 software.

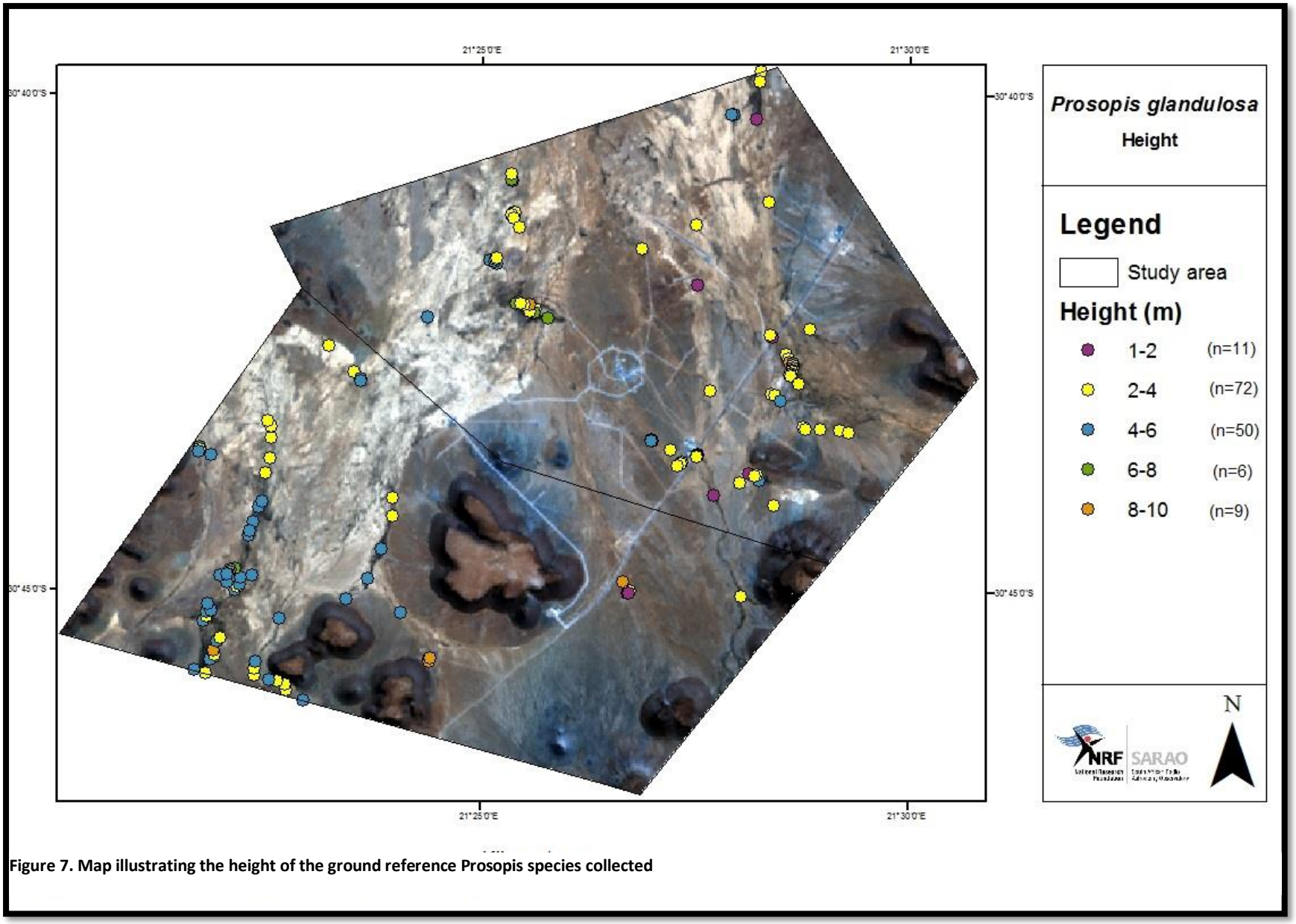



**Figure 7. Map illustrating the height of the ground reference Prosopis species collected**

## 3.4 Pre-processing

This process involves correcting distortions one may find in satellite imagery. Remotely sensed data need to be pre-processed prior to any analysis in order to remove noise and allow for easier interpretation of the satellite imagery (Xie *et al*., 2008).

Maintaining radiometric consistency in satellite images is a challenge as a result of the differences in the calibration or operation of the sensor systems acquiring satellite images, atmospheric conditions, solar angle and sensor view angle (Kerle *et al*., 2004; Chen *et al*., 2005). Due to the distortions that may be caused by the influences mentioned above, radiometric corrections need to be undertaken to create consistent satellite images that are captured under a range of conditions (Kelcey and Lucieer, 2012). Radiometric corrections are undertaken to extract absolute reflectance measurements and reduce the environmental effects (Kelcey and Lucieer, 2012).

To correct geometric distortions, geometric corrections have to be undertaken. This is done by attempting to establish a relationship between the satellite image's coordinate system and the geographic coordinate system. This may be achieved by using ground control points, the calibration data of the sensor and position and altitude when the image was captured (Xie *et al*., 2008).

**WorldView-3 Imagery**

The WorldView-3 satellite imagery was radiometrically and geometrically corrected by the supplier Digital Globe (Updike and Comp, 2010). The WorldView imagery was atmospherically corrected using Fast Line-of-sight Atmospheric Analysis of Hypercubes algorithm (FLAASH). FLAASH is an atmospheric correction tool provided by Environment for Visualizing Images (ENVI) software. WorldView-3 imagery is of high accuracy and greater quality and therefore may be used without any further processing.

**Landsat Images**

The Landsat images were atmospherically corrected using the ENVI 5.2Fast Line-of-sight Atmospheric Analysis of Hypercubes algorithm. Landsat Level-1 images, also known as terrain-corrected images were used in this study. Landsat Level-1 products are precision registered and orthorectified through a systematic process that involves ground control points and a digital elevation model. This means that most of the images provided by Landsat can be used as delivered by the United States Geological Survey (USGS) (Young *et al*., 2017). A visual assessment of all satellite images was conducted to ensure that all of the Landsat images were aligned.

## 3.5 Data Analysis

### 3.5.1 Image Classification of WorldView-3and Landsat Satellite Image

The Worldview-3 and Landsat satellite image was classified using Multi-layer Perceptron (MLP) Neural Network Classifier on ENVI 5.2 software. The MLP is the most commonly used neural network classifier in remote sensing (Mustapha *et al*. 2010). The Neural Network (NN) consists of three layers; namely the input layer, hidden layer and output layer (Petropoulos *et al*., 2010, Ndehedehe *et al*., 2013; Deilmai *et al*., 2014; Azi*et al.*, 2017). The three layers each consist of neural nodes, with all the nodes of a layer being connected to the nodes of the adjacent layers. The interconnection among nodes carries an associated weight and each node computes the weighted sum of the input and passes the sum through an activation function that provides the output value of the node (Manaf *et al*., 2018). The input layer represents the image used (spectral bands used for classification). The hidden layer may be described as the engine room of the neural network as it is used for computation. The output layer consists of the classification results with the generated land cover classes (Ndehedhe *et al*., 2013; Delmai *et al.,* 2014; Manaf *et al.,* 2018).

A number of parameters have to be set before a NN classification can be conducted. These include establishing the training threshold contribution, training rate, training momentum, the training Root Mean Square (RMS) exit criteria field and the number of hidden layers to be used. The training threshold contribution determines the size of the contribution of the inner weight with respect to the activation level of the node and it is used to adjust the changes to a node's internal weight (Petropoulos *et al*., 2010; Ahmadizadeh *et al*., 2014; Aziz *et al*., 2017). The training rate specifies the magnitude of the weight adjustment for the nodes. The training rate has a value between zero and one. A higher rate will improve the speed of training but will also increase the risk of oscillations or non-convergence of the training result (Petropoulos *et al*., 2010; Aziz *et al*., 2017). The training momentum is a parameter used to define the step of training rate and its effect is to encourage weight changes along the current direction (Petropoulos *et al*., 2010). The training RMS exit criteria define the root mean square error value at which the training should stop (Petropoulos *et al*., 2010; Aziz *et al*., 2017). Different quantities of training parameters were under trial and error and the output which provided better results was chosen. The training parameters selected consisted of one hidden layer, a training threshold contribution value of 0.9, training rate value of 0.2, a training momentum value of 0.9 and a training root mean square of 0.1. The training parameters selected in this study have been utilized in a number of studies and they provided the best outputs (Petropoulos *et al*., 2010; Ahmadizadeh *et al*., 2014; Aziz *et al*., 2017).

The classes selected were shrubland, built-up land, waterbodies, *Aloidendron dichotomum* (Quiver tree) and *Prosopis glandulosa*. The classes were selected based on the current land cover land use in

the study area. The class shrubland was selected as majority of the study area's vegetation type is Bushmanland Basin Shrubland, which may be characterized by slightly irregular plains dominated by dwarf shrubland, with succulent shrubs or perennial grasses (Thompson, 1996). The study area was originally a sheep farm but with the establishment of the SKA in the area, there have been buildings and other man-made structures constructed. These include telescopes, offices and roads. *Prosopis glandulosa* is by far the most dominant vegetation in the study area and there are populations of *Aloidendron dichotomum* in some of the hills. The study area also consists of numerous streams and man-made-dams. Figure 8 is a flow chart illustrating the steps followed to classify the 2016 Worldview image using a NN classification.

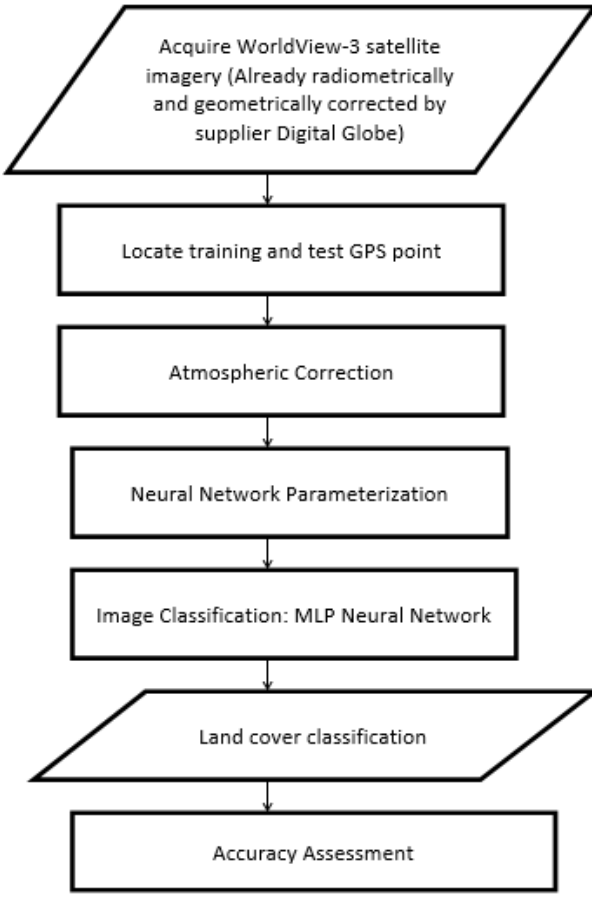



**Figure 8. Flowchart illustrating the processes followed when classifying the high resolution WorldView 3 image**

After the image classification, an accuracy assessment was conducted. This was done to compare the classified land cover map with the ground-truth data to evaluate how well the classification represented the real world. This process was performed by creating a Confusion Matrix table in ENVI 5.2 software. This process compares on a class by class basis the relationship between the ground truth data and the classified image and does so by computing the overall accuracy, producer accuracy

and user accuracy (Congalton, 1991). The overall accuracy is computed by dividing the total number pixels classified correctly by the total number of reference pixels. The producer accuracy (omission error) is calculated by dividing the total number of correctly classified pixels in each class by the total number of reference data pixels known to be of that class (Congalton, 1991). The user accuracy (commission error) is calculated by dividing the total number of correctly classified pixels in each class by the total number of pixels that were classifies in that class. This method of assessing accuracy is efficient as it represents the accuracies of each class and states the errors of inclusion and errors of exclusion (Congalton, 1991). In addition, the Kappa coefficient was calculated. This measures the extent of the classification accuracy (Butt *et al*., 2015). The Kappa coefficient measures the agreement between the classified image and the reference data pixels. A kappa value of 0 represents no agreement whereas a kappa value of 1 represents a perfect agreement (Butt *et al*., 2015). In total, 30% of the collected ground reference data was used to test the accuracy of the image classification.

### 3.5.2 Land Use Land Cover Change detection

Aland use land cover change detection analysis was conducted using Landsat satellite images, which were classified using the neural network algorithm. The training and test data was collected using high resolution aerial photographs. In total, 70% of the data was used for training, while the 30% was used for testing (accuracy assessment). The image classification and accuracy assessment were conducted in the ENVI 5.2 software. Table 4 presents the LULC classes used in Landsat classification, showing the training and testing data.

The change analysis was conducted on the IDRISI software. The IDRISI land cover land use change module provides a fast assessment of the quantitative changes of each land cover class (Eastman, 2016). This analysis is conducted by assessing change between times 1 and time 2 land cover maps. Change results are then illustrated in the form of graphs and maps, which present the gains and losses by each land cover class. Other variables calculated by this procedure include the net change and the contribution to change experienced by each land cover class (Mishra *et al*., 2014; Eastman, 2016). Figure 9 illustrates the processes followed to conduct the land cover change detection analysis.

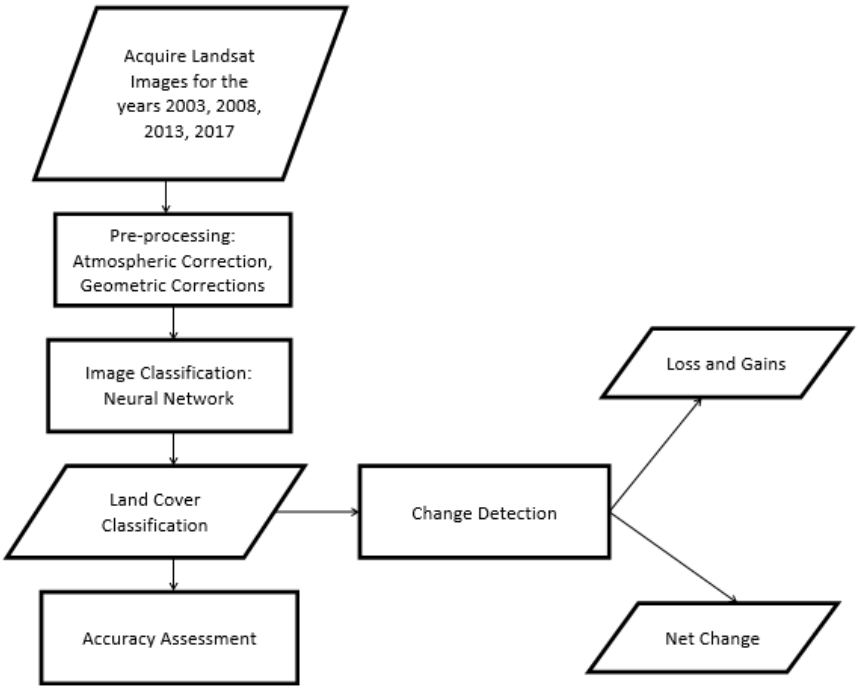



**Figure 9. Flowchart illustrating the processes followed when conducting the land use land cover change detection**

**Table 4. LULC classes showing the test and training data**

| **2003** | | | |
|---|---|---|---|
| **Class** | **Training** | **Test** | **Total** |
| Shrubland | 47 | 20 | 68 |
| Waterbodies | 28 | 12 | 40 |
| Built-Up Land | 49 | 21 | 70 |
| *Prosopis glandulosa* | 56 | 24 | 80 |
| **2008** | | | |
| **Class** | **Training** | **Test** | **Total** |
| Shrubland | 50 | 22 | 72 |
| Waterbodies | 35 | 15 | 50 |
| Built-Up Land | 45 | 20 | 65 |
| *Prosopis glandulosa* | 44 | 20 | 64 |
| **2013** | | | |
| **Class** | **Training** | **Test** | **Total** |
| Shrubland | 46 | 20 | 66 |
| Waterbodies | 29 | 13 | 42 |
| Built-Up Land | 42 | 18 | 60 |
| *Prosopis glandulosa* | 50 | 22 | 72 |
| **2017** | | | |
| **Class** | **Training** | **Test** | **Total** |
| Shrubland | 43 | 19 | 62 |
| Waterbodies | 28 | 12 | 40 |
| Built-Up Land | 45 | 19 | 64 |
| *Prosopis glandulosa* | 54 | 24 | 78 |

### 3.5.3 *Prosopis* Land Cover Change Prediction

The land cover change prediction procedure consists of 4 main stages, namely; the Change Analysis stage, Transition Potential Modelling stage, Change Prediction stage, and the Model Validation stage**.** Figure 10 illustrates the processes followed to conduct the land cover change prediction.

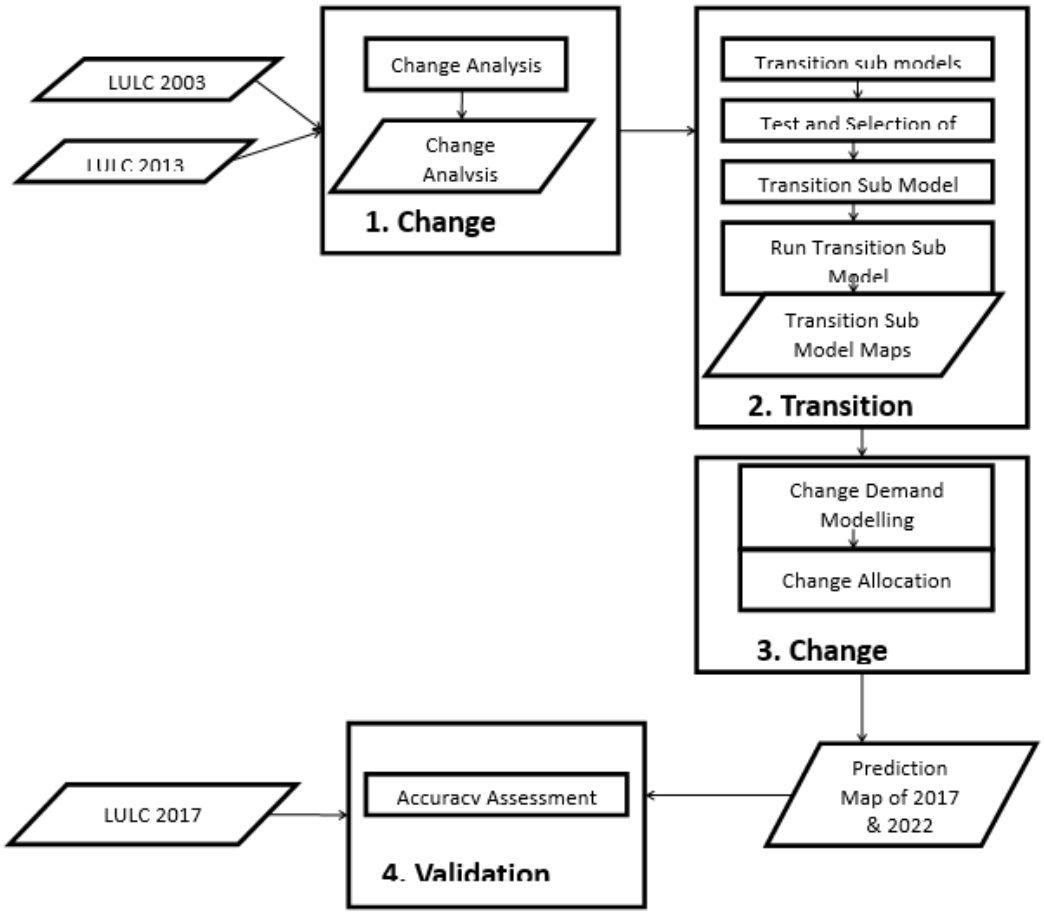



**Figure 10. Flowchart illustrating the processes followed when conducting the 2017 and 2022 land cover prediction**

**Change Analysis**

Future land cover predictions are based on the historical land cover change from time 1 to time 2 (Eastman, 2016). This study used land cover maps for the years 2003 and 2013 to predict the land cover for the years 2017 and 2022. A land cover land use map for the year 2017 was created to verify the accuracy on the prediction model, as 2017 satellite images are available to compare with the prediction map.

Changes between the years 2003 and 2013 were assessed. The changes that took place in this period represent the transitions from one class to another which is essential in order to identify dominant transitions to *Prosopis glandulosa* and other LULC classes.

**Transition Potential Modelling**

Transition Potential Modelling is the second step in the Change Prediction process. The aim of this step is to create transition potential maps which may be described as maps of suitability for each transition (Eastman, 2016). This process identifies the potential of the land to transition to another LULC type. Transition potential maps were created, and these were grouped into a sub-model where exploratory variables or predictor variables were identified (Eastman, 2016). This study used elevation, slope and distance to watercourses as predictor variables. These were selected based on literature indicating that these variables affect the establishment and spread of *Prosopis*.

The potential exploratory power of a variable can be tested to evaluate whether the variable or driving force is worth being considered. The Cramer's V test was used to assess the variables. Cramer's V is a correlation coefficient that ranges from 0 to 1, with variables with greater values being considered as more important than other variables (Roy *et al*., 2014).

There are three modelling algorithms that are available in LCM. These include the Logistic Regression, Multi-layered Perceptron Neural Network and Sim-Weight procedure. After the model variables were selected, the transition sub-model was modelled using the Multi-layered Perceptron Neural Network. The Multi-layered Perceptron Neural Network was selected in this study as it has been enhanced to provide an automatic mode that does not require any intervention by the user (Eastman, 2016). The LCM considers each transition as a separate sub-model but the Multi-layered Perceptron Neural Network allows for multiple transitions to be grouped into a single sub-model if it is considered that they all result from the same underlying driving forces (Roy *et al*., 2014; Megahed *et al*., 2015; Eastman, 2016).

**Change Prediction**

The change prediction procedure uses change rates calculated at the change analysis step as well as transition potential maps produced in the previous step (Megahed *et al*., 2015; Eastman, 2016). This procedure is responsible for determining the quantity of change in each transition through a Markov Chain analysis. The Markov chain analysis was utilized to obtain transition probability matrix, transition area matrix and a set of conditional probability images (Behera *et al*., 2012; El-Hallaq and Habboub, 2015). Behera *et al*. (2012) described the transition probability matrix as being a file with records of the probability that each land cover and land use class will change to every other class. A transition area matrix may be described as the area (in cells) expected to change in the next time period that also records the number of pixels that are expected to change from one land use and land cover type to another (Behera *et al*., 2012). Conditional probability maps are described as a

cartographical presentation of the transition probability matrix as they state the probability that each pixel will belong to the designated class in the next time period (Behera *et al*., 2012).

**Model Validation**

In order to ensure that the land cover/land use prediction for the year 2022 will produce reliable predictions, the model had to be validated using existing datasets (Hadi *et al*., 2014). The validation procedure involves the use of comparing the predicted land cover/land use areas with the actual present LULC areas. This study predicted the 2017 LULC through the model to produce a prediction map that was compared with the actual LULC map for the year 2017.

There are two approaches used to validate a model; namely the statistical approach and the visual approach.

***Visual approach***

The visual approach of validating a model refers to one visually comparing the predicted LULC areas with the actual present LULC areas. The visual approach was conducted to obtain a quick assessment of the spatial patterns. A simulated LULC map of 2017 was created using 2003 and 2013 LULC maps and environmental data (slope, distance to watercourses and elevation).

***Statistical approach***

The purpose of conducting statistical validation is to assess whether the real LULC map agrees with the prediction map (Nadoushan *et al*., 2015). The statistical approach evaluates how well the maps (real map and prediction map) agree in terms of the number of cells in each LULC class, and also how well the maps (real map and prediction map) agree in terms of the location of the cells in each class (Pontius *et al*., 2001; Roy, 2014; Nadoushan *et al*., 2015; Hua, 2017). To statistically test the strength of association between the real LULC map and the prediction map, the Cramer's V and Kappa Index of Agreement (KIA) was measured. These measures result in coefficients ranging from 0 to 1, with 0 meaning there is no correlation between the classes and 1 meaning there is a perfect correlation.

The VALIDATE module from IDRISI was used to measure the Kappa Index of Agreement. This module quantifies the agreement between the real LULC map and prediction map by calculating the Kappa index of agreement and its variants which are the $K_{no}$, $K_{location}$ and $K_{standard}$ (Hadi *et al*., 2014*;* Nadoushan *et al*., 2015). The $K_{no}$ states the overall agreement and can be utilized to evaluate the overall accuracy of the prediction (Hadi *et al*., 2014*;* Nadoushan *et al*., 2015). The $K_{location}$ indicates the level of agreement of location between the real LULC map (Hadi *et al*., 2014*;* Megahed *et al*., 2015). The

$K_{standard}$ shows the agreement extent in terms of each class (Hadi *et al*., 2014). A Kappa statistic of 1 indicates a perfect agreement and 0indicates an agreement due to chance (Nadoushan *et al*., 2015).

The CROSSTAB module from IDRISI was used to measure the Cramer's V coefficient. The CROSSTAB checks how two images are similar by performing image crosstabulation and cross correlation (Eastman, 2016). This includes comparing the categories in first map with those of the second and measures the association between the images. The Cramer's V determines the strength of association between variables (Dzieszko, 2014).

A confusion matrix table was also created to assess the accuracy of the prediction map. This process compares on a class by class basis the relationship between the ground truth data and the prediction map (Congalton, 1991). Ground reference points collected during the field survey were used to calculate the confusion matrix table as field work was conducted in 2017.

# 4. Results

## 4.1 2016 Worldview-3 Land Cover Classification

### 4.1.1 Results

Figure 12 is the 2016 land cover land use map of the study area classified using Worldview-3 high resolution satellite imagery. *Prosopis glandulosa* is estimated to cover an area of approximately 2.15 $km^2$. The overall accuracy of the classification was 76%. Table 5 is the Confusion Matrix table which compares on a class by class basis the relationship between the classified map and testing ground reference data. In total, 88% of *Prosopis* were accurately classified as this class, with 2% being misclassified as bare rock and 6% being misclassified as quiver trees. The high resolution WorldView image was able to detect small vegetated *Prosopis* patches.

In total, 74% were accurately classified as shrubland. *Aloidendron dichotomum* (Quiver tree) is sparsely spread along dolerite koppies in the study area. In total, 82.20% of *Aloidendron dichotomum* was accurately delineated. In total, 99% of the built-up environment was accurately classified. This includes the roads, buildings and telescope infrastructure in the study area.

The Kappa coefficient, which measures the agreement between the classified image and the reference data pixels, was 0.5. This shows a strong association between the classified image and reference data as a Kappa value of 1 represents a perfect agreement (Butt *et al*., 2015).

**Table 5. Confusion matrix for 2016 Worldview land cover classification**

| **2016 Land Cover Classification**<br><br>**Percent (%)** | | | | | | | | |
|---|---|---|---|---|---|---|---|---|
| **Class** | **Bare rock (%)** | **Bare soil (%)** | **Built-up land (%)** | **Quiver tree (%)** | ***Prosopis* (%)** | **Waterbodies (%)** | **Shrubland (%)** | **Total (%)** |
| **Bare rock** | 82.96 | 0.86 | 0 | 8.58 | 2.42 | 0 | 14.62 | 27.57 |
| **Bare soil** | 1.45 | 97.35 | 0.04 | 0 | 0.01 | 0 | 1.31 | 1.45 |
| **Built-up land** | 0.99 | 0 | 99.92 | 0.21 | 1.28 | 0 | 0.09 | 0.34 |
| **Quiver tree** | 5.98 | 0.08 | 0 | 82.20 | 6.52 | 0 | 7.17 | 6.96 |
| ***Prosopis*** | 2.89 | 0 | 0.04 | 5.11 | 88.59 | 0.05 | 2 | 2.36 |
| **Waterbodies** | 0 | 0 | 0 | 0 | 0 | 99.95 | 0 | 0.06 |
| **Shrubland** | 5.72 | 1.72 | 0 | 3.90 | 1.17 | 0 | 74.80 | 61.26 |
| **Total** | 100 | 100 | 100 | 100 | 100 | 100 | 100 | 100 |

Figure 11 illustrates the diagram of the RMS training in 1000 iterations. The RMS training plot defines the root mean square error value at which the training should stop (Petropoulos *et al*., 2010; Aziz *et al*., 2017). The RMS error is shown on the plot during training. If the RMS error decreases below the entered value, the training will stop. The RMS error on Figure 11 starts from approximately 0.7 and it drops rapidly to approximately 0.2. This plot shows that the networks RMS error drops rapidly as it learns. A well trained neural network should have a low RMS error at the end of the training phase, which is depicted on Figure 11. The classification was then executed.

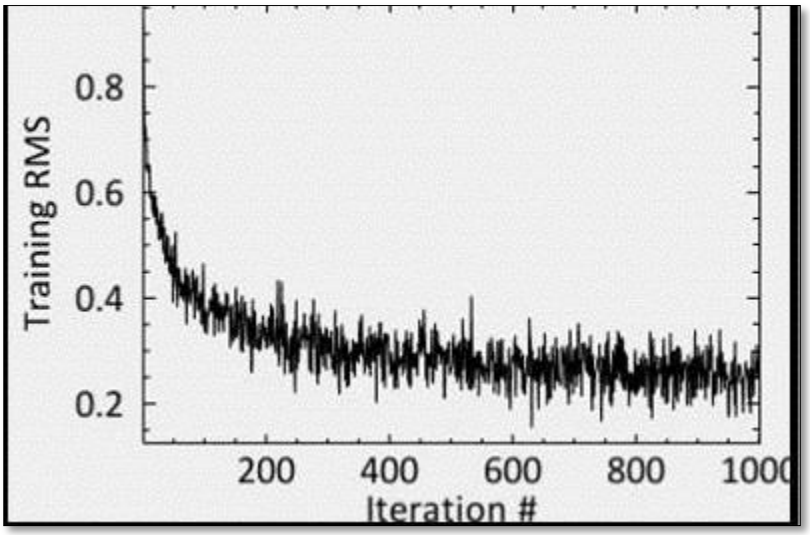



**Figure 11. RMS plot for the 2016 neural network classification**

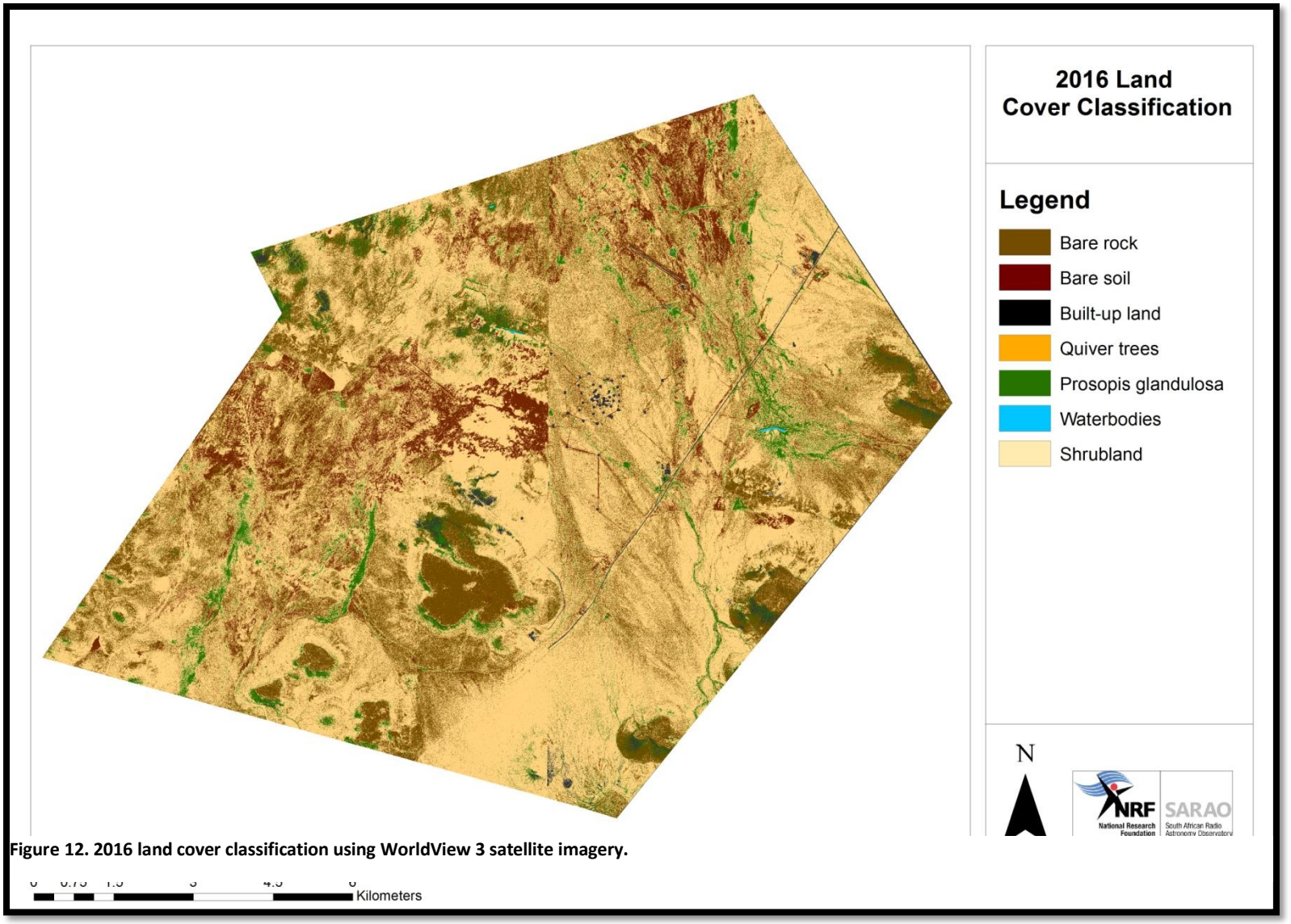



**Figure 12. 2016 land cover classification using WorldView 3 satellite imagery.**

## 4.2 Change Detection Analysis

### 4.2.1 Results

A change detection analysis was conducted using land cover/land use maps created with Landsat satellite images. Four classes were selected for the classification of the Landsat images. These are built-up land, waterbodies, *Prosopis glandulosa* and shrubland. *Aloidendron dichotomum* was not included as a class in these classifications as a result of the 30 m spatial resolution of Landsat images. These tree species are small and could not be delineated using a higher spatial resolution image of 1.24 m.

**2003 Land Cover Classification**

Figure 13 is the 2003 land cover land use map classified using a Landsat 5 ETM image. The classification had an overall accuracy of 98%, with a Kappa Coefficient of 0.8498. *Prosopis glandulosa* may be observed along drainage lines and two man-made dams in the study area. *Prosopis* covered an area of approximately 6.7 $km^2$ in the year 2003.

Table 6 is the confusion matrix table of the 2003 land cover classification. In total, 76.68% (569/742 pixels) of *Prosopis* were accurately classified, with the remaining 157/742 pixels (21.16%) being misclassified as shrubland. A total of 98.89% (11 328/ 11 328 pixels) of shrubland were accurately classified, with 0.11% (157/11 502 pixels) being misclassified as *Prosopis*. A total of 64.29% (9/14 pixels) of built up land were accurately classified with 35.71% (5/14 pixels) being misclassified as shrubland. In 2003, the SKA had not established in the area. The built-up land refers to the farmhouses as the study area was used for sheep farming prior the establishment of the SKA and Meerkat telescopes. Table 7 states the Producer and User Accuracy values.

**Table 6. Confusion matrix for 2003 Landsat 5 land cover classification**

| Class | *Prosopis glandulosa* (%) | Waterbodies (%) | Shrubland (%) | Built-up land (%) | Total (%) |
|---|---|---|---|---|---|
| ***Prosopis glandulosa*** | 76.68 | 0 | 0.11 | 0 | 4.80 |
| **Waterbodies** | 0.94 | 69.23 | 0 | 0 | 0.28 |
| **Shrubland** | 21.16 | 30.77 | 99.89 | 35.71 | 94.78 |
| **Built-up land** | 1.21 | 0 | 0 | 64.29 | 0.15 |
| **Total** | 100 | 100 | 100 | 100 | 100 |

**Table 7. 2003 Accuracy assessment statistics**

| Class | Commission (%) | Omission (%) | Commission (Pixel) | Omission (Pixel) |
|---|---|---|---|---|
| ***Prosopis glandulosa*** | 2.23 | 23.32 | 13/582 | 173/742 |
| **Waterbodies** | 20.59 | 30.77 | 7/34 | 12/39 |
| **Shrubland** | 1.51 | 0.11 | 174/11502 | 13/11341 |
| **Built-up land** | 50.00 | 35.71 | 9/18 | 5/14 |
| **Class** | **Producer accuracy (%)** | **User accuracy (%)** | **Producer accuracy (Pixel)** | **User accuracy (Pixel)** |
| ***Prosopis glandulosa*** | 76.68 | 97.77 | 569/742 | 569/582 |
| **Waterbodies** | 69.23 | 79.41 | 27/39 | 27/34 |
| **Shrubland** | 99.89 | 98.49 | 11328/11341 | 11328/11502 |
| **Built-up land** | 64.29 | 50.00 | 9/14 | 9/18 |

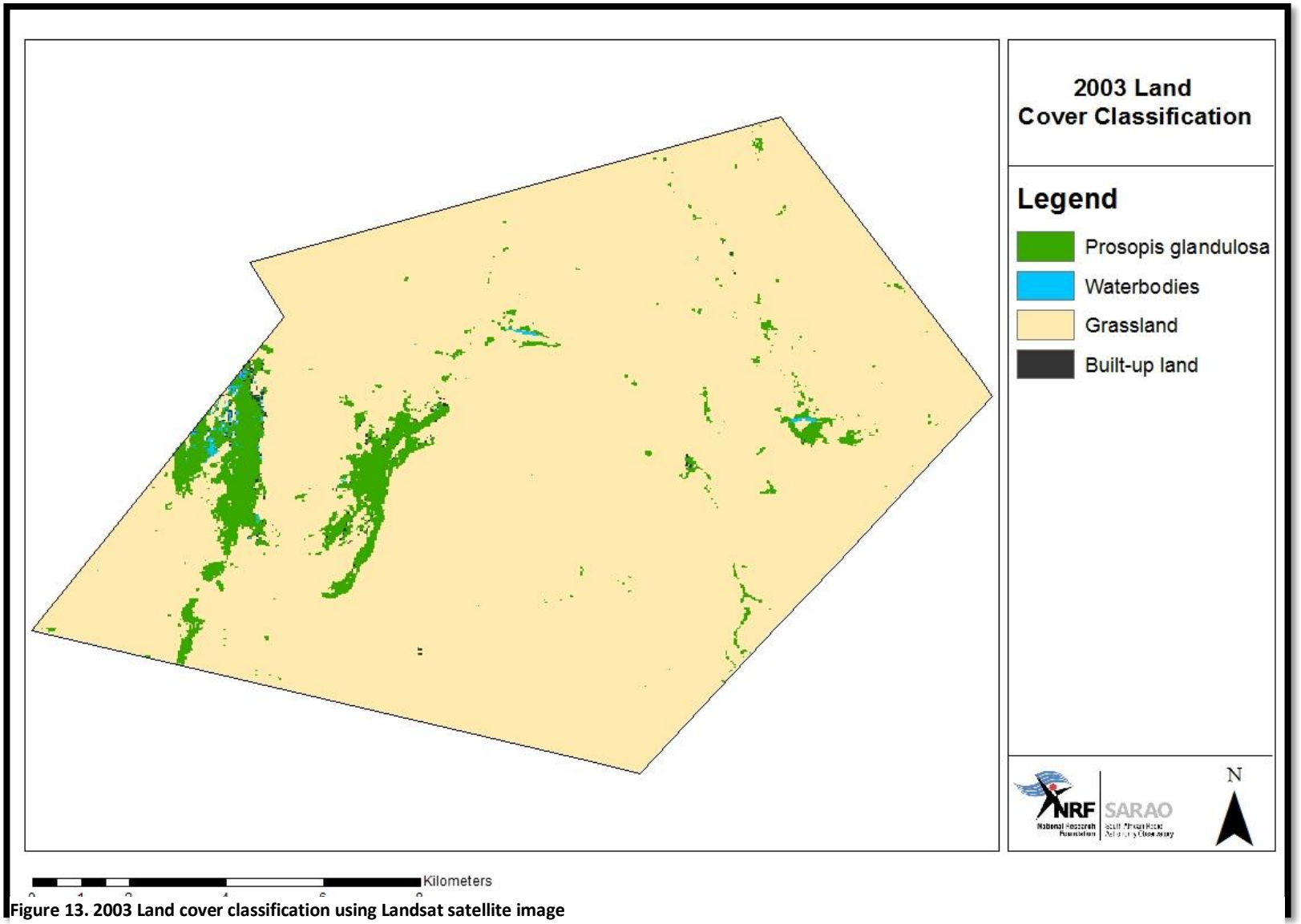



**Figure 13. 2003 Land cover classification using Landsat satellite image**

**2008 Land Cover Classification**

Figure 14 is the 2008 land cover land use map classified using a Landsat 5 ETM image. The land cover classification had an overall accuracy of 97%, with a Kappa Coefficient of 0.7439. *Prosopis* covered an area of approximately 6.5 $km^2$in the year 2008.

Table 8 is the confusion matrix table of the 2008 land cover classification. In total, 60.38% (448/742 pixels) of *Prosopis* were accurately classified, with only 39.62% (294 /742 pixels) being misclassified as shrubland. In total, 99.96% (11 336/11 341 pixels) of shrubland were accurately classified. Built-up land had a low classification accuracy. In total, 28.57% (4/14 pixels) were accurately classified as built-up land with 71.43% (10/14 pixels) being misclassified as shrubland. Table 9 states the Producer and User Accuracy values.

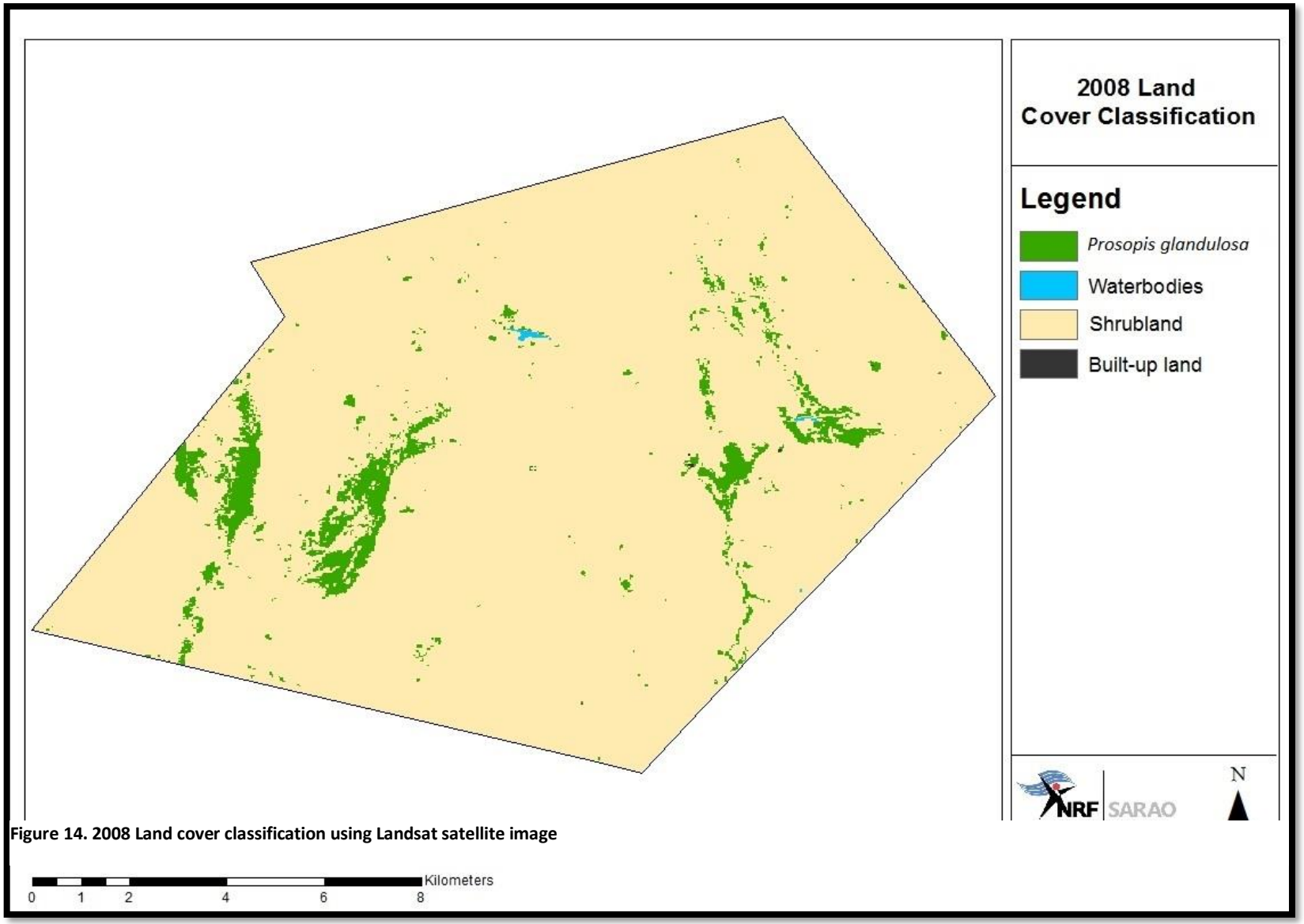



**Figure 14. 2008 Land cover classification using Landsat satellite image**

**Table 8. 2008 Confusion matrix**

| Class | *Prosopis glandulosa* (%) | Waterbodies (%) | Shrubland (%) | Built-up land (%) | Total (%) |
|---|---|---|---|---|---|
| ***Prosopis glandulosa*** | 60.38 | 0 | 0.04 | 0 | 3.72 |
| **Waterbodies** | 0 | 87.18 | 0 | 0 | 0.28 |
| **Shrubland** | 39.62 | 12.82 | 99.96 | 71.43 | 95.95 |
| **Built-up land** | 0 | 0 | 1 | 28.57 | 0.04 |
| **Total pixels** | 742 | 39 | 11341 | 14 | 12136 |

**Table 9 2008 Accuracy assessment statistics**

| Class | Commission (%) | Omission (%) | Commission (Pixel) | Omission (Pixel) |
|---|---|---|---|---|
| *Prosopis glandulosa* | 0.88 | 39.62 | 4/452 | 294/742 |
| Waterbodies | 0 | 12.82 | 0/34 | 5/39 |
| Shrubland | 2.65 | 0.04 | 309/11645 | 5/11341 |
| Built-up land | 20.00 | 71.43 | 1/5 | 10/14 |
| **Class** | **Producer accuracy (%)** | **User accuracy (%)** | **Producer accuracy (Pixel)** | **User accuracy (Pixel)** |
| *Prosopis glandulosa* | 60.38 | 99.12 | 448/742 | 448/452 |
| Waterbodies | 87.18 | 100.00 | 34/39 | 34/34 |
| Shrubland | 99.96 | 97.35 | 11336/11341 | 11336/11645 |
| Built-up land | 28.57 | 80.00 | 4/14 | 4/5 |

## 2003-2008 Change Detection

A change detection analysis was conducted for the year 2003-2008. Figure 15 presents the gains and losses that took place during this period. There was gain in *Prosopis* of an area of approximately 2.8 $km^2$and a loss of approximately 3 $km^2$. According to this analysis, there was an overall slight decrease in *Prosopis* of approximately 0.20 $km^2$in 5 years (2003-2008), resulting in an average loss rate of 0.04 $km^2$per year. Figure 16 states the net change that took place during this period.




**Figure 15. Gains and Losses graph for the year 2003-2008**

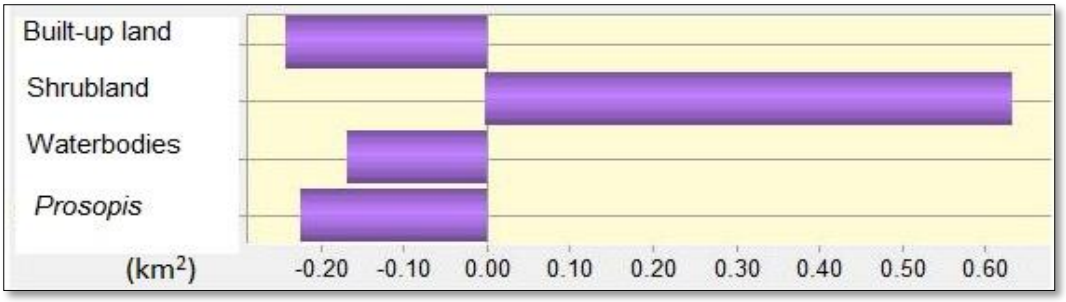



**Figure 16. Net change graph for the year 2003-2008**

## 2013 Land Cover Classification

Figure 17 is the 2013 land cover/land use map classified using a Landsat 8 satellite image. The overall accuracy for this classification was 96%, with a Kappa coefficient of 0.6135. *Prosopis* covered an area of approximately 5.7km$^2$ in the year 2013.

Table 10 is the confusion matrix table of the 2013 land cover classification. In total, 74.12% (336/453 pixels) of *Prosopis* were classified accurately, with 25.88% (117/453 pixels) being misclassified as shrubland. A total of 65.03% (238/366 pixels) of built-up land was accurately classified, with 32.15% (119/366pixels) being misclassified as shrubland. Built-up land refers to the SKA and Meerkat infrastructure that was being constructed in the area at the time. One may observe the road construction on Figure 17, which is the 2013 land cover land use map. Table 11 presents the producer and user accuracy values of the classification.

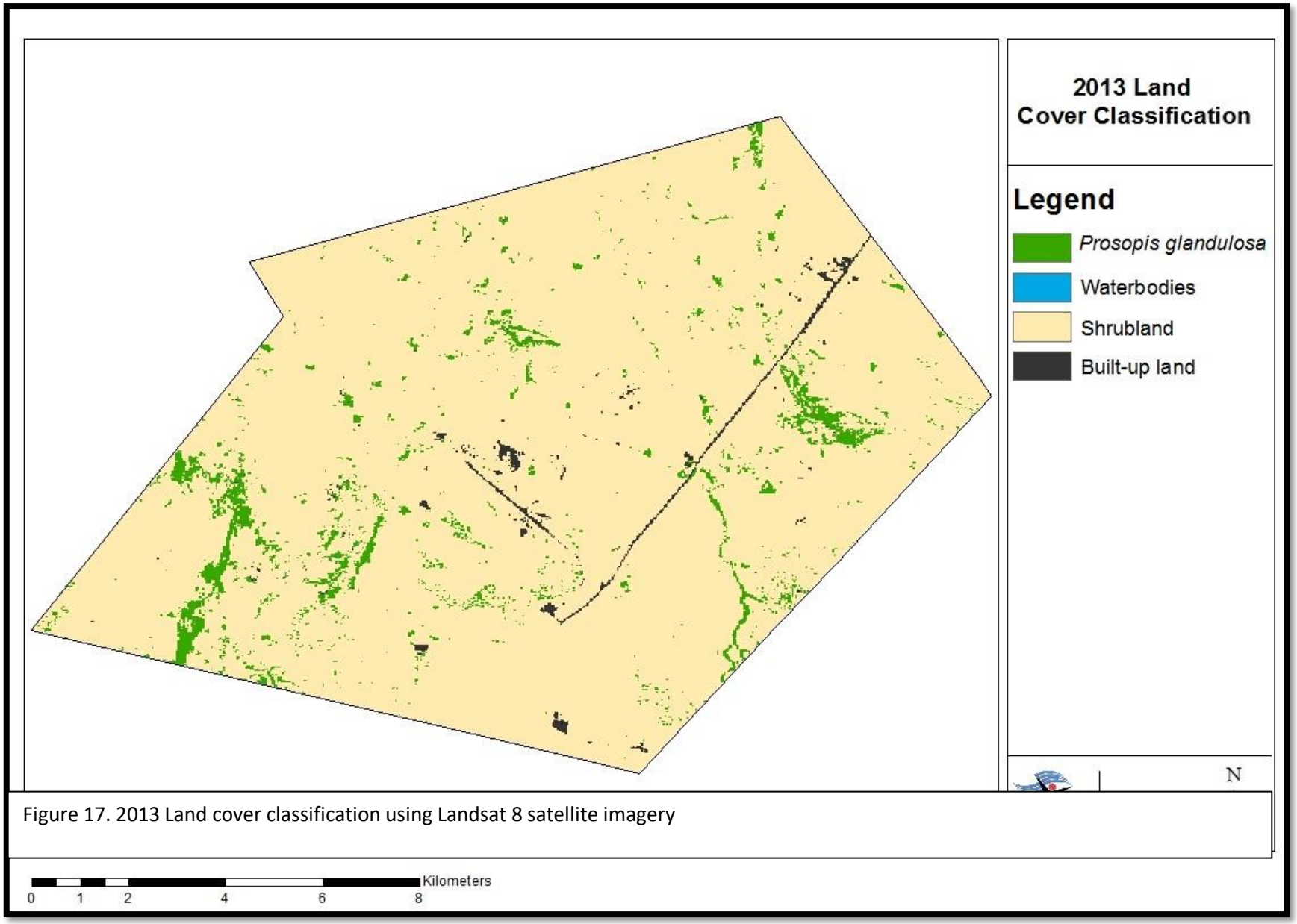



Figure 17. 2013 Land cover classification using Landsat 8 satellite imagery

**Table 10. Confusion matrix for 2013 Landsat land cover classification**

| Class | *Prosopis glandulosa* (%) | Waterbodies (%) | Shrubland (%) | Built-up land (%) | Total (%) |
|---|---|---|---|---|---|
| ***Prosopis glandulosa*** | 74.17 | 30 | 1.52 | 2.46 | 3.12 |
| **Waterbodies** | 0 | 0 | 0 | 0 | 0 |
| **Shrubland** | 25.83 | 70 | 98.31 | 32.51 | 95.64 |
| **Built-up land** | 0 | 0 | 0.17 | 65.03 | 1.24 |
| **Total** | 100 | 100 | 100 | 100 | 100 |

**Table 11. 2013 Accuracy assessment statistics**

| Class | Commission (%) | Omission (%) | Commission (pixels) | Omission (pixels) |
|---|---|---|---|---|
| ***Prosopis glandulosa*** | 51.16 | 25.83 | 352/688 | 117/453 |
| **Waterbodies** | 0.00 | 100.00 | 0/0 | 70/70 |
| **Shrubland** | 1.35 | 1.69 | 285/21095 | 358/21168 |
| **Built-up land** | 13.14 | 34.97 | 36/274 | 128/366 |
| **Class** | **Producer accuracy (%)** | **User accuracy (%)** | **Producer accuracy (Pixels)** | **User accuracy (Pixels)** |
| ***Prosopis glandulosa*** | 74.17 | 48.84 | 336/453 | 336/688 |
| **Waterbodies** | 0 | 0 | 0/70 | 0/0 |
| **Shrubland** | 98.31 | 98.65 | 20810/21168 | 20810/21095 |
| **Built-up land** | 65.03 | 86.86 | 238/366 | 238/366 |

**2008-2013 Change Detection**

A change detection analysis was conducted for the year 2008-2013. Figure 18 shows the gains and losses that took place during this period. There was a gain in *Prosopis* of an area of approximately 3.2 $km^2$ and a loss of approximately 4 $km^2$. Figure 19 illustrates the net change that took place in the period 2008-2013. According to this analysis, there was an overall decrease in *Prosopis* of approximately 0.8 $km^2$ in 5 years, resulting in an average decrease rate of 0.16 $km^2$per year. There was also a drastic decrease in shrublands during this period and this decrease in vegetation may be attributed to the increase in built-up land in the study area. Figure 20 presents the contributions to the net change in built-up land. Shrubland was major contributor to built-up land with *Prosopis* having a slight contribution. During this period, the construction of the SKA and associated infrastructure was taking place. This may be observed on Figure 17, which is the land cover map for the year 2013. Roads and telescope foundations were being constructed during this period.

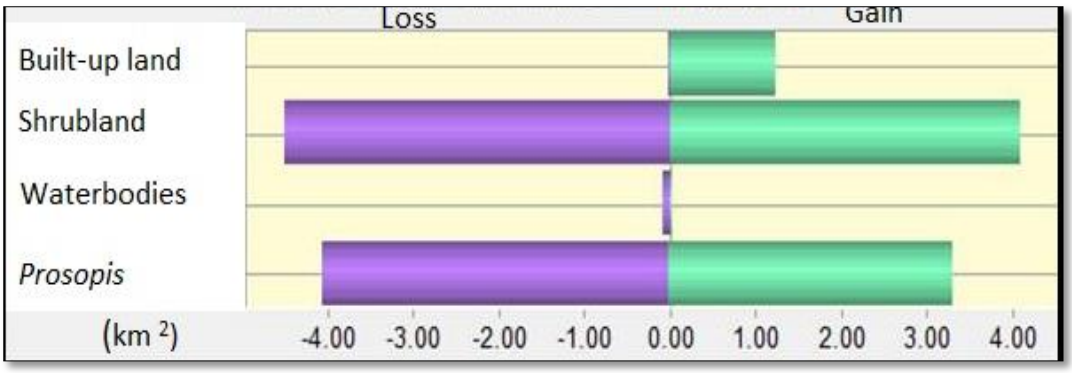



**Figure 17. Gains and Losses graph for the year 2008-2013**

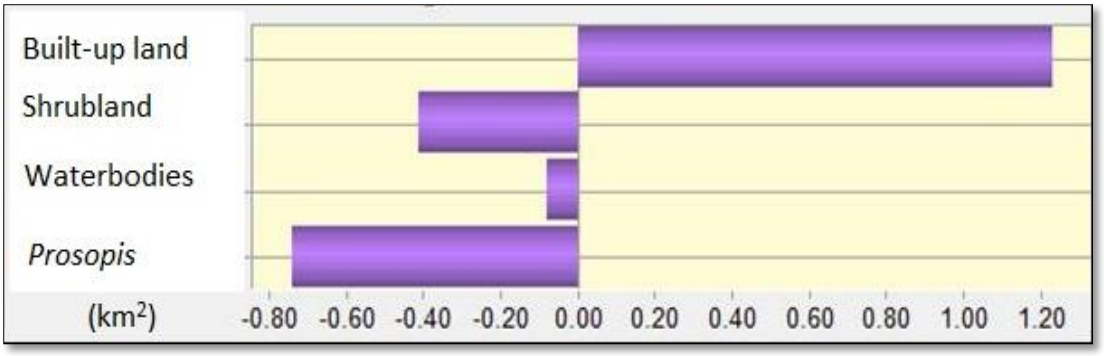



**Figure 18. Net change graph for the year 2008-2013**

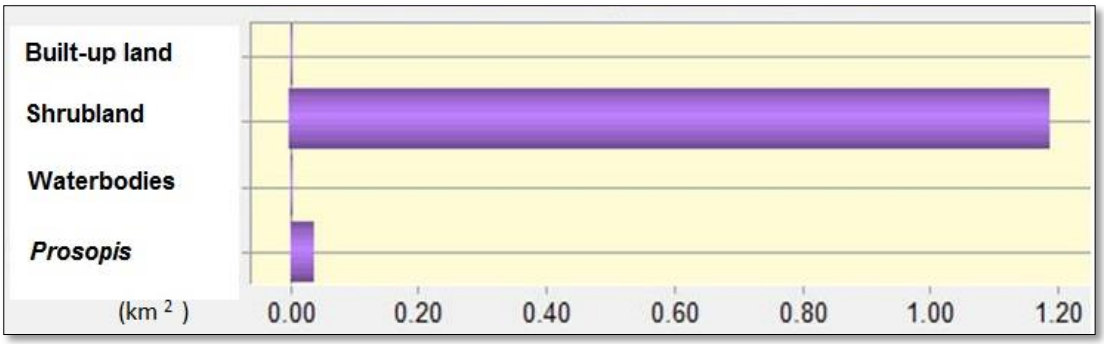



**Figure 19. Contributions to Net Change in Built-up land**

**2017 Land Cover Classification**

Figure 21 is the 2017 land cover map classified using a Landsat 8 satellite image. The classification had an overall accuracy of 96%, with a Kappa coefficient of 0. 5366. *Prosopis* covered an area of approximately 6.3 $km^2$ in 2017.

Table 12 is the confusion matrix table for the 2017 land cover classification. A total of 69.39% (331/477 pixels) of *Prosopis* were accurately classified with the remaining 30.61% (146/477 pixels) being misclassified as shrubland. A total of 97.64% (20 669/21 168 pixels) of shrubland were accurately classified. In total, 51.64% (189/366 pixels) of built-up land were accurately classified, with 47.24% (173/366 pixels) being misclassified as shrublands. Table 13 presents the producer and user accuracy values.

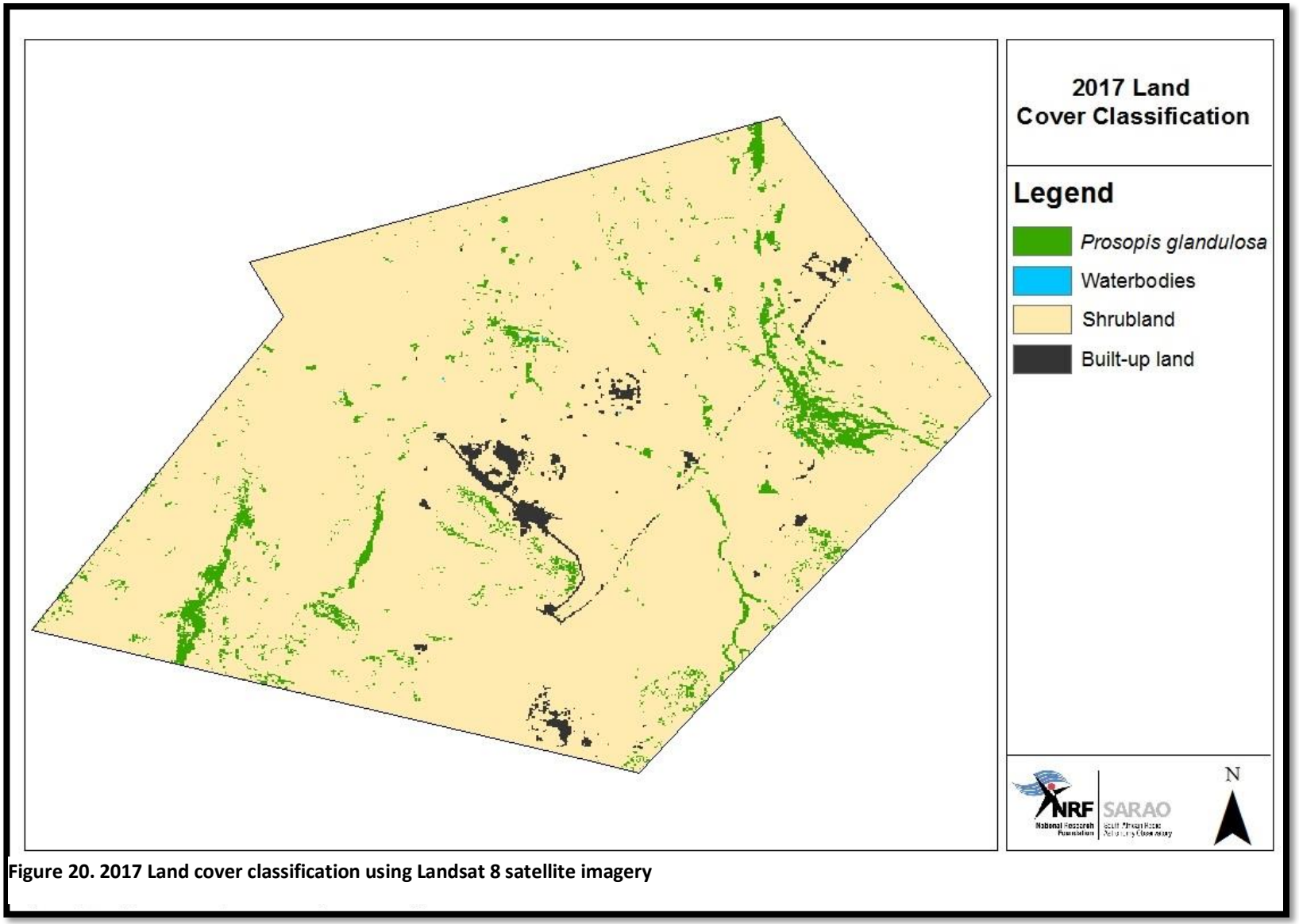



**Figure 20. 2017 Land cover classification using Landsat 8 satellite imagery**

**Table 12. Confusion matrix 2017 land cover classification**

| Class | *Prosopis glandulosa* (%) | Waterbodies (%) | Shrubland (%) | Built-up land (%) | Total (%) |
|---|---|---|---|---|---|
| ***Prosopis glandulosa*** | 69.39 | 23.08 | 1.90 | 1.09 | 3.38 |
| **Waterbodies** | 0 | 5.13 | 0 | 0 | 0.01 |
| **Shrubland** | 30.61 | 71.79 | 97.6 | 47.27 | 95.31 |
| **Built-up land** | 0 | 0 | 0.46 | 51.64 | 1.30 |
| **Total** | 100 | 100 | 100 | 100 | 100 |

**Table 13. 2017 Accuracy assessment statistics**

| Class | Commission (%) | Omission (%) | Commission (pixel) | Omission (pixel) |
|---|---|---|---|---|
| *Prosopis glandulosa* | 55.63 | 30.61 | 415/746 | 146/477 |
| Waterbodies | 0.00 | 94.87 | 0/2 | 37/39 |
| Shrubland | 1.65 | 2.36 | 347/21016 | 499/21168 |
| Built-up land | 33.92 | 48.36 | 97/286 | 177/366 |
| **Class** | **Producer accuracy (%)** | **User accuracy (%)** | **Producer accuracy (Pixel)** | **User accuracy (Pixel)** |
| *Prosopis glandulosa* | 69.39 | 44.37 | 331/477 | 331/746 |
| Waterbodies | 5.13 | 100.00 | 2/39 | 2/2 |
| Shrubland | 97.64 | 98.35 | 20669/21168 | 20669/21016 |
| Built-up land | 51.64 | 66.05 | 189/366 | 189/286 |

**2013-2017 Change Detection**

A change detection analysis for the years 2013-2017 was conducted. Figure 22 illustrates the gains and losses that took place for each class during this period. There was a gain in *Prosopis* of an area of approximately 3.2 $km^2$ and a loss of approximately 2.8 $km^2$. There was an overall increase of 0.4 $km^2$ in these tree species during this period and this is presented in Figure 23. This may be attributed to the extensive vegetation clearing that took place for the construction of infrastructure. This resulted in *Prosopis* species growing in these cleared environments and these species invading new areas. There was an average increase rate of 0.1 $km^2$ in the four years 2013-2017. There was a decrease in shrubland of approximately 4.5 $km^2$. This may also be as a result of the increase in built-up land. More infrastructure was being constructed during this period.

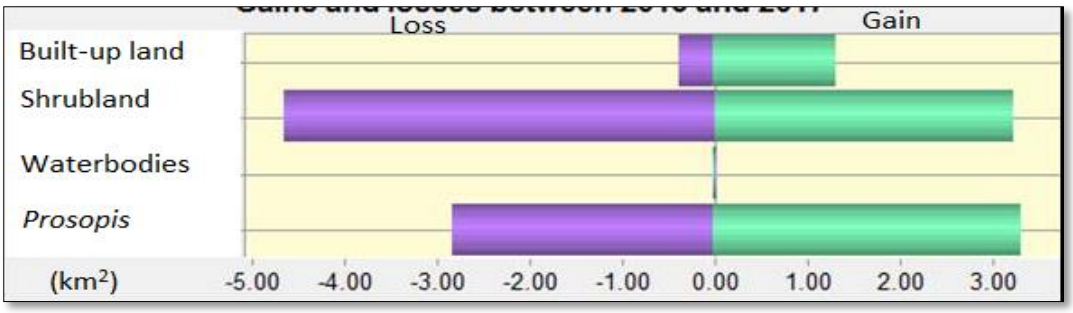



**Figure 21. Gains and losses for the year 2013-2017**

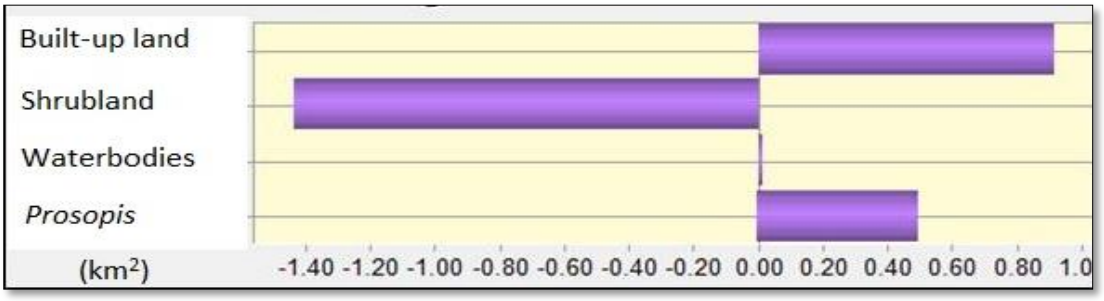



**Figure 22. Net change for the year 2013-2017**

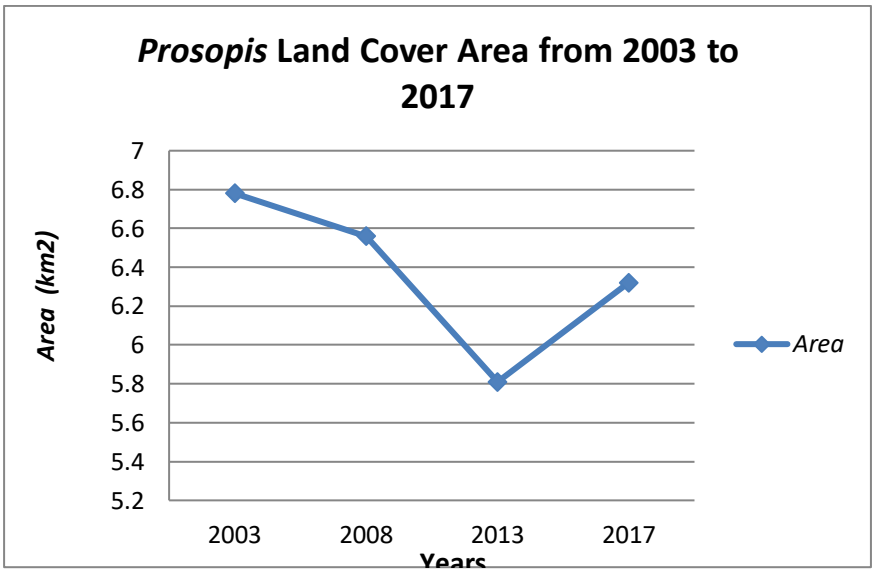



**Figure 23. *Prosopis* land over changes from 2003-2017**

Figure 24 illustrates the changes in *Prosopis* land cover from the year 2003-2017. Figure 25 illustrates the RMS training in 1000 iterations. The RMS training plot defines the root mean square error value at which the training should stop (Petropoulos *et al*., 2010; Aziz *et al*., 2017). The RMS error is shown on the plot during training. If the RMS error decreases below the entered value, the training will stop.

These plot shows that the networks RMS error drops rapidly as it learns. The classifications were then executed.

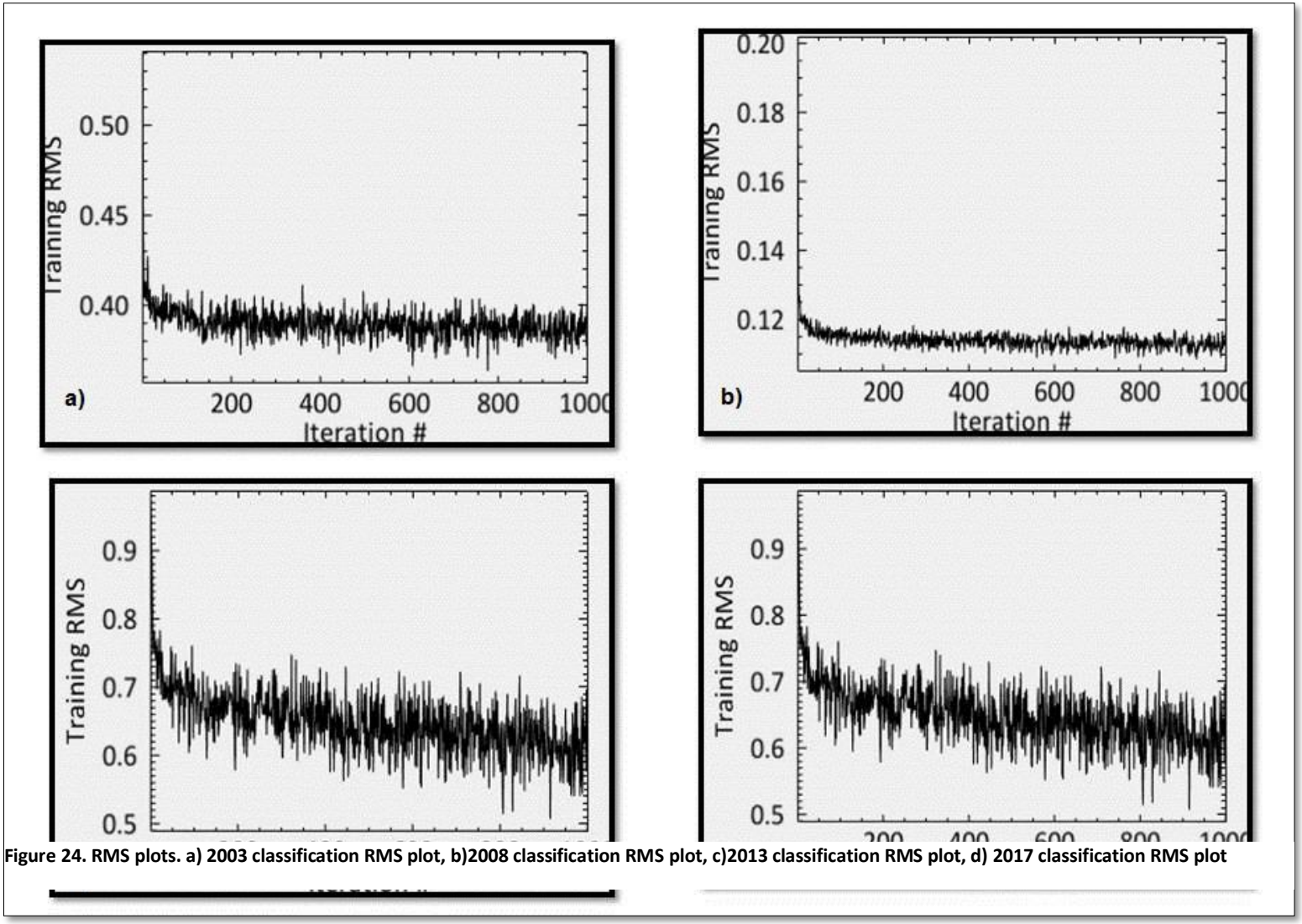



**Figure 24. RMS plots. a) 2003 classification RMS plot, b)2008 classification RMS plot, c)2013 classification RMS plot, d) 2017 classification RMS plot**

## 4.3 Change Prediction

### 4.3.1 Results

The land cover change prediction procedure consists of 4 main stages, namely; (1) change analysis stage, (2) transition potential modelling, (3) the change prediction stage and (4) the model validation stage.

**Change Analysis**

Land cover maps for the year 2003 and 2013 and ancillary environmental data (elevation, distance to watercourse and slope) were used for the land cover prediction. The first step, which is the change analysis, was conducted using the two classified land cover/land use maps. Figure 26 illustrates the gains and losses that took place during this period. This figure shows that there was approximately 3.5 $km^2$ of *Prosopis* gained and approximately 4.5 $km^2$ lost. There was an overall decrease in *Prosopis* during this period and this is mainly due to the increase in built-up land. *Prosopis* trees were cleared in specific parts of the study area for the construction of roads and telescopes resulting in a slight decrease in these tree species in the study area. There was an increase in built-up land of approximately 1.5 $km^2$ which includes roads, buildings and telescopes belonging to the SKA SA.




**Figure 25. 2003-2013 gains and losses graph for land cover prediction**

Figure 27 is a change map which illustrates the significant transitions that took place in the study area during the period 2003-2013. These transitions include; from grassland to built-up land, from grassland to *Prosopis* and from *Prosopis* to grassland. The areas that transition from grassland to built-up land refer infrastructure constructed by SKA during this period. The transition from grassland to *Prosopis* illustrates the invasion and expansion of the distribution of these species in the study area.

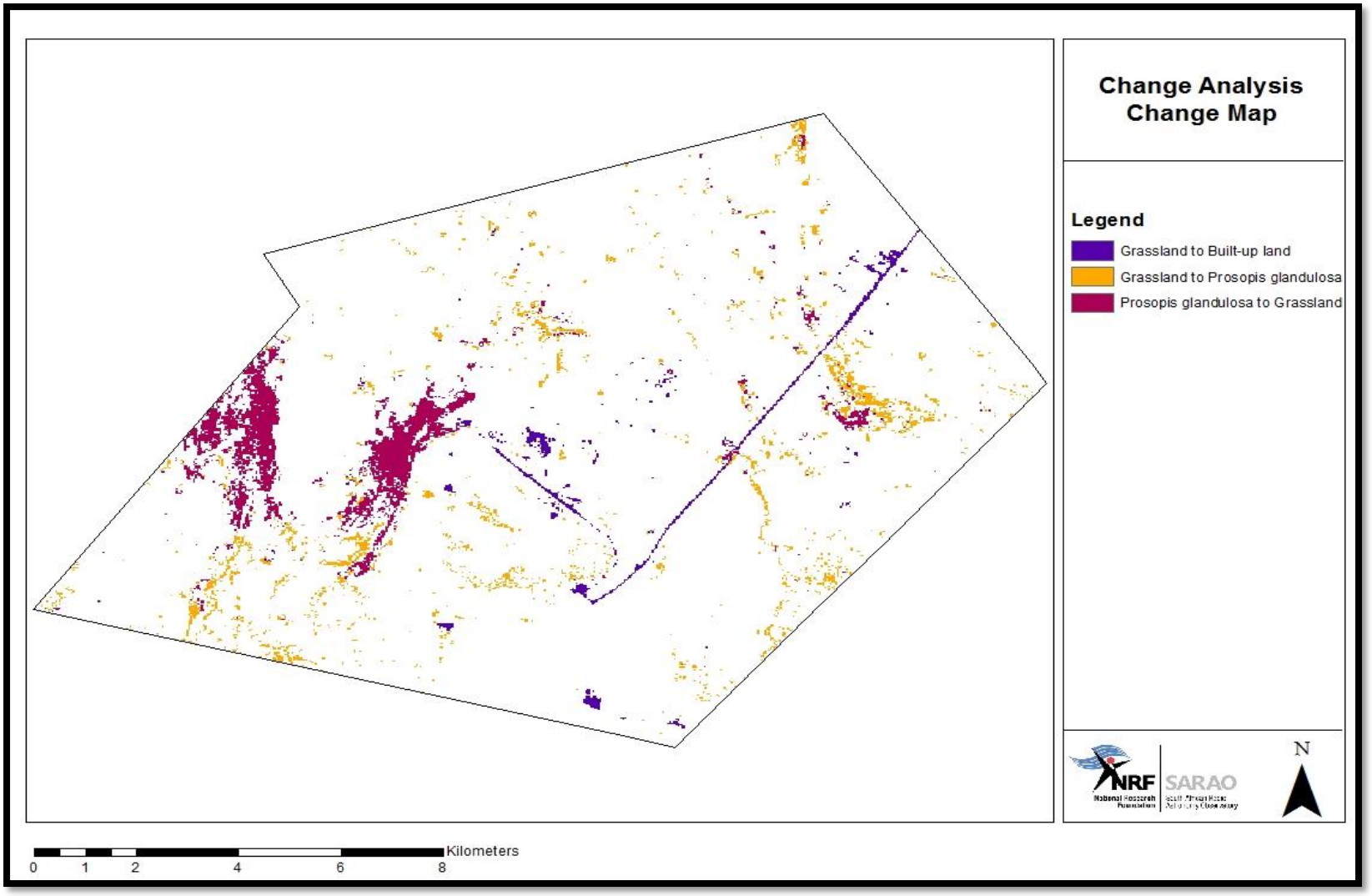



**Figure 26. 2003-2013 Change analysis change map for prediction model**

**Transition Potential Modelling**

Three driver variables were selected to develop the land cover change prediction model. These include slope, distance to water courses and elevation. The Land Change Modeller differentiates between static and dynamic variables, with static variables being those that do not change and dynamic variables being those that change over time (Eastman, 2009). The three driver variables used in this study were static. The elevation map was created using a 30 m SRTM DEM. The slope model was created in ArcGIS using the Spatial Analyst tool and the 30 m SRTM DEM. The distance to watercourses map was created by extracting drainage lines using the DEM and using the Distance Module in IDRISI to calculate the Euclidean distance from watercourses. This ancillary environmental data is depicted in Figure 28. These variables were selected based on literature which stated the establishment of these tree species is determined by the availability of water and the terrain (Wakie *et al*., 2014; Ndhlove *et al*., 2016; Meroni *et al*., 2017; Ng *et al*., 2017). The significance of these variables was tested using the Cramer's V value. LCM calculates this value automatically and shows the level of association between the exploratory variables and land cover categories (Eastman, 2009; Roy *et al*., 2014). The model illustrated that the most influential variable was elevation with a Cramer's V value of 0.1771, followed by the distance to water with a Cramer's value of 0.1611. According to Eastman (2009) a Cramer's V value of 0.15 or higher are useful.

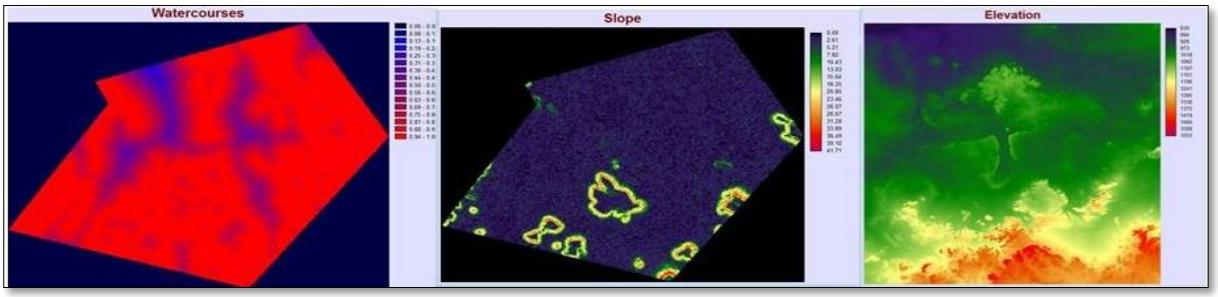



**Figure 27. Driver variables used in the change prediction model**

Once the driver variables were tested and selected as drivers of change, transition potential maps were created for each transition possibility. Transition potentials may be described as the likelihood of one land cover class to change into another (Roy *et al*., 2014). To create transition potentials, the MLP Neural Network modelling algorithm was employed. Transition potential maps were created based on the historical changes and selected driver variables (Roy *et al*., 2014). The MLP achieved an accuracy of 60% and a RMS value of 0.2.

Once the transition potential was calculated and the transition potential maps were created, the Markov chain analysis was conducted to determine the quantity of change in each transition (Behera

*et al*., 2012; Roy *et al*., 2014). The Markov chain analysis uses two input maps comparing the initial (T1) and second land cover (T2) to predict the future land cover (T3) using a transition probability matrix for the future (Roy *et al*., 2014). Behera *et al*. (2012) described the transition probability matrix as being a file with records of the probability that each land cover and land use class will change to every other class.

**2017 Land Cover Prediction**

Figure 29 is the 2017 land cover prediction map created using 2003 and 2013 land cover maps, ancillary environmental data and the IDRISI Land Change Modeller (LCM). The model predicted that *Prosopis* covered an area of 8 $km^2$ in 2017.

**Visual Model Validation**

In order to validate the model, a 2017 change prediction map was compared with the actual 2017 land cover map. Based on a quick visual inspection of the actual 2017 land cover map and the 2017 prediction land cover map, both maps appear to be very similar. The predicted quantity of *Prosopis* change is slightly greater than it really was, with the predicted map having an area of 8 $km^2$ and the actual land cover map having an area of *Prosopis* of approximately 6.3 $km^2$.

**Statistical Model Validation**

Table 14 illustrates the Kappa statistics parameters which assess the level of agreement between the real land cover/land use map and prediction map. This assists in measuring the accuracy of the model. All the Kappa values ($K_{no}$, $K_{location}$, $K_{standard}$) were above 0.9, which indicates the model had a high accuracy. This revealed that the model is suitable for accurate prediction of future LULC changes. Kappa statistics of 1 indicate a perfect agreement between the real map and the prediction map.

**Table 14. Statistical model validation**

| Kappa Parameter | Value |
|---|---|
| $K_{no}$ | 0.9197 |
| $K_{location}$ | 0.9468 |
| $K_{standard}$ | 0.9347 |

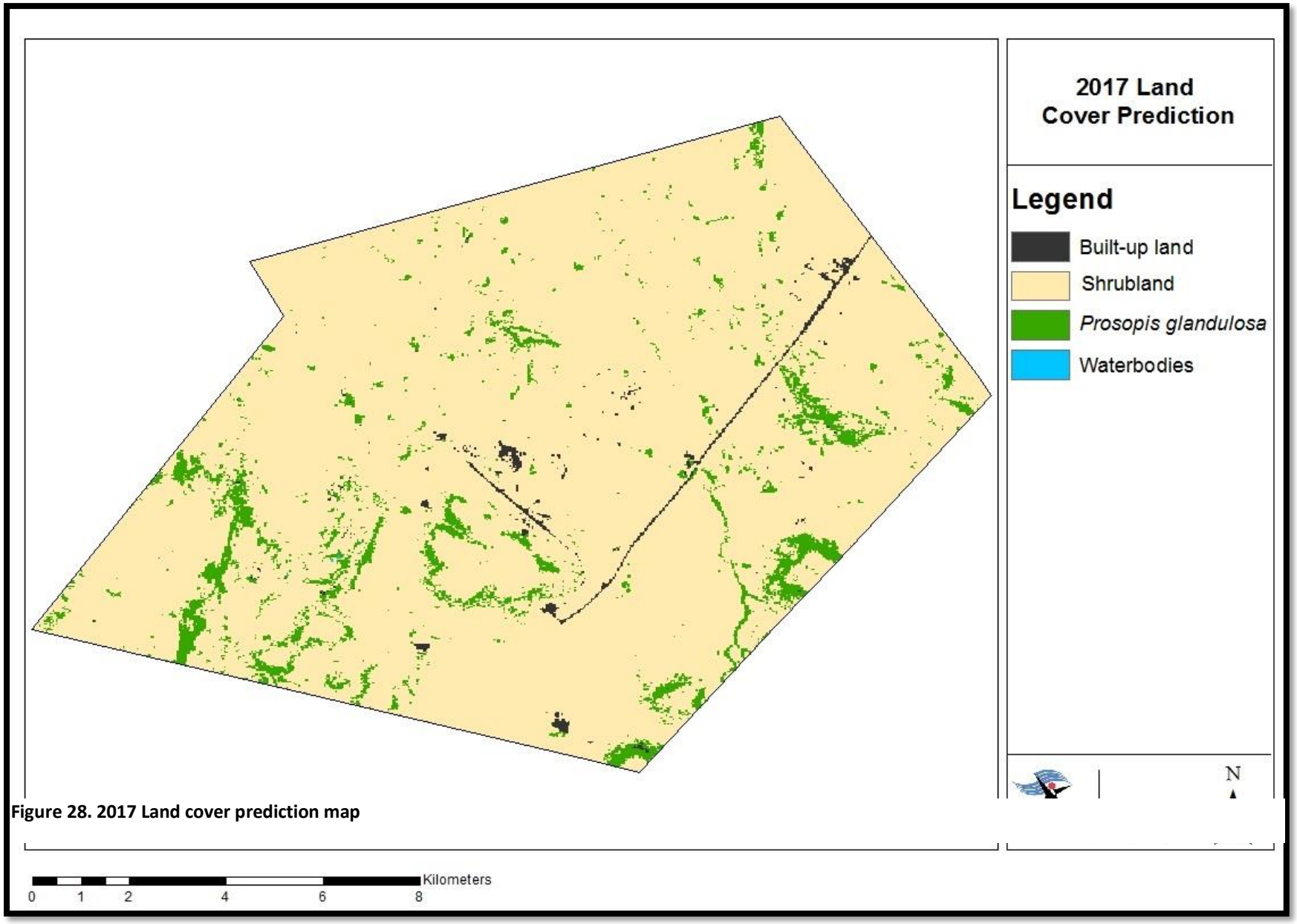
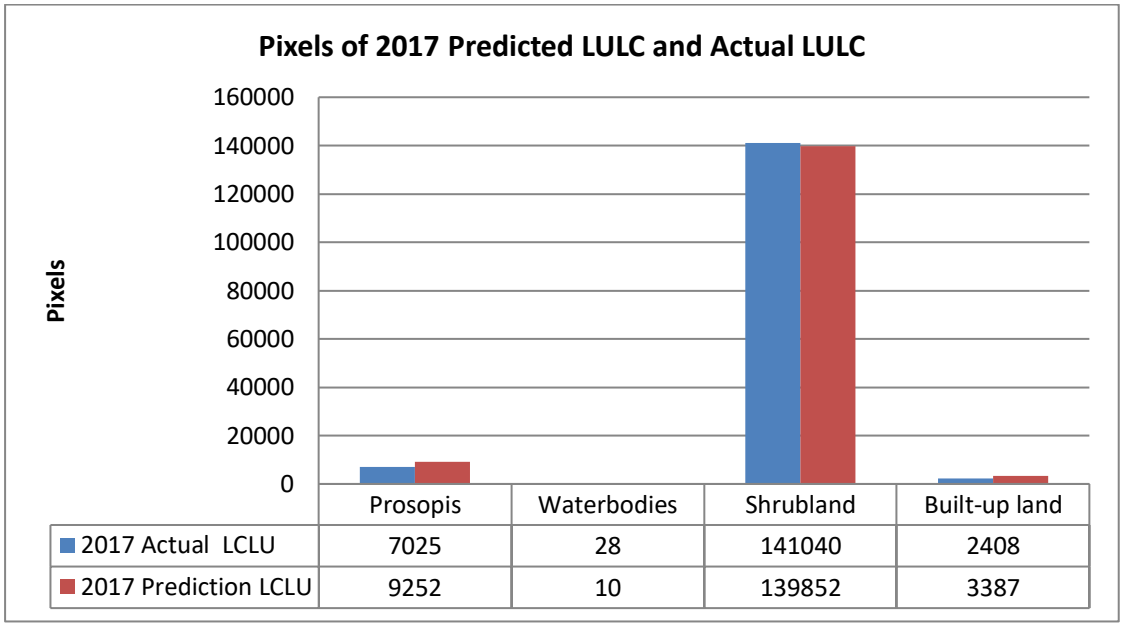



**Figure 28. 2017 Land cover prediction map**

The Cramer's V value, which measures the strength in association between the images had a value of 0.6. This means that there is a strong association between the predicted LULC map and the actual 2017 LULC map.

Figure 30 compares the pixels of each class in the real LULC map and predicted LULC map for the year 2017. The graph indicated that the model may have slightly over-predicted the land cover changes for *Prosopis*. The model estimated that are 9252 pixels of *Prosopis*, whereas there were 7025 pixels for this class based on the actual 2017 LULC map.




| | Prosopis | Waterbodies | Shrubland | Built-up land |
|---|---|---|---|---|
| 2017 Actual LCLU | 7025 | 28 | 141040 | 2408 |
| 2017 Prediction LCLU | 9252 | 10 | 139852 | 3387 |

**Figure 29. Pixel comparison of 2017 real LULC map and 2017 predicted LULC map**

A confusion matrix table was created using ERMMAT module (error matrix analysis) on IDRISI to establish the accuracy of the predicted land cover map using actual ground truth reference data. The prediction map had a Kappa coefficient of 0.8796. The agreement between the 2017 land cover prediction map and ground reference data was high, as a Kappa value of 1 represents a perfect agreement (Butt *et al*., 2015). Table 15 presents the confusion matrix table for the land cover predicted map of 2017. In total, 8488/11096 pixels (76.5%) were classified as *Prosopis*, with the remaining 2608 pixels (23.50%) being incorrectly predicted as shrubland.

**Table 15.Confusion matrix for 2017 prediction map.**

| | **Built-up land** | **Shrubland** | ***Prosopis*** | **Waterbodies** | **Total** |
|---|---|---|---|---|---|
| **Built-up land** | 1776/1776 (100%) | 0 | 0 | 0 | 1776 |
| **Shrubland** | 0 | 137 598/137 598 (100%) | 2608/11 096 (23.50%) | 0 | 140206 |
| ***Prosopis*** | 0 | 0 | 8488/11 096 (76.50%) | 0 | 8488 |
| **Waterbodies** | 0 | 0 | 0 | 31(100%) | 31 |
| **Total** | 1776 | 137598 | 11096 | 31 | 150501 |

## 2022 Land Cover Prediction

Predicting areas that are at risk from being invaded by alien invasive species is essential as this may prevent the further spread and establishment of these species. Areas favourable for these species need to be monitored, and species distribution models provide this information which can be used by land managers to inform their control and eradication strategies (Barbet-Massin *et al*., 2018).

This study predicted the LULC changes for the year 2017 by using LULC maps for 2003 and 2013. The validation of the model was satisfactory, revealing that the model is appropriate for predicting future LULC changes. A LULC prediction map for the year 2022 was then generated, using the same data that was utilized for the 2017 prediction. Figure 31 is the 2022 land cover prediction map. *Prosopis* is predicted to cover an area of approximately 9 $km^2$ in the year 2022. The density of these species is expected to increase in areas that had a moderate and dense density.

The study revealed the potential expansion of *Prosopis* species in the study area. The model predicted that there will be a significant increase in these species if proper preventative, control and eradication measures are not developed and implemented. Prediction maps can be used to inform these strategies which will assist in restoring damaged ecosystems and control the spread of these species. Construction activities which can influence the establishment of these species need to be monitored. Areas which are favourable for the establishment and growth of these species need to be constantly monitored to reduce the risk of invasion.

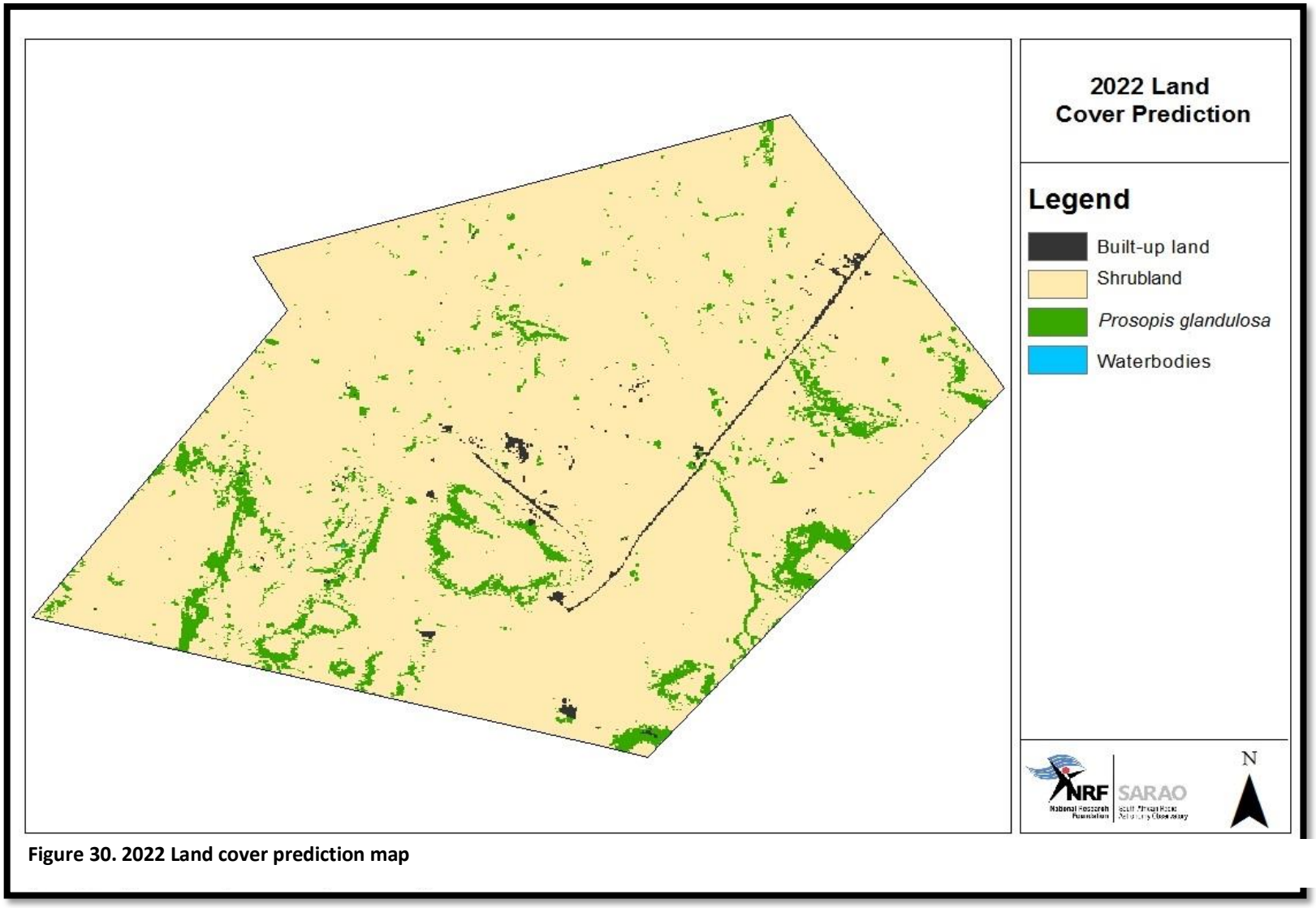



**Figure 30. 2022 Land cover prediction map**

# 5. Discussion

## 5.1 WorldView-3 Land Cover Classification

The use of high resolution satellite imagery to delineate *Prosopis* in the study area was successful. *Prosopis* species were observed to be along drainage lines, dams and boreholes in the study area. This was observed on Figure 16. The spatial distribution of these tree species corresponds with literature and field work observations. These species are mainly located in the lowest and wettest areas where there is water runoff (Boyle *et al*., 2014; Ngi *et al*., 2017). This is where the highest population density of *Prosopis* was found. The use of high resolution sensors allowed for the narrow linear zone of trees to be detected along riparian corridors. WorldView-3 has a spatial resolution of 1.24 m and consists of eight spectral bands (Table 1). The high spatial and spectral resolution allowed for detection *Prosopis* which established in small patches and also along linear habitats (Ng *et al*., 2017). *Prosopis* species were also observed around boreholes in the study area. This shows that these species are not entirely dependent on surface water. *Prosopis* species have long roots which allow them to exploit groundwater supplies (Geesingis *et al*., 2011).

Most of the invasions along the drainage lines have a dense canopy cover. This may be observed in Figure 6, which illustrates the density cover of the surveyed *Prosopis* invasions. Information on the abundance and distribution of these species is essential as this data informs the types of control and eradication strategies that must be implemented (Holdmes *et al*., 2008). The dense cover of *Prosopis* along these watercourses has a negative impact on the riparian ecosystem. These species negatively impact natural systems and biodiversity by altering their structures and functions resulting in native biodiversity being displaced and water yields being reduced (Charles and Dukes, 2008; Wakie *et al*., 2014; Le Maitre *et al*., 2000, 2015). Environmental managers therefore need to prioritize the clearing of these species in these areas before the density of these tree species intensifies into closed canopies (Holdmes *et al*., 2008). It would also be more cost effective controlling these species when their density is still sparse, moderate and dense; as more resources would be required if one attempts to clear invasions that are of a closed canopy cover.

The height of the *Prosopis* trees along these drainage lines ranges from 2 to 6 m. Figure 7 illustrates the heights of the surveyed *Prosopis*. A total of 72/148 (53%) of the surveyed sites had *Prosopis* trees with a height of 2-4 m. Out of the 72 trees that were 2-4 m high, 21 of them were observed to have a sparse density (29%). There were 11/148 (7%) sites that had trees with a height of 1-2 m. Out of the 11 sites, 5 had a sparse density (45%). This shows that these species are still establishing in the area.

A total of 50/148 (34%) of the surveyed sites had *Prosopis* trees with a height of 4-6 m. A total of 28/50 (56%) of the trees with a height of 4-6 m were observed to be related to densely populated. Half of the dense trees surveyed are of a height of 4-6 m. These areas should be considered as high priority areas and clearing should take place before these tree species intensify in density and further increase in height. This will make clearing efforts difficult and more resources will be required.

The use of a high resolution sensor allowed for not only large stands of trees to be detected, but also small trees, making this sensor ideal to delineate features in riparian zones, where moderate resolution sensors may not have detect these features. High resolution imagery has the potential to provide detailed information on invasive species at the species level. The main limitation of using high resolution satellite imagery is its availability. Acquiring these high resolution satellite images is expensive. Conducting long term time series analyses with these images is also a challenge as most of the advanced sensors were established in the 2000s. This affects the ability for managers to conduct long term detailed change analyses. The time to process these images was also a challenge. This study used an advanced classification algorithm. The classification algorithm was able to produce a land cover land use map with a high accuracy level, but high computational power was required and each classification ran for approximately 1 day.

## 5.2 Change Detection Analysis

A land cover land use change detection analysis was conducted using land cover land use maps created with Landsat satellite images. The spatial distribution and extent of *Prosopis* cover in the study area varies in the period 2003-2017. There are periods in which the species distribution decreases and periods where they increase, resulting in the species distribution and extent fluctuating over time.

In the period 2003-2008, there was an overall decrease in *Prosopis* of approximately 0.20 $km^2$. This may be observed in Figure 20, which is a graph illustrating the net change during this period. During this period, there was no construction of SKA infrastructure yet. There was an average decrease rate in *Prosopis* of approximately 0.04 $km^2$.For the period 2003-2008, the study area was still used for sheep farming. No SKA infrastructure development was taking place.

For the period 2008-2013, there was a larger decrease in *Prosopis* cover in the study area. There was an overall decrease in *Prosopis* of an area of approximately 0.8 $km^2$. This may be attributed to clearing of vegetation for the construction of infrastructure. There was an increase in built-up land of approximately 1.3 $km^2$ that took place in the study area. During this period, the SKA had acquired this land and the land use changed from sheep farming to astronomy infrastructure. The infrastructure

that was constructed during this period includes buildings, roads, construction camps and Meerkat telescopes which are shown as linear feature.

In the period 2003-2013, *Prosopis* species had been observed to decrease in area, as a result of these species and shrublands being cleared for the construction of SKA infrastructure. For the period 2013-2017, there was a sharp increase in *Prosopis* species of an area of approximately 0.4 $km^2$.

When *Prosopis* and other vegetation were actively been cleared for the construction of infrastructure in the study area, one may observe an overall decrease in these species. From the year 2013-2017, there was no heavy clearance of vegetation as the construction of infrastructure had already commenced, resulting in the re-growth of these species and them invading new cleared areas. It is essential for one to monitor the cleared areas regularly as *Prosopis* seedlings may emerge. It is important to remove seedling immediately to stop the reestablishment of these species (Holdmes *et al*., 2008). Construction activities such as excavations are vulnerable to *Prosopis* invasion. In this study, one may observe that with an increase in construction activities, there was an increase in *Prosopis* establishment and spread. The study has highlighted the importance of monitoring and maintaining areas where alien invasive plant species have been removed. Repeated follow-up treatments are required to ensure that seedlings do not re-establish and to assess if the affected ecosystems are restored.

Landsat satellite images can be utilized to conduct land cover land use change detection analyses as they have a historical archive of images, which new high-resolution sensors do not have. This makes the sensor more suitable for the change detection analyses but its spatial resolution may affect the level of detail one may obtain. The spatial resolution for Landsat images was a limitation as this sensor has a spatial resolution of 30 m, compared to 1.24 m spatial resolution for WorldView-3. The Worldview-3 image was able to delineate tree species along narrow water courses which were not detected in the Landsat land cover maps. Areas that had a *Prosopis* density of sparse to moderate were not detected on the Landsat images but were on the Worldview-3 image.

## 5.3 Change Prediction

Using land over/land use maps and ancillary environmental data, the land cover for the year 2017 and 2022 was predicted. The prediction accuracy of the 2017 land cover prediction map was tested using the actual 2017 land cover land use map. The two land cover maps appeared very similar with *Prosopis* species appearing in the same areas in both maps. Statistical measures of strength of association (Kappa Index of Agreement and Cramer's V coefficient) between the 2 images were calculated and these measures revealed that the model had a high level of accuracy. The Cramer's V coefficient which

determined the strength of association had a value of 0.6. The Kappa Index of Agreement statistics ($K_{no}$, $K_{location}$, $K_{standard}$) all had values above 0.9. These values indicate that there is a strong association between the predicted LULC map and real LULC map.

The area of *Prosopis* cover was calculated for both maps and the predicted quantity of *Prosopis* change was slightly greater than what it really was. *Prosopis* species covered an area of approximately 6.3 $km^2$ in 2017. The prediction map estimated *Prosopis* to cover an area of approximately 8 $km^2$for the year 2017. The 2017 prediction map had a high overall accuracy which proved that the model could produce a high accuracy prediction map

A 2022 prediction map was therefore created to simulate the LULC for the study area. The model predicted that in the year 2022, *Prosopis* will cover an area of approximately 9 $km^2$. *Prosopis* species are predicted to further invade along drainage lines and intensifying in density. Areas that had *Prosopis* species established in small groups are predicted to form into dense thickets.

# 6. Conclusions

This study was aimed at using high and moderate resolution satellite imagery to delineate the distribution of *Prosopis glandulosa*, to analyze the land cover changes over a 14 year period and to model future land cover changes. The objectives were successfully completed, proving how the use of remotely sensed data and GIS can be used to provide information that can then be used to effectively manage and control alien invasive plant species.

Spatial data, captured at the right scale provides information on the distribution of alien invasive plant species and their spatial extent, which is essential for monitoring the efficiency of the current management strategies and evaluating potential future invasions. Due to remotely sensed data being multi-temporal and cost effective than traditional survey methods, this tool can be used for natural resource management.

**Mapping the current distribution of *Prosopis***

WorldView-3 satellite images can be utilized to delineate alien invasive plant species such as *Prosopis* as a result of its high spatial and spectral resolution. The use of high resolution satellite images improves the accuracy of LULC maps resulting in detailed, more accurate maps which can be used by conservation managers for devising appropriate management and control strategies to reduce the spread of alien invasive plant species. The Worldview-3 image used to map these species was captured April, which is an ideal time for these species to be discriminated from other plant species in the area. This highlights the importance of the date in which images are captured as this will have an impact on the accuracy of the image classification. Image date selection is essential as in some cases, *Prosopis* has been observed to have a similar spectral signature with *Acacia* spp. This may result in these species being confused. It is therefore essential to select images captured during peak time of plant activity and Van den Berg *et al*. (2013) concluded that the most ideal images for the accurate delineation of *Prosopis* in the Northern Cape should be captured between February to May (Van den Berg *et al*., 2013; Meroni *et al*., 2017).

The limitation with using high resolution satellite imagery is their availability and cost. Sensors such as WorldView-3 have limited dates available as they were launched in the 2000s, whereas moderate resolution sensors such as Landsat consist of satellite images that date back to 1972. This allows for long term monitoring of the earth's surface to take place.

The image classification algorithm used was the Neural Network classifier which was conducted on ENVI software 5.2. Advance classifiers are able to delineate land cover classes more accurately than

traditional algorithms but using this advanced algorithm has a limitation. Advanced classifiers require high computational power. This resulted in the image classification procedure being time consuming.

**Change detection**

*Prosopis* species were successfully delineated using Landsat satellite images and a change detection analysis was conducted. One was able to observe the land cover changed in the study area for the period 2003-2017. *Prosopis* species are observed to slightly decrease for the period 2003-2013, but with the increase of built up land, which lead to the clearing of vegetation, it is observed that these species invade these cleared areas later. Construction activities have an impact on the spread of *Prosopis* in the study area. Seed dispersal needs to be monitored during construction as a result of construction vehicles spreading these seeds and land being exposed when vegetation is cleared. The Environmental Control Officer must monitor construction areas and make sure *Prosopis* species are removed by trained personnel prior construction to reduce the risk of seed dispersal.

The Landsat images used were captured between the months of October and November. This was as a result of the field work being conducted during those months. This was a limitation as this is not the most ideal month for *Prosopis* species to be mapped using satellite image but based on field studies of the study area, *Prosopis* is by far still the most abundant tree in the area. The availability of satellite images for a desired period is also a limitation. Landsat sensors have a temporal resolution of 16 days. This resulted in approximately two images available for an area per month. This had a negative impact on the study as some images had cloud cover, limiting the available images one could use for the study.

**Change Prediction**

The study was able to successfully simulate the spatial distribution and extent of *Prosopis* species in the study area for the year 2017 and 2022 through the use of LULC maps and ancillary environmental data (distance to watercourses, slope and elevation). Although these simulations were able to provide information on the trend of these species, there are limitations one needs to consider when using such predictions models. These include understanding that the outcomes of the predictions are dependent on the accuracy of the image classification. Landsat images, which have a moderate spatial resolution, were used in this model. The spatial resolution of a satellite image affects the image classification accuracy and the level of information one may obtain from that satellite image therefore affecting the prediction model accuracy.

# 7. Recommendations

For future studies, it is recommended that higher spatial and spectral resolution satellite images are used to create LULC maps that will be used for the change detection analysis and change prediction analysis. This is essential as these sensor characteristics have an impact on the image classification accuracy. When one attempts to use LULC maps to create prediction maps, the classification accuracy of these maps may affect land cover prediction accuracy.

# 8. References

Abdi, Z.D. 2011.*Mapping and managing the spread of* Prosopis juliflora *in Garissa County, Kenya*. MSc. thesis, Kenyatta University, Kenya.

Abdou, L., Diouf, A., Inoussa, M.M., Mamoudou, B.M., Illiassou, S.A. and Mahamane, A. 2016.Modeling the Geographic Distribution of *Prosopis africana* (G. and Perr.) Taub. in Niger. *Environment and Natural Resources Research*, *6*(2), 136-144.

Adam, E., Mureriwa, N. and Newete, S. 2017. Mapping *Prosopis glandulosa* (mesquite) in the semi-arid environment of South Africa using high-resolution WorldView-2 imagery and machine learning classifiers. *Journal of Arid Environments*, 145, 43-51.

Admasu, D. 2008. Invasive plants and food security: the case of *Prosopis juliflora* in the Afar region of Ethiopia. *FARM-Africa, IUCN*, 1-13.

Ahmadizadeh, S. 2014. Land use change detection using remote sensing and artificial neural network: Application to Birjand, Iran. *Computational Ecology and Software*, *4*(4), 276-288.

Amboka, A.A. and Ngigi, T.G. 2015. Mapping and Monitoring Spatial-Temporal Cover Change of *Prosopis* Species Colonization in Baringo Central, Kenya. *International Journal of Engineering Science Invention, 4(3)*, 50-55.

Andersen, H.E., McGaughey, R.J. and Reutebuch, S.E. 2005. Estimating forest canopy fuel parameters using LIDAR data. *Remote Sensing of Environment*, 94(4), 441-449.

Aziz, N., Minallah, N., Junaid, A. and Gul, K., 2017. Performance Analysis of Artificial Neural Network Based Land Cover Classification. *World Academy of Science, Engineering and Technology, International Journal of Environmental, Chemical, Ecological, Geological and Geophysical Engineering*, *11*(5), 412-416.

Barbet-Massin, M., Rome, Q., Villemant, C. and Courchamp, F., 2018. Can species distribution models really predict the expansion of invasive species? *PloS One*, *13*(3), e0193085, doi:10.1371/journal.pone.0193085.

Behera, M.D., Borate, S.N., Panda, S.N., Behera, P.R. and Roy, P.S., 2012. Modelling and analyzing the watershed dynamics using Cellular Automata (CA)–Markov model–A geo-information based approach. *Journal of Earth System Science*, *121*(4), 1011-1024.

Bhojvaid, P.P. and Timmer, V.R. 1998. Soil dynamics in an age sequence of *Prosopis juliflora* planted for sodic soil restoration in India. *Forest Ecology and Management*, 106(2), 181-193.

Bosch, J.M., Van Wilgen, B.W. and Bands, D.P. 1986. A model for comparing water yield from fynbos catchments burnt at different intervals. *Water SA*, *12*(4), 191-196.

Boyle, S.A., Kennedy, C.M., Torres, J., Colman, K., Pérez-Estigarribia, P.E. and Noé, U. 2014. High-resolution satellite imagery is an important yet underutilized resource in conservation biology. *PloS One*, *9*(1), e86908,doi:10.1371/journal.pone.0086908.

Burgiel, S.W. and Muir, A.A. 2010. *Invasive species, climate change and ecosystem-based adaptation: Addressing multiple drivers of global change*. Washington, DC, US and Nairobi, Kenya, Global Invasive Species Programme (GISP), 1-56.

Burkart, A. 1976.A monograph of the genus *Prosopis* (Leguminosae subfam. Mimosoideae): catalogue of the recognised species of *Prosopis*. *Journal Arnold Arboretum*, 57(4), 450-525.

Butt, A., Shabbir, R., Ahmad, S.S. and Aziz, N. 2015.Land use change mapping and analysis using Remote Sensing and GIS: A case study of Simly watershed, Islamabad, Pakistan. *The Egyptian Journal of Remote Sensing and Space Science*, *18*(2), 251-259.

Chamier, J., Schachtschneider, K., Le Maitre, D.C., Ashton, P.J. and Van Wilgen, B.W. 2012.Impacts of invasive alien plants on water quality, with particular emphasis on South Africa. *Water SA*, 38(2), 345-356.

Chander, G., Markham, B.L. and Barsi, J.A., 2007. Revised Landsat-5 thematic mapper radiometric calibration. *IEEE Geoscience and Remote Sensing Letters*, *4*(3), pp.490-494.

Charles, H. and Dukes, J.S. 2008.Impacts of invasive species on ecosystem services. *Ecological Studies*, 193, 217-237.

Chen, X., Vierling, L. and Deering, D. 2005.A simple and effective radiometric correction method to improve landscape change detection across sensors and across time. *Remote Sensing of Environment*, *98*(1),63-79.

Cho, M.A., Malahlela, O. and Ramoelo, A. 2015.Assessing the utility WorldView-2 imagery for tree species mapping in South African subtropical humid forest and the conservation implications: Dukuduku forest patch as case study. *International Journal of Applied Earth Observation and Geoinformation*,38,349-357.

Choge, S.K., Pasiecznik, N.M., Harvey, M., Wright, J., Awan, S.Z. and Harris, P.J.C. 2007.*Prosopis* pods as human food, with special reference to Kenya. *Water SA*, *33*(3), 419-424.

Choodarathnakara, A.L., Kumar, T.A., Koliwad, S. and Patil, C.G. 2012. Mixed pixels: a challenge in remote sensing data classification for improving performance. *International Journal of Advanced Research in Computer Engineering & Technology (IJARCET)*, *1*(9), 261-271.

Congalton, R.G. 1991. A review of assessing the accuracy of classifications of remotely sensed data. *Remote Sensing of Environment*, 37(1), 35-46.

De Alba, H. and Barros, J. 2012. Deforestation in the Kayabi indigenous territory: Simulating and predicting land use and land cover change in the Brazilian Amazon. *Proceedings of the III Coloquio Internacional en Geografia, Michoacán, México*, 21-24.

Deilmai, B.R., Kanniah, K.D., Rasib, A.W. and Ariffin, A. 2014. Comparison of pixel-based and artificial neural networks classification methods for detecting forest cover changes in Malaysia. *IOP Conference Series: Earth and Environmental Science,* 18(1), 012069, doi:10.1088/1755-1315/18/1/012069.

Dzieszko, P. 2014. Land-cover modelling using corine land cover data and multi-layer perceptron. *Quaestiones Geographicae*, *33*(1), 5-22.

Eastman, J.R. 2016.*IDRISI Terrset Manual*. Clark Labs-Clark University: Worcester, MA, USA.

Ehrenfeld, J.G. 2003. Effects of exotic plant invasions on soil nutrient cycling processes. *Ecosystems*, 6(6), 503-523.

El-Hallaq, M.A. and Habboub, M.O. 2015. Using Cellular Automata-Markov Analysis and Multi Criteria Evaluation for Predicting the Shape of the Dead Sea. *Advances in Remote Sensing*, *4*(01), 83-95.

Elith, J., Phillips, S.J., Hastie, T., Dudík, M., Chee, Y.E. and Yates, C.J. 2011. A statistical explanation of MaxEnt for ecologists. *Diversity and Distributions*, *17*(1), 43-57.

Felker, P., Clark, P.R., Laag, A.E. and Pratt, P.F. 1981. Salinity tolerance of the tree legumes: Mesquite (*Prosopis glandulosa* var. *torreyana, P. velutina* and *P. articulata*) Algarrobo (*P. chilensis*), Kiawe (*P. pallida*) and Tamarugo (*P. tamarugo*) grown in sand culture on nitrogen-free media. *Plant and Soil*, 61(3),311-317.

Fox, T.J., Knutson, M.G. and Hines, R.K. 2000. Mapping forest canopy gaps using air-photo interpretation and ground surveys. *Wildlife Society Bulletin*, 24(4), 882-889.

García-Sánchez, R., Camargo-Ricalde, S.L., García-Moya, E., Luna-Cavazos, M., Romero-Manzanares, A. and Manuel Montaño, N. 2012. *Prosopis laevigata* and *Mimosa biuncifera* (Leguminosae), jointly influence plant diversity and soil fertility of a Mexican semiarid ecosystem. *Revista de Biología Tropical*, 60(1), 87-103.

Geesingis, D., Al Khawlani, M. and Abba, M.L. 2004. Management of introduced *Prosopis* species: can economic exploitation control an invasive species? *Unasylva*, 217(55), 36-44.

George, C., Lochner, A. and Huisamen, B. 2011. The efficacy of *Prosopis glandulosa* as antidiabetic treatment in rat models of diabetes and insulin resistance. *Journal of Ethnopharmacology*, 137(1), 298-304.

Hadi, S.J., Shafri, H.Z. and Mahir, M.D. 2014. Modelling LULC for the period 2010-2030 using GIS and Remote sensing: a case study of Tikrit, Iraq. *IOP conference series: Earth and Environmental Science*, 20 (1), 012053, doi:10.1088/1755-1315/20/1/012353.

Haji, J. and Mohammed, A. 2013. Economic impact of *Prosopis juliflora* on agropastoral households of Dire Dawa Administration, Ethiopia. *African Journal of Agricultural Research*, *8*(9), 768-779.

Hancock, G.R., Martinez, C., Evans, K.G. and Moliere, D.R. 2006. A comparison of SRTM and high-resolution digital elevation models and their use in catchment geomorphology and hydrology: Australian examples. *Earth Surface Processes and Landforms*, *31*(11), 1394-1412.

Henderson, L. 1998. Southern African plant invaders atlas (SAPIA). *Applied Plant Science*, 12, 31-32.

Henderson, L. 1999. The Southern African Plant Invaders Atlas (SAPIA) and its contribution to biological weed control. *African Entomology*, 1, 159-163.

Henderson, L. 2007. Invasive, naturalized and casual alien plants in southern Africa: a summary based on the Southern African Plant Invaders Atlas (SAPIA). *Bothalia*, 37(2), 215-248.

Holmes, P.M., Esler, K.J., Richardson, D.M. and Witkowski, E.T.F. 2008. Guidelines for improved management of riparian zones invaded by alien plants in South Africa. *South African Journal of Botany*, *74*(3), 538-552.

Hoshino, B., Karamalla , A., Manayeva, K., Yoda, K., Suliman, M., Elgamri, M., Nawata, H. and Yasuda, H. 2012. Evaluating the invasion strategic of Mesquite (*Prosopis juliflora*) in eastern Sudan using remotely sensed technique. *Journal of Arid Land Studies*, 4, 1-4.

Hua, A.K. 2017. Application of Ca-Markov model and land use/land cover changes in Malacca River Watershed, Malaysia. *Applied Ecology and Environmental Research*, *15*(4), 605-622.

Jordan, C.F. 1969. Derivation of leaf-area index from quality of light on the forest floor. *Ecology*, 50(4), 663-666.

Joshi, C., de Leeuw, J. and van Duren, I.C. 2004. Remote sensing and GIS applications for mapping and spatial modelling of invasive species. *Proceedings of ISPRS*, 35, 669–677.

Kelcey, J. and Lucieer, A. 2012. Sensor correction and radiometric calibration of a 6-band multispectral imaging sensor for UAV remote sensing. *International Archives of the Photogrammetry, Remote Sensing and Spatial Information Science*, *39*, 393-398.

Kerle, N., Bakker, W.H., Grabmaier, K.A., Huurneman, G.C., van der Meer, F.D., Prakash, A., Tempfli, K., Gieske, A.S.M., Hecker, C.A., Janssen, L.L.F. and Parodi, G.N. 2004. *Principles of remote sensing: an introductory textbook*. ITC Educational Textbook Series, 2.

Köhl, M., Magnussen, S.S. and Marchetti, M. 2006. *Sampling methods, remote sensing and GIS multiresource forest inventory*. Springer Science & Business Media.

Kuloba, B.M., Van Gils, H., Van Duren, I., Moya, S.M. and Nene, S.M. 2011. Modeling cheetah, *acinonyx jubatus* fundamental niche in Kenya. *International Journal of Environmental Monitoring and Analysis*, 3(5), 317-330.

Le Maitre, D.C., Van Wilgen, B.W., Chapman, R.A. and McKelly, D.H. 1996. Invasive plants and water resources in the Western Cape Province, South Africa: modelling the consequences of a lack of management. *Journal of Applied Ecology*, 33, 161-172.

Le Maitre, D.C., Versfeld, D.B. and Chapman, R.A. 2000. The impact of invading alien plants on surface water resources in South Africa: a preliminary assessment. *Water SA,* 26(3), 397-408.

Le Maitre, D.C., Gush, M.B. and Dzikiti, S. 2015. Impacts of invading alien plant species on water flows at stand and catchment scales. *AoB Plants*, 7, 043, doi:10.1093/aobpla/plv043.

Liu, Y., Du, M. and Zhu, W. 2010. Examination Method and Implementation for Field Survey Data of Crop Types Based on Multi-resolution Satellite Images. *International Conference on Computer and Computing Technologies in Agriculture*, 344, 681-690.

Ma, Y. and Xu, R., 2010. Remote sensing monitoring and driving force analysis of urban expansion in Guangzhou City, China. *Habitat International*, *34*(2), 228-235.

Malahlela, O., Cho, M. A. and Mutanga, O. 2014. Mapping canopy gaps in an indigenous subtropical coastal forest using high-resolution WorldView-2 data. *International Journal of Remote Sensing*, 35(17), 6397-6417.

Malahlela, O.E., Cho, M.A. and Mutanga, O. 2015. Mapping the occurrence of *Chromolaena odorata* (L.) in subtropical forest gaps using environmental and remote sensing data. *Biological Invasions*, 17(7), 2027-2042.

Manaf, S.A., Mustapha, N., Sulaiman, M., Husin, N.A. and Hamid, M.R.A. 2018. Artificial Neural Networks for Satellite Image Classification of Shoreline Extraction for Land and Water Classes of the North West Coast of Peninsular Malaysia. *Advanced Science Letters*, *24*(2), 1382-1387

Megahed, Y., Cabral, P., Silva, J. and Caetano, M. 2015. Land cover mapping analysis and urban growth modelling using remote sensing techniques in greater Cairo region—Egypt. *ISPRS International Journal of Geo-Information*, *4*(3), 1750-1769.

Meroni, M., Ng, W.T., Rembold, F., Leonardi, U., Atzberger, C., Gadain, H. and Shaiye, M. 2017. Mapping Prosopis juliflora in west Somaliland with Landsat 8 satellite imagery and ground information. *Land Degradation & Development*, *28*(2), 494-506.

Milton, S.J. 2017. *Ecology and biodiversity assessment of the SKA Phase 1 in South Africa*. Specialist report for the SKA Strategic Environmental Assessment. CSIR, available at http://www.skaphase1.csir.co.za.

Mirik, M. and Ansley, R.J. 2012. Comparison of ground-measured and image-classified mesquite (*Prosopis glandulosa*) canopy cover. *Rangeland Ecology & Management*, 65(1),85-95.

Mishra, V.N., Rai, P.K. and Mohan, K. 2014. Prediction of land use changes based on land change modeler (LCM) using remote sensing: a case study of Muzaffarpur (Bihar), India. *Journal of the Geographical Institute" Jovan Cvijic", SASA*, *64*(1), 111-127.

Mucina, L. and Rutherford, M. 2004. *Vegetation map of South Africa, Lesotho and Swaziland*: *Shapefiles of Basic Mapping Units*. Beta version 4.0, National Biodiversity Institute, Cape Town, South Africa.

Mustapha, M.R., Lim, H.S. and Iafri, M.M. 2010. Comparison of Neural Network and Maximum Likelihood Approaches in Image Classification. *Journal of Applied Sciences*, *10*(22), 2847-2854.

Mwangi, E. and Swallow, B. 2005. Invasion of *Prosopis juliflora* and local livelihoods: Case study from the lake Baringo area of Kenya. *Conservation and Society,* 6(2), 130–140.

Nadoushan, M., Soffianian, A. and Alebrahim, A. 2015. Modeling land use/cover changes by the combination of Markov chain and cellular automata Markov (CA-Markov) models. *Journal of Earth, Environment and Health Sciences*, *1*(1), 16-21.

Ndehedehe, C., Ekpa, A., Simeon, O. and Nse, O. 2013. Understanding the neural network technique for classification of remote sensing data sets. *New York Science Journal, 6*, 26-33.

Ndhlovu, T., Milton, S.J. and Esler, K.J. 2016. Impact of *Prosopis* (mesquite) invasion and clearing on vegetation species composition and diversity in semi-arid Nama-Karoo rangeland, South Africa. *African Journal of Range & Forage Science*, 33(2), 101-110.

Ng, W.T., Rima, P., Einzmann, K., Immitzer, M., Atzberger, C. and Eckert, S. 2017. Assessing the Potential of Sentinel-2 and Pléiades Data for the Detection of *Prosopis* and *Vachellia* spp. in Kenya. *Remote Sensing*, *9*(1), 74, doi:10.3390/rs9010074.

Nouri, J., Gharagozlou, A., Arjmandi, R., Faryadi, S. and Adl, M. 2014. Predicting Urban Land Use Changes Using a CA-Markov Model. *Arabian Journal for Science & Engineering, 39*(7), 5565-5573.

Pasiecznik, N.M., Felker, P., Harris, P.J., Harsh, L., Cruz, G., Tewari, J.C., Cadoret, K. and Maldonado, L.J. 2001. *The 'Prosopis Juliflora'-' Prosopis Pallida. Complex: A Monograph*. HDRA,Coventry, 172pp.

Pejchar, L. and Mooney, H.A. 2009. Invasive species, ecosystem services and human wellbeing. *Trends in Ecology and Evolution*, *24*(9),497-504.

Petropoulos, G.P., Vadrevu, K.P., Xanthopoulos, G., Karantounias, G. and Scholze, M. 2010. A comparison of spectral angle mapper and artificial neural network classifiers combined with Landsat TM imagery analysis for obtaining burnt area mapping. *Sensors*, *10*(3), 1967-1985.

Pontius Jr, R.G., Cornell, J.D. and Hall, C.A. 2001. Modeling the spatial pattern of land-use change with GEOMOD2: application and validation for Costa Rica. *Agriculture, Ecosystems & Environment*, *85*(1-3), 191-203.

Pollock, J.J. 2015. *A Maxent-based Model for Identifying Local-scale Tree Species Richness Patch Boundaries in the Lake Tahoe Basin of California and Nevada*. Doctoral dissertation, University of Southern California, California.

Reaser, J.K., Meyerson, L.A., Cronk, Q., De Poorter, M., Eldrege, L.G., Green, E., Kairo, M., Latasi, P., Mack, R.N., Mauremootoo, J., O'Dowd, D., Orapa, W., Sastroutomo, S., Saunders, A., Shine, C., Thrainsson, S. and Vaiutu, L. 2007. Ecological and socioeconomic impacts of invasive alien species in island ecosystems. *Environmental Conservation,* 34, 98–111.

Richardson, D.M. and Van Wilgen, B.W. 2004. Invasive alien plants in South Africa: how well do we understand the ecological impacts? working for water. *South African Journal of Science*, *100*(1-2), 45-52.

Rosenbaum, P.R. and Rubin, D.B. 1983. The central role of the propensity score in observational studies for causal effects. *Biometrika*, *70*(1),41-55.

Roura-Pascual, N., Richardson, D.M., Krug, R.M., Brown, A., Chapman, R.A., Forsyth, G.G., Le Maitre, D.C., Robertson, M.P., Stafford, L., Van Wilgen, B.W. and Wannenburgh, A. 2009. Ecology and management of alien plant invasions in South African fynbos: accommodating key complexities in objective decision making. *Biological Conservation*, 142(8),1595-1604.

Roy, H.G., Fox, D.M. and Emsellem, K. 2014, June. Predicting land cover change in a Mediterranean catchment at different time scales. In: *International Conference on Computational Science and Its Applications* (pp. 315-330). Springer, Cham.

Sawal, R.K., Ratan, R. and Yadav, S.B.S. 2004. Mesquite (*Prosopis juliflora*) pods as a feed resource for livestock-A review. *Asian- Australasian Journal Animal Science*, *17*, 719-725.

Shackleton, R.T., Le Maitre, D.C. and Richardson, D.M. 2015. *Prosopis* invasions in South Africa: Population structures and impacts on native tree population stability. *Journal of Arid Environments*, 114,70-78.

Skakun, S., Kussul, N., Shelestov, A.Y., Lavreniuk, M. and Kussul, O. 2016. Efficiency assessment of multitemporal C-band Radarsat-2 intensity and Landsat-8 surface reflectance satellite imagery for crop classification in Ukraine. *IEEE Journal of Selected Topics in Applied Earth Observations and Remote Sensing*, *9*(8), 3712-3719.

Tessema, Y.A. 2012. Ecological and economic dimensions of the paradoxical invasive species *Prosopis juliflora* and policy challenges in Ethiopia. *Journal of Economics and Sustainable Development,* 3(8), 62-70.

Thompson, M. 1996. A standard land-cover classification scheme for remote-sensing applications in South Africa. *South African Journal of Science*, *92*(1), 34-42.

Turpie, J.K., Marais, C. and Blignaut, J.N. 2008. The working for water programme: Evolution of a payments for ecosystem services mechanism that addresses both poverty and ecosystem service delivery in South Africa. *Ecological Economics*, *65*(4), 788-798.

Updike, T. and Comp, C. 2010. Radiometric use of WorldView-2 imagery. *Technical Note*, 1-17.

Van den Berg, E.C., Kotze, I. and Beukes, H. 2013. Detection, quantification and monitoring of *prosopis* in the Northern Cape Province of South Africa using remote sensing and GIS. *South African Journal of Geomatics*, *2*(2),68-81.

Van Klinken, R.D. and Campbell, S.D. 2001. The biology of Australian weeds. 37. *Prosopis L*. species. *Plant Protection Quarterly*, *16*(1), 2-20.

Van Klinken, R.D., Shepherd, D., Parr, R., Robinson, T.P. and Anderson, L. 2007. Mapping mesquite (*Prosopis*) distribution and density using visual aerial surveys. *Rangeland Ecology & Management*, 60(4), 408-416.

Van Wilgen, B.W. and Lange, W.D. 2011. The costs and benefits of biological control of invasive alien plants in South Africa. *African Entomology*, *19*(2), 504-514.

Van Wilgen, B.W., Cowling, R.M., Marais, C., Esler, K.J., McConnachie, M. and Sharp, D. 2012. Challenges in invasive alien plant control in South Africa. *South African Journal of Science*, *108*(11-12), 8-11.

Van Wilgen, B.W., Richardson, D.M., Le Maitre, D.C., Marais, C. and Magadlela, D. 2001. The economic consequences of alien plant invasions: examples of impacts and approaches to sustainable management in South Africa. *Environment, Development and Sustainability*. 3(2), 145-168.

Wakie, T.T., Evangelista, P.H., Jarnevich, C.S. and Laituri, M. 2014. Mapping current and potential distribution of non-native Prosopis juliflora in the Afar Region of Ethiopia. *PloS one*, *9*(11), e112854,doi:10.1371/journal.pone.0112854.

Weltzin, J.F., Archer, S.R. and Heitschmidt, R.K. 1998. Defoliation and woody plant (shape *Prosopis glandulosa*) seedling regeneration: potential vs realized herbivory tolerance. *Plant Ecology*, 138(2), 127-135.

West, A.M., Kumar, S., Brown, C.S., Stohlgren, T.J. and Bromberg, J. 2016. Field validation of an invasive species Maxent model. *Ecological Informatics*, *36*, 126-134.

Wilson, J.R., Ivey, P., Manyama, P. and Nänni, I. 2013. A new national unit for invasive species detection, assessment and eradication planning. *South African Journal of Science*, 109(13), 0111,doi:10.1590/sajs.2013/20120111.

Wise, R.M., Van Wilgen, B.W. and Le Maitre, D.C. 2012. Costs, benefits and management options for an invasive alien tree species: the case of mesquite in the Northern Cape, South Africa. *Journal of Arid Environments*, 84, 80-90.

Xie, Y., Sha, Z. and Yu, M. 2008. Remote sensing imagery in vegetation mapping: a review. *Journal of Plant Ecology*, *1*(1), 9-23.

Yang, W., Hou, K., Yu, F., Liu, Z. and Sun, T. 2010. A novel algorithm with heuristic information for extracting drainage networks from raster DEMs. *Hydrology and Earth System Sciences Discussions*, *7*(1), 441-459.

Young, N.E., Anderson, R.S., Chignell, S.M., Vorster, A.G., Lawrence, R. and Evangelista, P.H. 2017. A survival guide to Landsat preprocessing. *Ecology*, *98*(4), 920-932.

Zachariades, C., Hoffmann, J.H. and Roberts, A.P. 2011. Biological control of mesquite (*Prosopis* species) (Fabaceae) in South Africa. *African Entomology*, *19*(2), 402-415.

Zhou, L. and Yang, X. 2008. Use of neural networks for land cover classification from remotely sensed imagery. *The International Archives of the Photogrammetry, Remote Sensing and Spatial Information Sciences*, *37*, 575-578.

Zimmerman, H. and Pasiecznik, N.M. 2005. *Realistic approaches to the management of Prosopis species in South Africa*. Policy brief, Pretoria, Prepared by the Agricultural Research Council for the HDRA organic organisation and funded by the UK Department for International Development (DFID). https://www.gov.uk/dfid-research-outputs/realistic-approaches-to-the-management-of-prosopis-species-in-south-africa.